Using Plasma Polymerised Allylamine to Culture Hepatocytes in *In-vitro* Fluidic Bioreactors

By Chafika Dehili, MPharm (Hons)

Thesis submitted to the University of Nottingham for the degree of Doctor of Philosophy

September 2007

Table of Contents

Table of Figures

Abstract

Tissues constituting mammalian organisms are finitely organised 3-D multicellular structures where cell-cell and cell-matrix interactions are important modulators of functionality. The liver, being the site of metabolism in mammals, is extensively employed in *in-vitro* studies such as toxicology, drug testing and liver replacement. Most existing liver models have been static, homogenous 2-D models which have shown limited morphological and functional characteristics of *in-vivo* liver. With the improved understanding of the liver, these models became more sophisticated to comprise various liver and non-liver cell types, various configurations of extracellular matrix and complex scaffold supports, including fluidic systems.

Fluidic supports for liver cells *in-vitro* are reported in this work and two different types were investigated. The first one was a glass based microfluidic system with hexagonal structure to mimic the liver lobule. The second one was a standard flat-plate fluidic chamber made of plastic (Ibidi channel). For the purpose of improving the attachment of the cells and the performance of the bioreactors examined, various substrate coating procedures were evaluated. The main coating techniques employed were collagen in two forms, adsorbed and gel, and plasma polymerised allylamine (ppAAm).

The plasma coating procedures utilised in this work changed the surface properties of the substrate used by increasing the levels of nitrogen and improving hydrophilicity as demonstrated by x-ray photoelectron spectroscopy and contact angle measurements. The ppAAm penetrated both etched glass channels of the hexagonal

bioreactor and the flat-plate chamber. The ppAAm films on etched glass channels had similar properties to the films produced on the glass surrounding the channels and coverslips. The ppAAm films obtained in the flat-plate chamber were different and they were characterised with a gradient of chemicals and hydrophilicity. This was because the Ibidi chamber is a closed environment and the plasma vapour infiltrated through the inlet and outlet at the ends of the channel.

The attachment and functionality of primary rat hepatocytes seeded onto ppAAm films were evaluated using ppAAm coated coverslips and compared to coverslips coated with collagen gel. This demonstrated that both collagen gel and ppAAm improved the attachment, albumin secretion and 7-Ethoxyresorufin-O-deethylase (EROD) activity of the cells compared to uncoated glass.

The hexagonal glass bioreactor showed poor attachment of liver cells and this was enhanced with ppAAm coating. The Huh-7 cells incubated into ppAAm coated hexagonal bioreactor died and detached after incubation with media flow. One of the reasons for this was poor cellular attachment. An improved attachment, but not viability, was observed when the cells were seeded using the biotin-avidin technique. The ppAAm coated flat-plate chamber demonstrated low adhesion of primary rat hepatocytes. However, these channels showed good attachment when collagen type I was adsorbed onto the surface. The viability and functionality, when measured using albumin secretion and EROD, of primary rat hepatocytes were maintained for 5 days in closed fluidic circuit in mono-culture and co-culture with 3T3 cells. These promising results could be exploited to further develop these systems for *in-vitro* culture of liver cells.

Acknowledgments

I would like to thank my supervisor, Kevin Shakesheff, for his supervision and support during the course of this PhD. I also thank Morgan Alexander for his supervision and help with the plasma work. I express many thanks and gratitude to Pauline Lee who started this project and assisted me during the first two years. Many thanks go to my internal examiner, John Aylott, and other members of the pharmacy school that contributed to useful discussions about the project during meetings and seminars. I am also thankful to EPSRC and the Algerian Government for funding.

I thank all the members of the tissue engineering group from 2003 to 2007 for being a great team, especially the liver group (Pauline, Rob, Laura, Liqiong, John) and the small community of D16 (Alex, Mischa, Andrew, Soopie and Ruby). Many thanks go to all the technicians in the pharmacy school particularly Mrs Marshall for being there as a friend as well.

I sincerely thank Mieke Heyde and Rabia Bourkiza for being there when I needed them and of course for proof reading my thesis. Special thanks go to Marta Silva for her friendship and support since the start of my PhD and particularly for accompanying me in the laboratory at the early hours of the day. Many thanks are attributed to Cat and Mischa for their help with XPS analysis and contact angle.

My friends and family have been great during this time and the list is long. All the friends I met in the tissue engineering labs have been very friendly and helpful. My housemates and the little Arab group of friends did a wonderful job dealing with my stressful and unhappy moments. They also provided me with help and advice from culturing hepatocytes (Magda) to fixing my computer (Hich and Momen) and fun (girls and boys). Special thanks to Lilia and Rawan for being there for retail therapy after the stressful lab days.

My parents, brothers and sisters provided me with lots of encouragement that enabled me to finish my PhD. You are the best "papa et mama" and I dedicate this to you.

Publications and Presentations

The followings were attended meetings where some of the work reported in this thesis has been presented:

Poster presentation: Hepatocytes Users Group, Valencia, Spain, 11th to 13th of November, 2004. Plasma based surface modification for tissue engineering purposes: the effects on hepatocyte attachment and functionality.

Poster presentation: Tissues and Cells Engineering Society, Queen's Mary Hospital, London, 20th to 21st of June, 2005. Primary rat hepatocytes cultured on plasma polymerised allylamine.

Poster presentation: World Congress on Tissue Engineering and Regenerative Medicine, Pittsburgh, USA, 25th t0 27th of April, 2006. Assessment of a novel microfluidic bioreactor for *in-vitro* liver engineering.

School Seminars

School of Pharmacy second year presentation, University of Nottingham, 24th of January, 2005. Micro-liver Project I.

School of Pharmacy third year presentation, University of Nottingham, 19TH of December, 2005. Micro-liver Project II.

Publications

DEHILI, C., LEE, P., SHAKESHEFF, K. and ALEXANDER, M. (2006). Comparison of primary rat hepatocyte attachment to collagen and plasma-polymerised allylamine on glass. *Plasmas Process Polym*, **3**, 474-484.

Abbreviations

BE	Binding energy
BSA	Bovine serum albumin
° C	Degree Celsius
cm	centimetre
cm^2	centimetre square
CoA	Co-enzyme A
CYP	Cytochrome
2-D	Two-dimensional
3-D	Three-dimensional
DMEM	Dulbecco's Modified Eagle Media
DMSO	Dimethyl sulphoxide
dyn/cm^2	Dyne per square centimetre
ECM	Extra-cellular matrix
EGTA	Ethylene glycol-bis (β-aminoethylether)- N, N, N', N'-tetraacetic acid
ELISA	Enzyme linked immunosorbent assay
EROD	7-Ethoxyresorufin-O-deethylase
eV	Electron volt
Ex/em	excitation/emission
FCS	Foetal calf serum
FITC	Fluorescein isothiocyanate
FWHM	Full width at half maximum
g	Gram
GK	Glucokinase
Gpase	Glucose-6-phosphatase
H	Height
HMDS	Hexamethyldisilazane
HRP	Horse-radish peroxidase
HRP Ab	Horse-radish peroxidase conjugated antibody
hrs	Hours
H_2SO_4	Sulphuric acid
IMS	Industrial methylated spirits

kDa	Kilodalton
kV	Kilo volts
L	Length
L-15	Leibovitz-15 medium
l	Litre
MHz	Megahertz
M	Molar
mg	Milligram
mins	minutes
µl	Microlitre
ml	Millilitre
µg	Microgram
mm	Millimetre
mM	Millimoles
nm	Nanometer
NaCl	Sodium chloride
NPCs	Non-parenchymal cells
P450	Cytochrome P450
Pa	Pascal
PBS	Phosphate buffered saline
PDMS	Poly(dimethylsiloxane)
PGS	Poly(glycerol sebacate)
PLA	Poly(LD-lactic acid)
PLLA	Poly(LD-lactic acid)
PLL	Poly(L-lysine)
pmol	Picomole
ppAAm	Plasma polymerised allylamine
PRH	Primary rat hepatocytes
rpm	Revolutions per minute
SD	Standard deviation
SEM	Scanning electron microscopy
sem	Standard error of the mean
T_3	Triiodotyronine
T_4	Thyroxin

TBS	Tris buffered saline
3-D	Three-dimensional
TMB	3,3',5,5'-Tetramethylbenzidine
U	Unit
UV	Ultraviolet
v/v	Volume in volume
VLDL	Very low density lipoproteins
W	Watt
w	Width
w/v	Weight in volume
XPS	X-ray photoelectron spectroscopy

Chapter One

General Introduction

1.1 Introduction

The liver is the largest gland in the human body. It weighs about 1.5 kg in the adult constituting 2% of the body weight. The liver is located in the right upper quadrant of the abdominal cavity, in contact with the diaphragm. It is anatomically divided into two lobes, right lobe and left lobe, by the falciform ligament. Each lobe is subdivided into two smaller lobes. The subdivision of the organ into circulatory sectors and segments is currently employed in hepatobiliary surgery. Hepatic lobules are the smallest grossly visible units of the liver. They comprise various cell types forming curved sheets of cells enfolding different cavities. The lobules are surrounded by a network of connective tissue and numerous inputs, including blood vessels, nerves, bile ducts and lymphatic vessels.

This complex structure of the organ is vital for its diverse functions and the survival of the organism. These roles include: 1) Metabolism and storage of the nutrients (carbohydrates, proteins and lipids) received from the gastro-intestinal tract after absorption. This makes the liver responsible for the preservation of the organism's energy supply. 2) Detoxification or degradation of endogenous and exogenous substances including body wastes and drugs. This permits their removal by the bile or the urinary tract. 3) Synthesis of a mixture of plasma proteins such as albumin, clotting factors and transferrin. The liver may also contribute to their degradation. 4)

Participate in the maintenance of systemic hormone levels by degrading most hormones and releasing some humoral factors. 5) Storage of iron, vitamins and the activation of vitamin D with the participation of the kidneys. 6) Liver macrophages play a role in immune surveillance particularly towards bacteria (Sasse *et al.*, 1992; Desmet, 1994; Jones, 1996).

All the cells in the liver participate in the accomplishment of the previous functions. This is carried out under the control of the autonomic nervous system, the circulating hormones and the concentration of the target substrate in the blood. Any defect in the system can result in an abnormal state leading to disease conditions that can be fatal. Thus, understanding the unique organisation of the liver, its functions and its interactions with the other parts of the organism in both normal and pathological states is essential.

The complexity of this organ renders research in this area intricate and challenging. The liver has been studied for many years and various aspects of the liver structure and function have been identified and characterised. However, there is still lack in the understanding of this organ that makes replicating it in an *in-vitro* liver model difficult. Various attempts at this have been undertaken and numerous liver models have been developed with an improved functionality to the conventional 2-D mono-culture of hepatocytes. These models exploited different properties of the liver including extra-cellular matrix, various liver cells and fluidics (Allen and Bhatia, 2003; Powers *et al.*, 2002). Developing a liver model has two main applications and these are *in-vitro* toxicity studies during drug development and artificial organ transplant or external liver support system.

In this chapter, the available literature around the liver, culture of liver cells *in-vitro,* and the *in-vitro* liver models is reviewed. First, the structural and functional zonation of the liver will be examined. Secondly, the challenges hindering the study of liver tissue *in-vitro* will be discussed. The final section will cover the available *in-vitro* liver models, the basis behind their development, their advantages and disadvantages.

1.2 The Liver

1.2.1 Structural Units of the Liver

Over the years, various units relating the structure and function of the liver have been defined and recognised. These are the classic lobule, the portal lobule, the primary lobule, the acinus and the choleon.

The classical lobule was first described by Kiernan and it consists of the hexagonal structure of liver cells with central vein and six portal triads at the vertices (Figure 1.1, Figure 1.2) (Rappaport *et al.,* 1954; Rappaport, 1958). The size of each lobule is approximately 0.7 x 2 mm (Jones, 1996). The classical lobule architecture is clearly observed in certain species, including pigs, whose livers contain thick bands of connective tissue bordering the lobules (Figure 1.1). This model appears to be incomplete and difficult to identify in man. However, the visualisation of the central vein and hepatic triads improves the identification of approximate borders and boundaries (Desmet, 1994; Jones, 1996). The blood from the portal triads enters intralobular structures, called sinusoids, and drains towards the central vein. During this period, the parenchymal cells and the blood stream exchange various substances (Desmet, 1994; Jones, 1996).

(a)

(b)

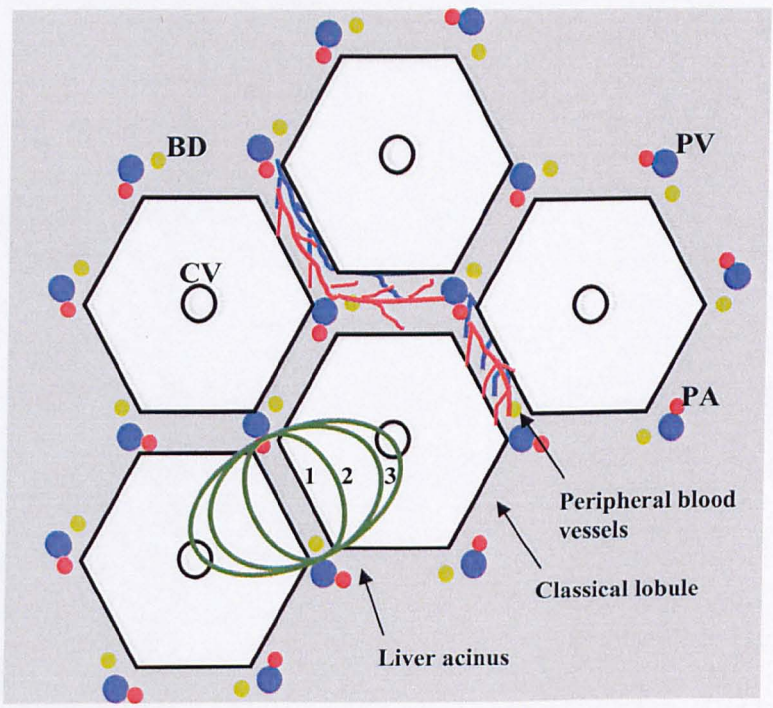

Figure 1.1 **(a)** Section in pig liver showing the lobulisation in the liver (http://www.udel.edu/biology/Wags/histopage/colorpage/clg/clgllp.GIF) (Parikh 2004). **(b)** Schematic diagram representing the structure of the liver and its functional units. The acinus and the classical lobule are the most recognized functional and structural units of the liver (CV: central vein, PV: portal vein, PA: portal artery, BD: bile duct, 1: zone 1, 2: zone 2, 3: zone 3).

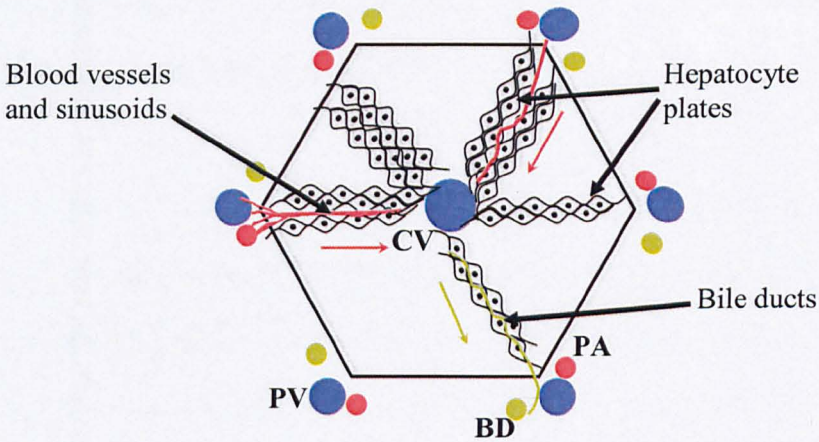

Figure 1.2 Schematic diagram of the liver lobule and the hepatocyte plates CV: central vein, PV: portal vein, PA: portal artery, BD: bile duct).

The portal lobule was proposed by Mall at the beginning of the twentieth century (Rappaport *et al,* 1954). This model is based on the portal triads forming the centre of the unit and the central veins on the peripheries.

The primary lobule is a way of refining the structure of the classical lobule. The unit consists of the cone-shaped structure of liver tissue produced by two neighbouring portal venules (Desmet, 1994; Saxena *et al.,* 1999). Every six to eight single units assemble to form the classical lobule.

The acinus is the region of the parenchyma that surrounds the blood supply from the peripheral afferent vessels and draining in to the central vein (Figure 1.1) (Rappaport *et al.,* 1954; Rappaport, 1958). The acinus is frequently described as having 3 zones, reflecting parts of the parenchyma that receive sinusoidal blood of different properties (Figure 1.1.). The periportal zone (zone 1) is located around the portal triads and afferent vessels, and the perivenous (pericentral or centriolobular) zone located near the central vein (zone 3). The cells in zone 1 receive blood that is high in nutrients and oxygen, whereas the cells in zone 3 receive blood that is much lower in nutrients and oxygen. These regions can be further subdivided into several parts depending on the criteria used. For example, the proximal and distal subdivision of the each zone was described in relation to enzyme expression as some enzymes are only expressed in the first or last quarter of the acinus (Jungermann and Kietzmann, 1996). An intermediate zone, zone 2, is described between the periportal (zone 1) and the centriolobular (zone 3) zones (Figure 1.1.) (Rappaport *et al.,* 1954). The cells in zone 1 are first to regenerate and last to endure necrosis, while the cells that

receive much poorer blood (zone 3) are less resistant to hepatotoxins and damage (Jones, 1996).

The choleon describes the bile secretory function of the liver. The unit consists of the bile canalicli and the biliary ductules.

1.2.2 Composition of the Liver

The different constituents of the liver are described in this section. These are the parenchymal and non-parenchymal liver cells, the extracellular matrix, blood, lymph, nerve, bile supplies.

a) Parenchymal Cells: Hepatocytes

Hepatocytes are the predominant cellular component of the liver. They constitute 80% of its volume and 60% of its total cell number (Daoust, 1958). They are large polyhedral cells arranged in curved wall-like structures (muralium) of anastomosing plates around the lacunae. The lacunar region contains sinusoids that mix and carry the blood from the portal veins and arteries to be drained in the central vein. On the basolateral surface, the hepatocytes are in contact with sinusoids, while they face their adjacent hepatocytes on the apical surface and form bile canaliculi. The lacunar space does not communicate freely with the interlobular region due to the presence of a limiting plate of hepatocytes surrounding the lobule. The plate forms a nearly continuous barrier with fenestrations to allow the passage of small branches of veins, arteries and bile ducts.

Hepatocytes are highly active cells and contain various organelles including nuclei, mitochondria, lysosomes, Golgi apparatus, endoplasmic reticulum, cytoskeletal structures (Sasse *et al.*, 1992; Desmet, 1994; Jones, 1996)

The hepatocytes are polarised parenchymal cells with three morphologically distinctive membrane domains, sinusoidal, intercellular and bile canalicular, that take part in diverse functions. The sinusoidal domain constitutes 37% of the total cell surface and links hepatocytes indirectly with hepatic endothelial cells (Weibel *et al.*, 1969). The two types of cells are separated by the space of Disse which contains fluid and matrix components (plasma and collagen types I, III, IV and V: reticular network) (Horn *et al.*, 1986; Sasse *et al.*, 1992; Jones, 1996). The main characteristic of the hepatocytes in this region is the microvilli and the presence of proteins including pumps (sodium pump), carrier-mediate transport complexes, and receptors (e.g. hormone receptors, immunoglobulin A) which are involved in hepatocyte-bloodstream exchange (Nathanson and Boyer, 1991; Volpes *et al.*, 1991). The intercellular domain connects the hepatocytes with their neighbouring hepatocytes. It is the largest domain constituting half the total surface area of the cells (Weibel *et al.*, 1969). In this domain the cells attach and communicate via a range of junctional complexes, including tight junctions, intermediate junctions, desmosomes and gap junctions (Desmet, 1987). The bile canalicular is the apical region of the hepatocellular membrane and contains tight junctions which form the canalicusinusoidal barrier and separate the bile from the blood stream (Desmet, 1987).

Hepatocytes contain large nuclei that are usually spherical of different sizes. Liver cells are mostly multinucleated with different ploidy classes. These properties vary and they depend on the species of interest, their age, their mitotic activity, their endocrine regulation, and their spatial distribution within the liver. With regards to the spatial distribution of parenchymal cells in rat liver, in the perivenous zone the layer of cells adjacent to the terminal hepatic venule contain a higher percentage of binucleated cells comparing to the rest of the zone (Geller, 1965). In the portal zone, binucleated cells with diploid nuclei are abundant. In the intermediate zone, tetraploid and octoploid nuclei containing cells can be observed (Geller, 1965; Hildebrand and Karcher, 1984).

Various studies of different organelles of the hepatocyte in different species revealed a pattern of diversity in their distribution along the acinus. These include mitochondria, lysosomes, smooth and rough endoplasmic reticulum, Golgi complex and cytoskeletal structures. The distribution of these organelles in the hepatocytes of the various regions of the acinus has been found to be linked to the distribution of hepatocyte functionality.

b) Sinusoidal Liver Endothelia

Liver endothelial cells measure 130 μm^3 and are equally spread throughout the parenchyma (Sasse *et al.*, 1992). The cells are largely flat with the nuclei projecting into the sinusoids (Horn *et al.*, 1986; Sasse *et al.*, 1992). They are characterised by sieve plates of grouped fenestrations. The fenestrations allow the exchange of blood substances between the bloodstream and the perisinusoidal space. The fenestrae can be larger in the periportal region compared to the centriolobular area (Jones, 1996).

However, they are more numerous in the perivenous area leading to a larger filtering capacity (Bouwens *et al.,* 1992; Burt *et al.,* 1993). Substances of varying sizes, including macromolecules, can access the space of Disse via the fenestrae. Despite being different from normal endothelial cells, sinusoidal endothelial cells have similar functions that include participating in active transport, coagulation, fibrinolysis, inflammation, immune responses, regulation of blood pressure, angiogenesis, lipid metabolism and synthesis of stromal components (Yokota, 1985; Rieder *et al.,* 1992).

c) Kupffer Cells

Kupffer cells are liver macrophages and represent the largest group of fixed macrophages. They are specialised in the phagocytosis of large particles within the range 0.1-0.8 μm (Sasse *et al.,* 1992). These cells measure 250 μm^3 and they are not evenly distributed in the parenchyma as they are predominant in the portal zone (Sasse *et al.,* 1992). Moreover, they are commonly seen at the sites of sinusoidal branching where they protect the region (Jones, 1996). Kupffer cells are a part of the endothelial lining having most of their surface area facing the blood stream in the sinusoids (Sasse *et al.,* 1992). However, these cells are highly mobile and can travel to reach the space of Disse or separate from the endothelial layer and travel along the lumen (MacPhee *et al.,* 1992; Sasse *et al.,* 1992). The cells contain a rich cytoplasm with various organelles permitting the completion of their phagocytotic and digestive functions and the production of proteases, lymphokines and prostaglandins (Wardle, 1987; Sasse *et al.,* 1992; Desmet, 1994) .

d) Stellates (Fat Storing Cells, Perisinusoidal Cells, Ito Cells)

Stellates are situated in the perisinusoidal space with cytoplasmic extensions enveloped by the endothelial lining. Their main function is the metabolism and the storage of lipids and vitamin A. 25.3% of their volume represents fat content in normal rat liver (Sasse *et al.,* 1992). However, this can vary in different regions of the liver and in abnormal states. Stellates in the perivenous zone, for example, contain very low quantity of fat droplets and have been described as empty fat storing cells (Yokota, 1985; MacPhee *et al.,* 1992). In this area of the lobule Stellates are less abundant than in the periportal region (Jungermann and Kietzmann, 1996). These cells are able to contract and therefore, can regulate the width of the sinusoidal lumen and the blood flow (Wisse *et al.,* 1991; Pinzani *et al.,* 1992; Sasse *et al.,* 1992). Their contractile features are calcium-dependent and may be the outcome of the contraction of their actin filaments (Wisse *et al.,* 1991; Pinzani *et al.,* 1992). Observations of Stellates in fibrogenesis lead to the suggestion that they may play the role of resting fibroblasts being activated in abnormal conditions to participate in intralobular fibrogenesis (Geerts *et al.,* 1990; Sasse *et al.,* 1992). This is enforced by their capability to synthesise connective tissue components, including collagen types I, III, and IV. Moreover, transitional forms, between lipocytes and fibroblasts, of cells can be observed (Jones, 1996).

e) Pit Cells

They are large granular lymphocytes derived from the peripheral blood. They possess natural killer activity and therefore, are the defensive element of the liver against viral infection and tumour metastasis (Sasse *et al.,* 1992; Desmet, 1994; Jones, 1996). Pit cells are more numerous in the periportal zone than in the

centriolobular region (Bouwens *et al.*, 1992; Burt *et al.*, 1993). This may contribute to difference in the sensitivity between the periportal and centriolobular to tumour cells and damage.

f) Connective Tissue

The liver is encapsulated within a thin connective tissue (Glisson's capsule) that propagates to the internal spaces of the organ. This is covered with a single layer of flat peritoneal mesothelial cells on the outer of the organ. The capsule is present on the entire surface of the liver and it is thickest around the inferior vena cava and at the porta hepatis (Jones, 1996). Although the size of the connective tissue in healthy human liver is small, it represents a key element in the structure of the organ. It is the supporting framework of the internal parenchyma that holds all the structures together and divides the liver into lobules (Jones, 1996). In addition, the connective tissue ensheaths most of the vessels and nerves and therefore, secures their pathway (Jones, 1996).

The portal canal (portal area or portal space) is the connective tissue that lies in the interlobular space. It can vary in size depending on its position in the branching of veins, arteries and bile ducts. The stroma is the connective tissue that ensheaths the hepatic artery, the portal vein, the bile duct, the lymphatic vessels and the nerves in the interior of the liver (Jones, 1996).

The composition of the connective tissue differs along the lobule with respect to the type of collagen and adhesion proteins. This can alter the communication between the cells and consequently affects their functions. In the periportal zone, collagen

types IV and V and the major adhesion protein laminin dominate, whereas, in the centriolobular zone, collagen types I, III, and VI and the adhesion protein fibronectin dominate (Reid *et al.*, 1992).

g) Blood Supply

The liver is the only organ to receive two different blood supplies (Figure 1.3). It is supplied with fresh oxygenated blood through the hepatic artery and this consists of approximately 25% of the afferent blood volume (Figure 1.3). The arterial hepatic vessels branch from the celiac trunk and enter the liver, ensheated in connective tissue stroma, at the hepatic porta. The other 75% of the blood entering the liver is venous blood from the portal vein. This blood is rich in nutrients and chemicals but poor in oxygen (Figure 1.3). Unlike other organs, the majority of afferent blood in the liver is venous gathered from the gastrointestinal tract for metabolism. This makes the liver the organ responsible for first pass metabolism and the selection of the substances penetrating the circulation (Jones, 1996).

The hepatic portal vein and artery lie together with the bile duct in the liver, forming the portal triads seen under the microscope in the classical lobule. In this, the blood vessels branch to form terminal portal arterioles and venules that run along the peripheral region of the classical lobule. In the intralobular space, the blood from arteries and veins is mixed in the sinusoids to facilitate the exchange between the blood stream and the parenchymal cells (Jones, 1996).

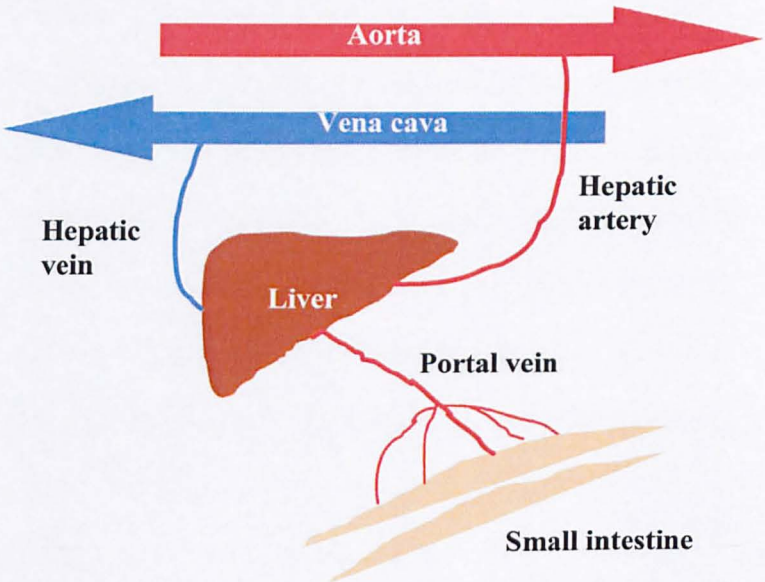

Figure 1.3 Schematic diagram illustrating the blood supply to the liver.

h) Biliary System

Bile travels in the opposite direction to the afferent blood (Jones, 1996). It collects in the bile canaliculi that are located at the apical surfaces of adjacent hepatocytes. The bile then moves down in these structures via the different zones of the lobule from the zone 3 at the centriolobular region to zone 1 at the portal triad. Various techniques, including quantitative electron microscopy and light microscopy, showed that the size of the biliary space of the bile canaliculi increases from the central to the portal region (McIndoe, 1928; Jones *et al.,* 1976). After that, the bile crosses the limiting plate via the small terminal bile ductules that are also called the canal of Hering. The canals of Hering lead to larger bile ductules in the periphery of the classical lobule and these are linked to the terminal bile ducts (Jones, 1996).

i) Lymphatic System

The most accepted theory is that the formation of lymph in the liver occurs primarily in the space of Disse (Niiro and O'morchoe, 1986; Yamamoto and Philips, 1986; Jones, 1996; Saxena *et al.,* 1999). The lymph is composed of plasma filtered from the sinusoidal blood stream. The hepatic lymph travels down to occupy the periportal space of Mall. This is the area in between the portal connective tissue and the limiting plate. At this location the lymph diffuses through the space of Mall and the connective tissue to enter the portal lymphatic capillaries. The liver has other lymphatics which include the superficial loose plexus of lymphatic vessels that surrounds the organ beneath the capsule, the lymphatic capillary plexus lying next to the portal vein, artery and bile ducts of the triads.

j) Nerve Supply

The human liver is innervated by a predominating sympathetic system, and parasympathetic nerves (Amenta *et al.*, 1981; Jones, 1996; Saxena *et al.*, 1999). The sympathetic system forms a rich perivascular plexus of adrenergic nerve fibres around the blood vessels. From this location, the nerve fibres branch to supply the lobule via the sinusoids. These branches generate small terminal branches that supply perisinusoidal cells and hepatocytes. Parasympathetic (cholinergic) system, on the other hand, has little presence around the sinusoids and hepatocytes. It innervates intrahepatic and extrahepatic branches of the portal vein, hepatic artery and hepatic vein.

The blood and nerve supplies might modulate the roles of the parenchyma affecting their distribution in the lobule. Afferent nerves carry information from the central nervous system to regulate the function of the liver, while the blood transport oxygen, humoral factors and various substrates to the liver.

1.2.3 Liver Function and its Distribution

Currently, the central lobule, the acinus and their subdivisions are the most recognised regions of the liver. The zones of the acinus differ in their composition, enzymes produced and metabolic pathways carried out resulting in the description of metabolic zonation of the parenchyma (Table 1.1) (Jungermann and Katz, 1989; Gebhardt, 1992; Jungermann and Kietzmann, 1996).

Periportal zone		Perivenous zone	
Metabolism	Enzyme or protein involved	Metabolism	Enzyme or protein involved
General metabolism		General metabolism	
• Oxidative enzyme metabolism	Succinate dehydrogenase	• Glycolysis	Glucokinase
• Fatty acid oxidation	β-Hydroxybutyryl-CoA dehydrogenase	• Lipogenesis	Fatty acid synthase
• Gluconeogenesis	Glucose-6-phosphatase		
• Cholesterol synthesis	Hydroxymethylglutaryl-CoA reductase		
• Ureagenesis	Carbamoyl phosphate synthetase		
Drug metabolism		Drug metabolism	
• Bile acid production		• Monoxygenation	Cytochrome P450
• Glutathione peroxidation	Glutathione peroxidise	• Glutathione conjugation	
		• Glucuronidation	UDP-glucuronosyl transferase

Table 1.1 Zonation of metabolic functions and the related enzymes.

a) Carbohydrate Metabolism

Glucose is the major energy source in humans and the liver has the crucial role of maintaining its availability and concentration in the bloodstream. For this purpose, the liver stores surplus glucose to release it when necessary. In humans, a considerable quantity of glucose absorbed during meals is taken up by the liver where it is either used in glycogen synthesis or degraded to pyruvate. During fast periods, the liver maintains the glucose levels by glycogenolysis and gluconeogenesis from lactate, amino acids and glycerol (Jungermann and Katz, 1989; Jungermann and Kietzmann, 1996).

Figure 1.4 summarises the distribution of the pathways of carbohydrate metabolism in the liver. In the absorptive phase after meals, perivenous cells take up most glucose and use it to synthesise glycogen in order to replenish glycogen stores. When the stores approach saturation, glucose is degraded to lactate that is transported in the circulation to the periportal zone. Lactate is used in the periportal region for the synthesis of glycogen via gluconeogenesis. Observations in rats at the end of the absorptive state revealed the presence of glycogen in all hepatocytes with a minor predominance in the periportal region. This slight predominance is reversed in the postabsorptive phase (between meals) because glycogen is degraded at a faster rate in the periportal zone. This leads to larger glycogen stores remaining in the centriolobular region for a longer period. During the postabsorptive phase, glycogen is degraded in the periportal zone to glucose. Later, it is degraded in the centriolobular zone to lactate which recirculates to the periportal region for consumption in gluconeogenesis.

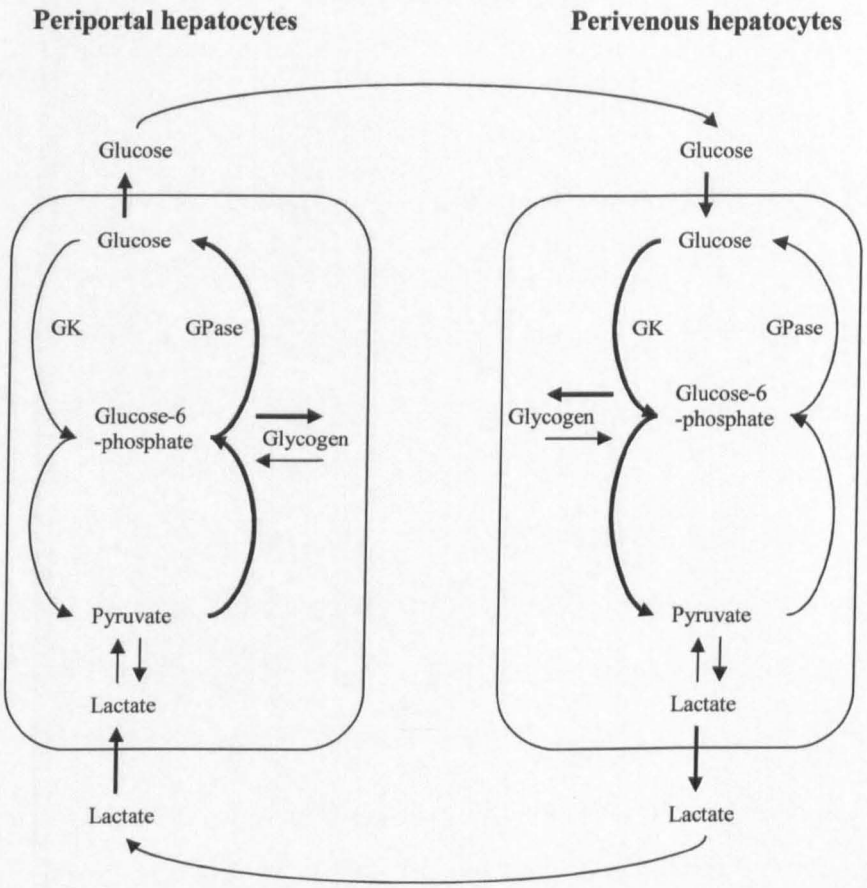

Figure 1.4 Schematic diagram demonstrating the distribution of carbohydrate metabolism in hepatocytes. Lactate generation is highest in the perivenous hepatocytes, while gluconeogenesis from lactate predominates in periportal hepatocytes (The thickness of the arrows represent the predominance of the pathway, GK is glucokinase and GPase is glucose-6-phosphatase; adapted from Radziuk and Pye, 2001).

This dynamic concept is currently accepted to occur in most mammals (Jungermann and Katz, 1989; Gebhardt, 1992; Jungermann and Kietzmann, 1996; Radziuk and Pye, 2001).

The exact pathway by which glycogen is synthesised has not been identified until recently. Unlike muscle, the liver synthesises glycogen through the indirect conversion of glucose to pyruvate and lactate and finally to glycogen (Jungermann and Kietzmann, 1996).

The pathways of both degradation and oxidative energy metabolism, which are involved in gluconeogenesis, predominate in the periportal region because it has a higher capacity of activity of the enzymes involved, including β-hydroxybutyryl-CoA dehydrogenase, alanine aminotransferase, succinate dehydrogenase, malate dehydrogenase and cytochrome oxidase. The aerobic requirement of oxidative energy metabolism is well supported in the periportal zone as cells there receive higher levels of oxygen than those of the pericentral zone. Conversely, hepatocytes of the pericentral region are poor in oxygen and contain a higher quantity and activity of enzymes mediating glycolysis compared to the periportal zone. Glycolysis is a less aerobic process that can occur in the absence of oxygen and requires the activity of glucokinase and pyruvate kinase (Jungermann and Katz, 1989; Gebhardt, 1992; Jungermann and Kietzmann, 1996; Radziuk and Pye, 2001). When the effects of oxygen levels on carbohydrate metabolism were studied in rat hepatocyte cultures, physiological oxygen levels in both periportal and perivenous hepatocytes were essential for an efficient carbohydrate processing (Jungermann and Kietzmann, 1997; Jungermann and Kietzmann, 2000).

b) Lipid Metabolism

The liver receives fatty acids directly from the small intestine via the circulation, but it can also synthesise fatty acids from various substrates, including glucose and ethanol. Fatty acids are produced in the skeletal muscle and adipose tissue from the hydrolysis of chylomicron triglycerides in the presence of lipoprotein lipases. A considerable quantity of dietary fat is stored in the adipose tissue, in the form of triglycerides, and released when required as an energy source. In the early postabsorptive state, fatty acids are released from the adipose tissue to generate energy via β-oxidation. During starvation and exercise, the rate of fatty acids release from the adipose tissue increases to synthesise ketone bodies, which are essential alternative energy source for tissues particularly the brain. In the liver, fatty acids react with glycerol to synthesise triglycerides which are exported in the form of very low-density lipoproteins (VLDL), or pre-β-lipoproteins. The zonation of these functions is less apparent than carbohydrate metabolism. The perivenous zone is specialised in the synthesis of VLDL during the absorptive phase, while the periportal region favours β-oxidation and ketogenesis during the postabsorptive state (Table 3.1) (Jungermann and Katz, 1989; Gebhardt, 1992; Jungermann and Kietzmann, 1996; Radziuk and Pye, 2001).

The metabolism of glucose, ethanol, amino acids and lactate generates acetyl-CoA, the basic structure in the *de- novo* synthesis of fatty acids. Most enzymes involved in this pathway are more active in the perivenous zone creating a dominance of *de novo* fatty acids synthesis in this area (Table 3.1). Examples of these enzymes include ATP citrate lyase, acetyl-CoA carboxylase, and fatty acid synthase. However, this distribution was found to differ between sexes when studied in rats (Jungermann and

Katz, 1989; Gebhardt, 1992; Jungermann and Kietzmann, 1996; Radziuk and Pye, 2001). In addition, the liver synthesises and secretes cholesterol into the bloodstream. This activity occurs mostly in the periportal zone where the participating enzymes are more active and bile acid secretion is highest (Jungermann and Katz, 1989; Gebhardt, 1992; Jungermann and Kietzmann, 1996; Radziuk and Pye, 2001).

c) Amino Acids Metabolism

Amino acids are recycled in the body and protein degradation can replenish most amino acids stores. Dietary amino acids are used in energy generation daily. The main two waste products of amino acid metabolism are carbon dioxide and ammonia. The liver eliminates ammonia by the synthesis of urea or conversion into glutamine. Glutamine synthesis occurs in the perivenous cells where hepatocytes are rich in catalytic enzymes, including glutamine synthetase. Glutamine synthetase mediates the incorporation of ammonia and glutamate to produce glutamine. Urea formation is predominant in the periportal area (Table 1.1) where glutamine carbon is used in glucose synthesis and nitrogen is used in the urea production. The major enzymes involved in this pathway, including carbamoylphosphate synthetase, ornithine carbamoyl transferase, arginine succinate synthetase and arginase, are highest in the periportal and proximal perivenous zones (zone 2) (Jungermann and Katz, 1989; Gebhardt, 1992; Jungermann and Kietzmann, 1996; Tsiaoussis *et al.*, 2001; Newsholme *et al.*, 2003).

d) Xenobiotic Metabolism

Xenobiotics are degraded via two-phase pathways generating excretable products. Phase 1 is the oxidation of the substrate which is catalysed by cytochrome P450

enzymes. The product of this phase enters phase 2 reactions and these are conjugation reactions with glucuronic, or sulphuric acid, or glutathione. Studies have revealed that the oxygenation reactions are preferentially located in the centriolobular region where the glucuronic conjugation is commonest, while the sulphuric conjugation predominates in the periportal zone (Table 1.1). However, there is a contradicting data about the distribution of glutathione conjugation because the quantity of glutathione is highest in the periportal zone, whereas the activity of the enzymes participating in the conjugation, including glutathione-S-transferase of types E, B, and C, is highest in the perivenous area (Jungermann and Katz, 1989; Gebhardt, 1992; Jungermann and Kietzmann, 1996; Tsiaoussis *et al.,* 2001; Newsholme *et al.,* 2003).

This distribution of activities can change due to induction after xenobiotic exposure. Examples of this include the dose dependent effects of phenobarital. Phenobarbital induces the production of cytochrome P450 2B form at both moderate and high doses. However, the location of the expression along the acinus depends on the dose. At moderate doses, the cytochrome P450 2B is observed in the perivenous region only, whereas at large doses the expression of the enzymes is extended to the periportal region as well (Bars *et al.,* 1989).

e) Protective Metabolism

Metabolism of natural substrates or exogenous substances can generate toxic metabolites. The degradation of various xenobiotics (e.g. bromobenzene) produces electrophiles through cytochrome P450 side reaction. These electrophiles increase the synthesis of reactive oxygen species that are the main cause of hepatotoxic

necrosis. P450 isoenzymes predominate in the centriolobular region and therefore the reactive oxygen species, including hydrogen superoxide, superoxide radical anion and hydroperoxidase, are commonest in these hepatocytes. The detoxification pathway consists of reduction by glutathione peroxidase which predominates in the perioportal zone together with glutathione leading in to a more sensitive perivenous zone (Jungermann and Kietzmann, 1996; Lindros, 1997). Moreover, chronic drug exposure contributes to the vulnerability of perivenous hepatocytes because many drugs induce the expression of different forms of cytochrome P450 enzymes. This provokes an imbalance between phase 1 and phase 2 detoxifying enzymes resulting in cell damage (Lindros, 1997). Although necrosis is frequently observed in the centriolobular region, necrosis in the periportal zone can be predominant with some hepatotoxins, including allyl alcohol (Lindros, 1997). The problem in this situation is the high efficiency by which the periportal hepatocytes take up allyl alcohol and convert it by alcohol dehydrogenase into aldehyde acrolein, a toxic compound. Aldehyde acrolein is eliminated through glutathione conjugation, but after the depletion of glutathione in the periportal hepatocytes it attacks macromolecules and causes cellular damage.

f) Bile Synthesis

There are two mechanisms by which hepatocytes accumulate bile acids and release them into the biliary system. The first one is the *de novo* synthesis of bile acids (bile-salt independent) from cholesterol. The second mechanism is the uptake of bile acids from the gastrointestinal tract (bile-salt dependent) via the portal vein and secreting them to the bile. The volume of areas rich in Golgi complexes and canaliculi, and the quantity of canalicular ATPase are higher in the periportal zone than in the

perivenous. These participate in the circulation of bile acids and therefore, indicate the predominance of bile cycling in the periportal zone of the liver (Jones *et al.*, 1978). Both the uptake of bile acids from the blood and their modification and secretion is concentrated in the periportal region (Jungermann and Katz, 1989; Gebhardt, 1992; Fitz, 1996; Jungermann and Kietzmann, 1996). The *de novo* synthesis of bile acids from preformed cholesterol and its secretion predominate in the perivenous area because many enzymes involved (e.g. cholesterol 7α-hydroxylase) dominate in this zone and the damage of this zone lead to a significant decrease in bile flow. Moreover, cells in the prerivenous area have been described as a reservoirs which can be activated during periportal damage to contribute to bile-salt dependent synthesis (Jungermann and Katz, 1989; Kanno *et al.*, 2000).

g) Gene Expression

Expressing the right genes at the right time is crucial for the hepatocytes to function. The zonation of gene expression in hepatocytes can be classified into gradient versus compartment zonation or dynamic versus stable zonation. Gradient versus compartment zonation of gene expression have been shown, indicating either a gradient of distribution along the sinusoids or restriction to one region only. Examples of this type include gene expressing glucokinase (gradient) and glutamine synthetase (compartment). Dynamic versus stable zonation represents the genes that adapt to certain conditions and others which remain stable despite the changes in the environment. For illustration, tyrosine aminotransferase expression is dynamic, whereas glutathione synthetase expression is stable (Gebhardt, 1992; Christoffels *et al.*, 1999).

Hormones and drugs are the main factors that affect gene expression in hepatocytes (Oinonen *et al.*, 1996). For illustration, pituitary-dependent hormones are involved in the zonation of certain cytochrome P450 genes.

1.2.4 Sinusoidal Gradient

The sinusoids carry blood in the liver and supply various chemicals to liver cells. These chemical including oxygen, hormones nutrients and drugs, influence the zonation of liver function. The tension of oxygen is approximately 60 to 65 mm Hg in the periportal zone and decreases in the pericentral zone to approximately 30-35 mm Hg. Moreover, the volume of liver tissue occupied by sinusoids is lower in zone 1 and increases as blood travels along the lobule. Hepatocytes at the periportal zone are rich in oxygen and nutrients. There is another oxygen gradient between the centre of the sinusoid and the hepatocytes and their intracellular domains. This gradient drives the diffusion of oxygen into the parenchymal cells where the tension of oxygen is about 25 mm Hg.

The concentration gradients of carbon substrates, including glucose, lactate and amino acids, are shallow and their impacts on the functions of hepatocytes are probably minimal. On the other hand, some substrates and products, such as ammonia, bile acids, and ketone bodies, show a sharp concentration gradient. Different mediators produced by the liver do not have an equal distribution in the lobule. Extracellular ATP, prostaglandins, thromboxanes and leukotrienes are inactivated by the distal perivenous hepatocytes forming a concentration gradient with the periportal area.

Various hormones are degraded in the liver. Their passage within the blood along the sinusoids initiates their uptake and degradation. Thus their concentrations in the blood decrease forming a concentration gradient between the periportal and centriolobular zones (Jungermann and Kietzmann, 1996). About 50% of glucagon, noradrenaline and cortisol and 80% of adrenaline are degraded during their passage through the liver. In addition, blood insulin decreases by approximately 50% between meals and 15% after meals. Conversely, other hormones, including triiodothyronine (T_3), increase by formation. The precursor of T_3, thyroxin (T_4), decreases via deiodenation by about 40%, while T_3 increases by about 50% (Jungermann and Katz, 1989).

1.3 *In-vitro* Liver Cell Culture

1.3.1 Challenges of *In-vitro* Liver Cell Culture

Over the years, isolated primary cell cultures have been the most widely used culture method of liver cells *in-vitro*. However, under conventional techniques, the cells have limited survival of one to two weeks and express a loss of functionality (Guillouzo, 1998; LeCluyse *et al.*, 1996). The factors involved in this phenomenon are related to three stages: cell isolation, seeding and attachment.

Cell isolation is currently carried out using the two-step collagenase perfusion method developed by Seglen. The procedure isolates hepatocytes from other liver cells, ECM and other liver components and destroys the closed 3-D architecture of the organ. The cells suspended in media have a short survival time of about two hours if they are not seeded. The various solutions, buffers, supplements and the

media used in these procedures affect the survival rate and the functionality of isolated cells. Species, age, sex, liver disease and genetics are other related factors. The duration of the procedure and the handling of the animal and the liver can influence the yield and the quality of the cells (Guillouzo, 1998; LeCluyse *et al.*, 1996).

The composition of the media, the properties and the architecture of the surface onto which the cells adhere affect the survival and the functionality of hepatocytes. Matrigel and collagen type I gel have been reported to improve the survival and the functionaliy of the cells (including cytochrome P450 and albumin). This was largely attributed to the maintenance of 3-D cell morphology of the cells on the gels or in between a two layer sandwich (Griffith and Swartz, 2006; Guillouzo, 1998; LeCluyse *et al.*, 1996). When the hepatocytes are in a 2-D layer, they adapt a flat morphology and this decreases their receptor numbers which leads to a decrease in cell-cell contact and cell-soluble factor interactions. Seeding the cells on a supporting 3-D scaffold, on the other hand, has been demonstrated to maintain 3-D morphology, survival and functionality. Examples of these scaffolds include the alginate sponges which were found to improve the survival and the functionality of hepatocytes via aggregation under specific conditions (Glicklis *et al.*, 2000; Yang *et al.*, 2001)

In addition, culturing another cell type with the hepatocytes has been proven to enhance their survival and functionality. Co-cultures of primary hepatocytes with either other primary cells or cell lines, including stellates and 3T3 cells, have been described in literature (Bhandari *et al.*, 2001; Bhatia *et al.*, 1998; Thomas *et al.*, 2005). The co-cultures can have the same forms as mono-cultures including

heterogeneous 2-D layers, heterogeneous cell aggregates, heterogenous cells in gel sandwiches, heterogeneous cells entrapped in natural or synthetic biodegradable polymers (Bader *et al.*, 1996; Bhatia *et al*, 1999; Griffith and Swartz, 2006; Guillouzo, 1998; LeCluyse *et al.*, 1996; Toh *et al.*, 2005). Zinchenko and co-workers cultured primary rat hepatocytes and kupffer cells onto micropatterned surfaces and demonstrated a superior functionality to mono-culture during a 10 day period (Zinchenko *et al.*, 2006).

Currently, the interest in these 3-D heterogeneous cell culture techniques is high and improving their performance and reliability is important for future *in-vitro* and *in-vivo* studies. These models, however, lack the sophisticated liver structures and have limitations in nutrients and oxygen transport into the cells. Recently and with the advances in microtechnologies and microfluidics, more promising liver models are being explored.

1.3.2 *In-vitro* Fluidic Liver Models

a) Flat Membrane Bioreactor

The flat membrane bioreactor (FMB) was developed by Bader and colleagues to clinically support patients with acute liver failure until they receive appropriate surgery and fully recover. Therefore, the FMB should perform various liver functions to support the patient's failed liver (Bader *et al.*, 2000; Langsch and Bader, 2001).

The bioreactor consisted of a polycarbonate plate covered with gas-permeable membrane in which primary pig hepatocytes and non-parenchymal cells (NPCs)

were cultured in a sandwich configuration. There were connections, at the sides of the plate, which allowed continuous perfusion of the media. To increase the number of cells seeded to the bioreactor, seven stackable gas-permeable membrane modules were used. The performance of hepatocytes in this liver model was assessed for various liver functions including albumin secretion (ELISA), ammonia elimination (L-glutamate dehydrogenase assay) and urea synthesis (enzymatic urease method), diazepam biotransformation (HPLC) and detection of phase I and phase II biotransformation enzymes using 7-Ethoxyresorufin-O-Deethylation (EROD) assay, 7-Ethoxycumarin-O-Deethylation (ECOD) assay, UDP-Glucuronosyltransferation (UGT) assay and Sulfotransferation (ST) assay in the presence and absence of different inducers including phenobarbital, 3-methylcholanthrene, clofibrate, isoniazid and rifampicin (Bader *et al.*, 2000; Langsch and Bader, 2001).

Pig primary hepatocytes in the single FMB model were able to perform basic and induced phase I and phase II metabolism for 2 to 3 weeks. The multi-plate bioreactor could hold as many cells as needed without affecting oxygen supply and cells specific functions, such as albumin secretion, were similar to *in-vivo* levels. Diazepam was metabolised in the multi-plate bioreactor to the same metabolites obtained in *in-vivo* humans and high levels of ammonia were eliminated resulting in high urea secretions (Bader *et al.*, 2000; Langsch and Bader, 2001).

b) Flat-plate Bioreactor

Several groups studied liver cells in the flat-plate bioreactor. Tilles and associates investigated the effects of oxygen and shear stress on hepatocytes in the flat-plate bioreactor in both mono- and co-cultures with 3T3 cells. Their goal was to optimise

the flat-plate bioreactor to offer a potential bioartificial liver device for clinical hepatology. The flat-plate bioreactor was constructed from a glass slide that was pre-coated with collagen gel. The final dimensions of the cell culture chamber were 25 mm (width), 75 mm (length), 85-500 μm (height). The main finding of their research was the importance of oxygen in a fluidic system for maintaining primary rat hepatocyte viability along the channel. Their work also highlighted the detrimental effects of shear stress on cell viability and functionality (Tilles *et al.*, 2001). This investigation was fundamental for the future applications of the flat-plate bioreactor. The effects of shear stress on hepatocytes were found to be reduced when a grooved substrate was used instead of the flat-plate. In addition, the grooved surface facilitated a more organised culture of two cell types (Park *et al.*, 2005).

The flat-plate bioreactor designed by Bhatia's group was employed to investigate the effects of oxygen gradient on the zonation of cell function. Their bioreactor consisted of a microscope slide (38 × 75 mm) placed in a bioreactor block which was designed with inlets (attached to syringe pump) and outlets for media transport. The microscope slide was secured in position using silicone lubricant and a stainless steel bracket with 6 screws. The final dimensions of the media containing compartment of the chamber were approximately 28 mm (w) × 55 mm (L) × 100 μm (H). Primary rat hepatocytes or co-cultures of primary rat hepatocytes and 3T3 fibroblasts were cultured on glass slide which was coated with collagen type I. The slide was introduced into the bioreactor circuits 1 to 7 days after cell isolation. Flow rates and oxygen concentrations were optimised in order to achieve adequate perfusion and physiological oxygen gradient and prevent damaging fluid shear effects (Allen and Bhatia, 2003, Allen *et al.*, 2005).

Hepatocyte function and toxicity in the flat plate bioreactor was assessed and compared to conventional hepatocyte monolayer and to *in-vivo* liver. The activation of glucagons-dependent PEPCK gene was affected by oxygen gradient in hepatocyte only cultures in the flat plate bioreactor. It showed similar distribution to *in-vivo* liver where it was highest near the inlet (periportal) and lowest in the outlet region (pericentral). The induction of cytochrome P450 CYP2B by Phenobarbital in hepatocytes and co-cultures also demonstrated hetergenous distribution similar to *in-vivo* liver. These patterns of gene expression distributions were primarily mediated by physiologic oxygen gradients and were absent in when supraphysiologic oxygen gradients were applied. Other factors including nutrients and hormone gradients can influence this zonation and this was demonstrated by changes in CYP2B and CYP3A induction by phenobarbital in the co-cultures when dexamethasone and EGF were added. The toxicity of acetaminophen in both hepatocytes and co-cultures was studied in the flat plat bioreactor and was localised to the outlet region which is similar to the centrilobular damage seen *in-vivo*. However the concentration used to achieve this was (15 mM) lower than the concentration needed (20 mM) to cause moderate toxicity in static monolayer cultures. The mechanism of acetaminophen-induced toxicity in the flat plate bioreactor was not investigated but it was thought to be similar to *in-vivo* toxicity, which is attributed to an increase in reactive intermediates and a decrease in glutathione and oxygen levels in this region (Allen and Bhatia, 2003, Allen *et al.*, 2005). This illustrated that the flat plate bioreactor is beneficial in toxicity studies.

c) Microfabricated Array Bioreactor

The bioreactor consisted of a scaffold which was fabricated by deep reactive ion etching of double-sided polished silicon wafers to form channels (wall surface favours cell adhesion, top and bottom discourages adhesion). This was covered at one side with a filter which was secured with a support scaffold. This scaffold-filter-scaffold sandwich was housed in either a macro-reactor fabricated from stainless steel and glass or micro-reactor (internal dimensions 8 mm × 3 mm) fabricated from polycarbonate. Both reactors had one inlet and two outlets (for top and bottom compartments of the bioreactor). The bioreactor was seeded with single cell suspensions or pre-aggregated spheroids of primary rat hepatocytes. The spheroids were aggregated for 2 to 3 days before seeding them into the scaffold. The flow was modelled to supply the cells with adequate oxygen levels and prevent shear stress induced damage of the system (Powers *et al.*, 2002a; Powers *et al.*, 2002b; Sivaraman *et al.*, 2005).

This bioreactor promoted the formation of liver like tissue from single cell suspension after 2 weeks of incubation. The tissue was viable after the incubation time and pre-aggregates showed improved and stable functionality (albumin and urea secretions) and morphological stability in the first week compared to single cells. This was mainly attributed to cell selection during cell aggregations in spinner flasks where more viable cells form aggregates because of enhanced cadherin experession. The other suggested reason was that NPCs in single cell suspension might not adhere as fast as hepatocytes (NPCs have low density compared to hepatocytes) and the formed tissue after that aggregation stage will have less NPCs compared to pre-aggregated cells.

In long term studies comparing spheroids cultured in this bioreactor with spheroids cultured under static conditions, it was demonstrated that the cells in this bioreactor maintained high functionality which was an order of magnitude higher than static. Morphologically, the tissue formed in the bioreactor showed tight junctions, glycogen storage and bile canaliculi. This improved functionality and morphology might have been affected by the distribution of media containing nutrients, oxygen, various metabolites and shear stress (Powers *et al.*, 2002a; Powers *et al.*, 2002b; Sivaraman *et al.*, 2005).

When the gene expression of various factors (HNF and CEBP-β) and genes (basal and induced cytochrome P450 genes) involved in hepatic specific function were investigated, this model was found to be superior to other models, including collagen sandwich, and closer to *in-vivo* liver. While various factors and genes were established to be down-regulated in the static collagen sandwich, they were maintained in this model of liver tissue. Recent publications reported that this bioreactor was scalable to comprise 40 to 1000 chambers to meet the needs of drug development research and toxicology studies (Powers *et al.*, 2002a; Powers *et al.*, 2002b; Sivaraman *et al.*, 2005).

d) Poly(dimethylsiloxane) (PDMS) Fabricated Microfluidic Bioreactors

The first bioreactor to be discussed is the membrane based bioreactor developed by Fujii's group. The permeable membrane was fabricated from PDMS or polyester and it was fitted in between two PDMS thick layers which had one inlet and one outlet each side. This created a 10 cm x 10 cm x 100 μm chamber for cell culture with media flowing from the inlet to the outlet of each side or permeating the membrane

and leaving through the outlet of the opposite side. This structural set-up was aimed to mimic hepatocyte plates and the sinusoids. The bioreactor was coated with collagen type I and seeded with primary rat hepatocytes. The assessment of the cell attachment, morphology and functionality was carried out using primary rat hepatocytes over a 15 day period. The cells formed aggregates which were characterised with bile canalicular networks. Albumin secretion and ammonium detoxification were found to be highest in both PDMS and polyester membrane bioreactors when compared to cells cultured in well plates or inserts at day 15 and day 4 respectively (Ostrovidov *et al.*, 2004).

Furthermore, PDMS was used in the fabrications of microfluidic structures by Leclerc. The PDMS was cured in pre-fabricated moulds and coated with collagen prior to cell culture. The closed loop set-up contained the microfluidic bioreactor, culture media, peristaltic pump and a bubble trap. Various structures with different dimensions were fabricated and analysed. These microfluidic bioreactors were examined using liver and other cells such as osteoblasts (Leclerc *et al.*, 2004a; Leclerc *et al.*, 2004b; Leclerc *et al.*, 2006). The manufactured microstructures were intended to increase cell numbers in *in-vitro* devices in order to simulate the liver and be used for transplantation or *ex-vivo* liver support systems. Single and multi-layer (stacking of single) structures were examined and used to maintain functional HepG2 cells were maintained for 2 weeks (Leclerc *et al.*, 2004a; Leclerc *et al.*, 2004b). PDMS was found to be an appropriate substrate for culturing hepatocytes *in-vitro* as it is oxygen permeable. However, being not biodegradable limits its exploitation in liver transplantation. Therefore, transferring these microstructures from PDMS into

biodegradable systems have been investigated in order expand their use for *in-vivo* implantation (Leclerc *et al.*, 2004a).

e) Microfluidic Channels Filled with Cells in Collagen Matrix

Collagen is the most widely employed ECM protein in hepatocyte culture. In the work published by Toh and colleagues, collagen was used as part of fluidic bioreactor to maintain hepatocytes in a 3-D morphology. The bioreactor was composed of a microfluidic channel (200μm × 200μm × 1 cm) manufactured from PDMS and glass. The channel was constructed with two inlets which enabled the perfusion of cells and collagen through one inlet and terpolymer, media or PBS via the second inlet. The terpolymer, HEMA-MMA-MAA, was employed for coacervation reaction with methylated collagen and collagen gel formation. The functionality of rat primary hepatocytes measured by EROD assay after 24 hrs in this bioreactor was found to be comparable to static micro-capsules of hepatocytes (Toh *et al.*, 2005). These results were extended to one week period and other cells were investigated in this system including HepG2 and bone marrow mesenchymal stem cells (Toh *et al.*, 2007). The benefits of this bioreactor could be disputed because the entrapment of hepatocytes in the collagen matrix limits cell-to-cell interactions which are essential for hepatocyte survival and functionality.

f) Other Bioreactors

Most of the developed liver bioreactors reported in this chapter are non-biodegradable. This limits their use to *in-vitro* studies and *ex-vivo* liver support devices. In order to exploit the benefits of microfluidics *in-vivo*, Bettinger and co-workers synthesised a biocompatible and biodegradable polymer for the fabrication

of microfluidic scaffolds. The elastomer synthesised was poly(glycerol sebacate) (PGS) which could be turned into microfluidic structures by moulding and stacking techniques. For cellular attachment, the devices were pre-coated with collagen before cell seeding. When the attachment and functionality of HepG2 cells was examined, attachment was found to be dependent on seeding densities and albumin production was comparable to available literature (Bettinger *et al.*, 2006).

Another promising technique for liver cell culture is patterning the distribution of the cells in microfluidic chips. Ho and colleagues employed enhanced field-induced dielectrophoresis (DEP) to align liver cells, including hepatocytes (HepG2 cells) and endothelial (human umbilical vein endothelial cells) cells, into radial patterns simulating their alignment in the liver lobule (Ho *et al.*, 2006).

Various other liver models exist in the tissue engineering field, including the ones based on aggregates and scaffolds. However, for the purpose of the studies covered in this thesis, this chapter concentrated on fluidic bioreactors. Fluidic liver cell models are expanding rapidly with promising outcome for application in both laboratory and clinical settings.

1.4 Surface Coating and Characterisation Prior to Cell Culture

Coating surfaces with extracellular matrix (ECM) proteins has been routinely used for cell culture *in-vitro*. Collagen has been widely employed in liver cell culture and it can be deposited in an adsorbed thin layer or as a gel. The source of ECM and particularly collagen is biological and has its drawbacks, including variation between

batches. In addition, some of the microfluidic structures are two small to allow for a layer of collagen gel. For these reasons, alternative coating techniques are being considered. Plasma processing techniques, for example, have been used for the modification of numerous polymeric materials in routine tissue culture and tissue engineering (Chu *et al.*, 2002). Various chemicals have been utilised in activation, grafting, or coating surfaces to promote attachment of targets including cells. These include oxygen (Yang *et al.*, 2002), ammonia (Hamerli *et al.*, 2003b; Yang *et al.*, 2002), acrylic acid (France *et al.*, 1998; Manso *et al.*, 2004; Whittle *et al.*, 2002), allylamine (France *et al.*, 1998; Hamerli *et al.*, 2003a; Harsch *et al.*, 2000; Whittle *et al.*, 2002), allyl alcohol (Whittle *et al.*, 2002), isopropyl alcohol (Mitchell *et al.*, 2004), and butylamine (Tseng and Edelman, 1998). The plasma modified surfaces could be employed to enhance cellular adhesion directly or indirectly. The indirect methods include the immobilisation of ECM proteins, which contain RGD peptides for cellular attachment, to amine and acid groups deposited by the plasma polymerisation (De Bartolo *et al.*, 2005; Carlisle *et al.*, 2000).

1.4.1 Plasma Polymers

Plasma processing has been documented to be more beneficial for cell culture and tissue engineering applications over other coating procedures. The main reasons for this are the production of sterile samples which are preferred in cell culture (Chu *et al.*, 2002); the high stability of the plasma polymerised polymers when exposed to rinsing and autoclaving (Dehili *et al.*, 2006; Harsch *et al.*, 2000); the good penetration into complex structures including 3-D porous scaffolds (Barry *et al.*, 2005; Barry *et al.*, 2006); the resistance to flow (Tseng and Edelman, 1998) and the compatibility to patterning techniques.

Plasma polymerisation is a method dependent on the formation of energetic plasma species (e.g. electrons, ions, neutral and radicals) in the transformation of vapour phase monomers (e.g. allylamine and acrylic acid) to polymeric coatings. Explaining the mechanisms that regulate the formations of the deposit has been challenging and different theories exist. Broadly, the first one cites the recombination of radicals (Yasuda, 1985), whereas the second theory suggests that the ion-neutral reaction in the plasma is important (O'Toole *et al.*, 1995). Moreover, recent work invokes the importance of the monomer chemistry in the relative activity of these two mechanisms (Barton *et al.*, 2005). Independent of to which of these theories one subscribes, at conditions resulting in a low degree of monomer fragmentation the polymeric film deposited preserves a large proportion of the monomer functional group. In the case of plasma polymerised allylamine (ppAAm), primary amines are retained in the deposit from the monomer whilst imine functionalities are also formed during or shortly after deposition at lower power (Shard *et al.*, 2004). Despite the role of the substrate in the adhesion of the produced deposits, plasma polymerization coating chemistry is independent of the substrate. In the work reported in the following chapters, oxygen plasma pre-etch was used to maximise interface binding between substrate and ppAAm.

1.4.2 Surface Characterisation

In order to understand the behaviour of the cells on the various surfaces utilised in this work, surface characterisation using x-ray photoelectron spectroscopy and contact angle was performed.

a) X-ray Photoelectron Spectroscopy (XPS)

XPS is a method used to determine the chemical properties of surfaces. The XPS analysis comprises two main steps, the photo-ionisation and energy dispersive steps. During the photo-ionisation stage, the surface of the sample is bombarded with x-rays leading to the absorption of photons, ionisation of atoms on the surface and the emission of core electrons. The emitted photoelectrons are dispersed and quantified according to their energies using an electron energy analyser. Using a mono-chromated source of radiation and conservation of energies (BE = PE –KE, where BE is the binding energy, PE is the energy of the photon and KE is the kinetic energy of the electron) enables the determination of binding energies of atoms from the data generated with the energy source analyser. This is plotted into spectra and analysed with the aid of databases and the available literature of known elements and chemical structures in order to find out the properties of the surface. These include the elemental composition of the surface of the substrate, the possible functional groups forming the surface and the approximate depth of the coating. The chemical properties of the surfaces established by XPS analysis can be utilised to predict the physical properties of the surface including wettability. The XPS analysis of surface has been widely employed to investigate the properties of plasma polymers and plasma processed surfaces including ppAAm as illustrated in this work. Moreover, the results collected from XPS analysis provide an understanding of cellular adhesion to a surface and its mechanisms (Tilinin *et al.*, 1996; Baraldi *et al.*, 2003).

b) Contact angle

Contact angle is determined as the angle that a liquid drop forms in contact with a solid surface. The analysis of the measurements obtained can be used to determine

the hydrophilic properties of the surfaces. Contact angle measurements are also employed to establish surface tension and energy using Young's equation ($\gamma_{lv}\cos\theta = \gamma_{sv} - \gamma_{sl}$, where γ is interfacial tension between l and v, s and v, s and l and l is liquid, v is vapour, and s is solid). There are various types of contact angle which can be classified under either static or dynamic contact angles and these include intrinsic, equilibrium, receding, advancing, Wenzel, composite and apparent contact angles (Kumar and Prabhu, 2007). Liquids of known properties are employed in contact angle measurements. In contact with the substrate surface, the liquid drop attains a shape that is favoured by the surface tension and energies. The drop can spread over a large area of the surface to form a thin layer of liquid, spread on an area of the surface keeping some shape of the circular drop, or maintain the circular droplet shape with minimum contact with the surface. These three behaviours of liquids on surfaces relate to very hydrophilic, moderately hydrophilic and hydrophobic characteristics of surfaces respectively (Kumar and Prabhu, 2007).

1.5 Aims and Objectives

The work reported in this thesis is the investigation of various fluidic systems for *in-vitro* culture of liver cells. Two bioreactors were studied, the first was structurally based on the hexagonal liver lobule and made of glass. The second one was a commercially available plastic slide chamber purchased from Ibidi (Germany). Various cells were examined in the two systems including primary rat hepatocytes and cell lines such as Huh-7 and FGC4 cells. The aim of the work was to examine the two models and optimise them for *in-vitro* cell culture. One of the objectives was to find an ideal surface for cell seeding. For this reason, part of the work focused on

assessing various coating techniques including collagen coating and plasma polymerisation. The thesis is divided into an introductory chapter, materials and methods chapter, four results chapters and finally conclusions and future work.

The objectives to achieve these aims are:

- Examine plasma polymerised allylamine as a coating technique for cell culture and compare it to other methods such as collagen (Chapter Three, Four and Five)
- Assess and optimise the hexagonal glass system (Chapter Four)
- Assess and optimise the Ibidi chamber (Chapter Five)
- Investigate the survival and function of primary rat hepatocytes in the Ibidi chamber over a 5 day period (Chapter Six).

Chapter Two

General Materials and Methods

2.1 Introduction

This chapter summarises the materials and methods employed in the experiments performed in relation to cell culture, morphology, viability and functionality assessment. More detailed experimental procedures are explained in the result chapters and appendices

2.2 Animals

Male Wistar rats, weighing between 170 and 190 grams, were obtained from the University of Nottingham Biomedical Service unit. The rats were housed in small groups on soft bedding in 12-hour light/dark cycle environment and given a free access to commercial food and tap water.

2.3 Chemicals

Unless otherwise stated all chemicals and reagents were purchased from Sigma, UK. These are: β-glucuronidase enzyme, dicoumarol, Dimethyl sulphoxide (DMSO), 7-ethoxyresorufin, 7-hydroxyresorufin, ethylene glycol-bis (β-aminoethylether)- N, N, N', N'-tetraacetic acid (EGTA), trypan blue, percoll, nicotinamide, dexamethasone, insulin, 10x HBSS, HEPES, Sodium bicarbonate, 0.01% poly(L-lysine) (PLL), hexamethyldisilazane (HMDS), sulphuric acid (H_2SO_4), 3,3',5,5'-

tetramethylbenzidine supersensitive (TMB), Tris buffered saline (TBS), bovine serum albumin (BSA), Tween-20 and carbonate-bicarbonate capsules. William's E, Dulbecco's Modified Eagle Media (DMEM), Ham's 12 media, Leibovitz-15 (L-15), foetal calf serum (FCS), antibiotic/antimycotic, and L-glutamine were obtained from Invitrogen, UK. Phosphate buffered saline (PBS), chloroform, ethanol, sodium hydroxide, industrial methylated spirits (IMS), BD Blunt Fill Needle 18G and T75 Nunc flasks were purchased from Fisher Scientific and chemicals, UK. Protein block solution was obtained from DAKO-Cytomation, UK. Poly(D,L-lactic acid) (PLA) (Purasorb®, Netherlands), rat tail collagen type I (Upstate, NY), 7X detergent and Cellagen solution AC-3 (0.3%) (ICN Biomedicals, Ohio), live/dead® viability and cytotoxicity kit for animal cells (Molecular probes, UK), glutaraldehyde and osmium tetroxide (TAAB, Berkshire, UK), albumin (rat) ELISA quantitation kit and sheep anti-rat albumin (Bethyl Laboratories, Alexis Corporation, UK).

2.4 Plastic- and glass-ware

Costar flat bottom and high binding polystyrene 96-well plates (Corning, NY, USA), cell culture polystyrene 6-well and 24-well plates (Falcon, Becton and Dickinson Ltd., Oxford, UK), glass coverslips (Scientific Laboratory Supplies, UK).

2.5 Primary hepatocyte isolation

Hepatocytes were isolated from the animals using a two-step end of lobe perfusion technique adapted from the method described by Seglen in 1976 (Seglen, 1976). All procedures were performed under sterile conditions. A peristaltic pump was set at

flow 25 ml/minute. A water bath containing all the buffers and tubing was set at 37° C to maintain the temperature of the buffers at around 37° C when they reach the liver lobes. The liver was removed from the animal and the flat and median lobes were used to isolate the cells. The lobes were trimmed to expose the blood vessels and then placed on a platform funnel (Figure 2.1, 2.2, 2.3). The lobes were then cannulated with one plastic cannula each. The cannulas were joined with Y stainless steel connector which was attached to long plastic tubing. A bubble trap was placed between the peristaltic pump and the long tubing to prevent bubbles to reach the liver tissue. In order to flush out the blood, the lobes were perfused with a gassed chelating buffer containing EGTA (0.5 mM) for approximately 10 minutes (Appendix 1.4). The EGTA chelates calcium and therefore disturbs tight junctions. After that, the lobes were perfused with a gassed collagenase buffer for 15 to 20 minutes (Appendix 1.5). The collagenase digests the tissue and it was recycled through the system. The cells were released in serum containing William's E medium (Appendix 1.8) by opening the capsule and mincing the tissue with scissors and forceps (Figure 2.3). The cell suspension was then filtered through 64 μm sterile gauze into 50 ml falcon tubes and centrifuged at 350 rpm for 3 minutes. The pellet was re-suspended in 20 mls of medium before counting. The viability of the cells was assessed using trypan blue exclusion method. The cells were counted in a modified Neubauer counting chamber under a light microscope. The cells that did not take the dye were counted and judged as viable and then the total cell number was counted. The viability was calculated as number of viable cells as percentage of the total cell number. The cells from each lobe were kept separate and the lobe with the best viability and total cell number was used for further purification.

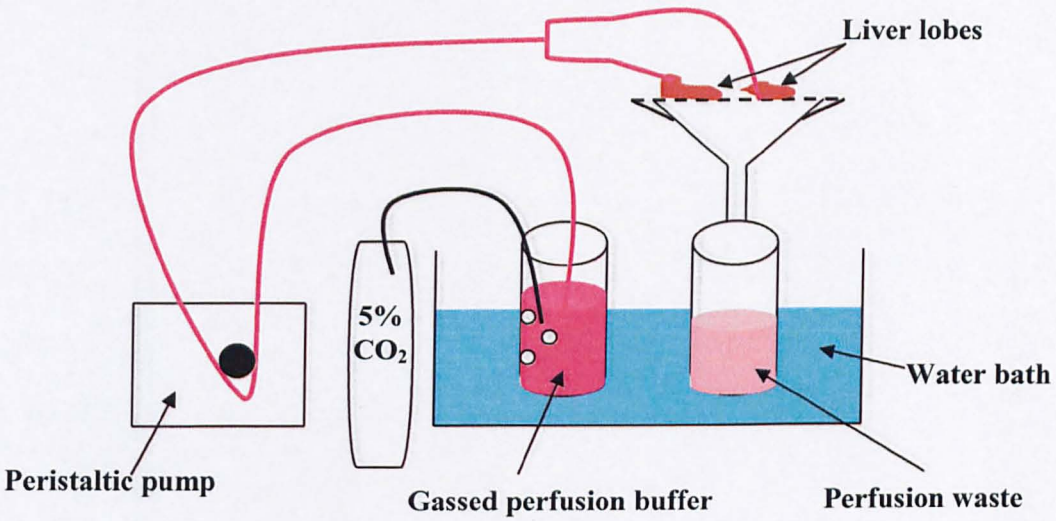

Figure 2.1 Schematic diagram of rat hepatocyte perfusion method.

Figure 2.2 A photograph of the set-up of primary rat hepatocyte isolation using the two-step collagenase perfusion method adopted from Seglen (Seglen, 1976).

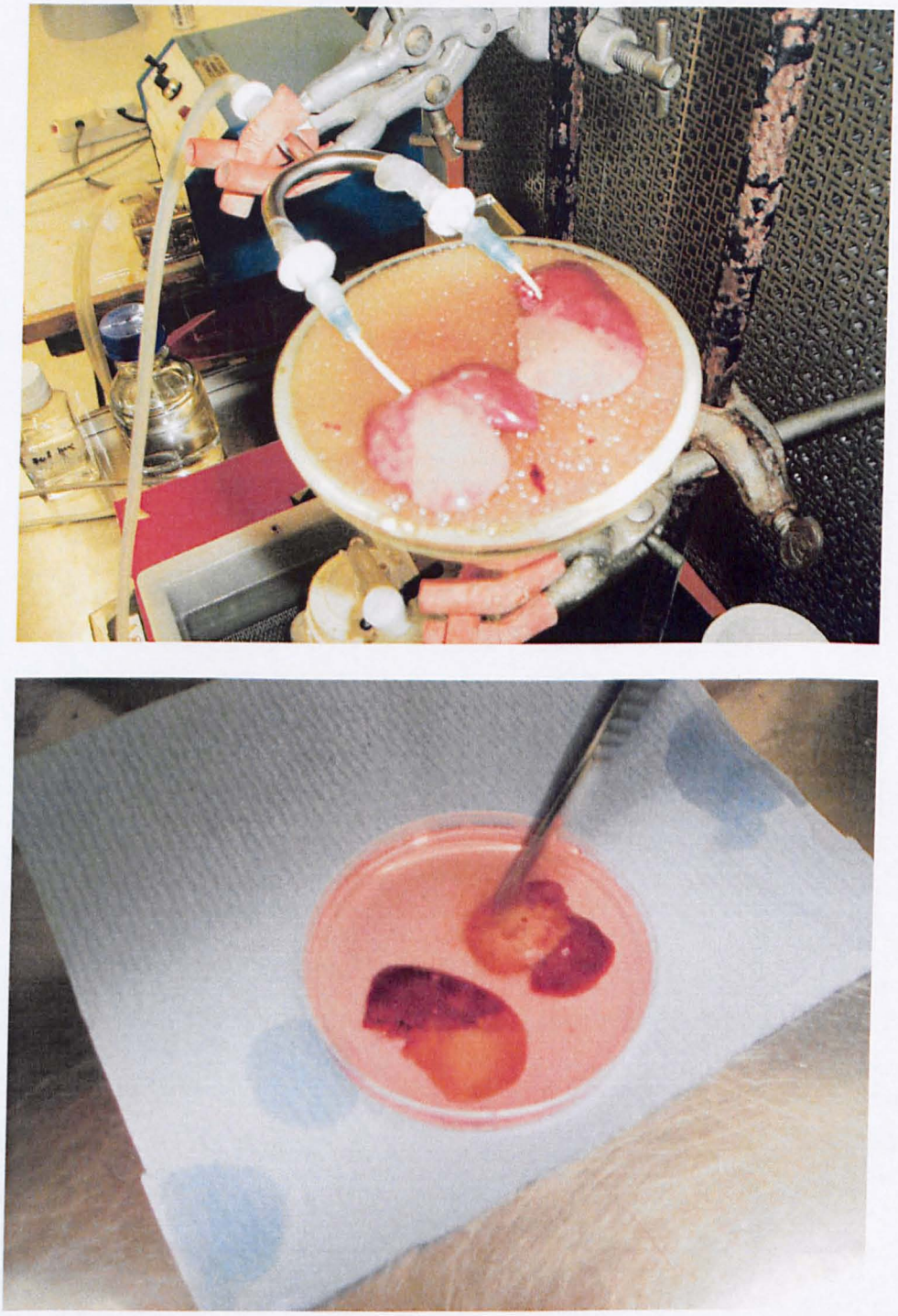

Figure 2.3 Photographs of the liver lobules during the two-step collagenase perfusion method and the release of the perfused liver cells.

The pellet was re-suspended in 10 mls of medium before adding 10 mls of 90% percoll (Appendix 1.7) and centrifuging at 525 rpm for 10 minutes using the Sigma 3K15 centrifuge. At this stage, the pellet was re-suspended again in medium and the viability was assessed as previously described. A viability of at least 80% was used for further experimental work.

L-15 media was employed during hepatocyte isolation and culture in some of the experiments. William's E and L-15 media were supplemented with L-glutamine and antibiotics/antimycotics. Serum containing William's E and L-15 media were supplemented with 10% foetal calf serum (FCS) (Appendix 1.8). Serum-free William's E and L-15 were supplemented with nicotinamide (5 mM), dexamethasone (0.4 μg/ml) and insulin (10 μg/ml). L-15 medium was used in the absence of 5% CO_2 (Appendix 1.8).

2.6 Huh-7 Cell Culture

Huh-7 cells (human hepatoma) were donated from Surrey University. The cells were cultured in Dulbecco's Modified Eagle Media (DMEM) supplemented with 10% FCS, 2mM L-glutamine and antibiotic/ antimycotic (100 U penicillin, 100 μg streptomycin, 250 ng amphotericin B) (Appendix 1.8). The cells were cultured in T75 Nunc flasks and incubated in humidified atmosphere with 5% CO2 at 37° C. At 70 to 80 % confluency, the cells were passaged by incubation in 5 ml of trypsin/EDTA solution for 2 mins. After that, 20 ml of media was added to deactivate trypsin/EDTA and the cells suspension was centrifuged at 1300 rpm using MSE Mistral 1000 centrifuge (Scientific Laboratory Supplies, UK) for 3 mins. The

supernatant was then aspirated and the cells were re-suspended in 20 ml of media. In order to obtain a single cell suspension, the cells were passed gently through a needle about a dozen of times (BD Blunt Fill Needle 18G).

2.7 FGC4 Cell Culture

FGC4 cells (rat hepatoma) were a gift from the toxicology group. The cells were cultured in Ham's 12 media supplemented with 10/% FCS, 2mM L-glutamine and antibiotic/ antimycotic (100 U penicillin, 100 μg streptomycin, 250 ng amphotericin B) (Appendix 1.8). The cells were cultured in T75 Nunc flaks and incubated in humidified atmosphere with 5% CO2 at 37° C. At 70 to 80 % confluency, the cells were passaged by incubation in 3 ml of trypsin/EDTA solution for 2 mins. After that, 20 ml of media was added to deactivate trypsin/EDTA and the cells suspension was centrifuged at 500 rpm using MSE Mistral 1000 centrifuge (Scientific Laboratory Supplies, UK) for 3 mins. Supernatant was then aspirated and the cells were re-suspended in 20 ml of media.

2.8 Cell culture conditions

All cell culture manipulations were performed using aseptic procedures in class I laminar flow cabinet (primary cells only) or class II microbiological safety cabinet (primary cells and cell lines). Otherwise stated, the cells were incubated at 37° C in humidified atmosphere with 5% CO_2 in air.

Generally PRH and Huh-7 cells were plated at 1×10^5 cells/cm^2 and FGC4 at 5×10^5 cells/cm^2 in the experiments performed. Any deviations are reported in individual result chapters.

2.9 Microscopy

2.9.1 Phase-contrast and fluorescent microscopy

An inverted Leica microscope (Leica model DMIRB/RED) was used to visualise the cells and the images were captured using Leica DC200 digital imager (Leica, UK). Nikon Eclipse TS100 (Nikon, UK) was also used in some experiments.

Nikon SMZ1500 stereomicroscope (Nikon, UK) was used to examine the cellular distribution in the hexagonal channels and the Ibidi plate as it allowed their observation at low magnifications. The images from both Nikon microscopes were captured and analysed using the accompanying camera (Nikon DS-5M-L1 Digital Sight Camera System) and software.

2.9.2 Confocal Microscopy

Confocal microscopy was carried out using the Leica TCS SP confocal microscope (Leica, UK) and the associated software. After positioning the sample and adjusting the parameter on the Leica program, the samples were scanned. The argon (Ar) laser was used and the excitation selected was 488 nm. The range of emission wavelength was narrowed for both the green and red detection of FITC and the live/dead stain in

order to limit the background. The software provided was used to analyse the images captured and create the 3-D views.

2.10 Live/dead staining

Live/dead staining was performed to assess the attachment and survival of hepatocytes on the glass channels. The culture medium was removed and the channels washed three times with PBS. The live/dead working solution (Appendix 3) (4 μM ethidium homodimer-1 and 2 μM calcein AM in serum-free medium) was added to the cells and incubated for 30 to 40 minutes in the dark at 37° C. After this time, the staining solution was removed and the cells were washed again three times with PBS. The glass channels were visualised using fluorescence microscopy with 450-490 excitation filter (ex/em 495/635 ethidium homodimer-1, ex/em 495/515 calcein AM). Live/dead staining shows the proportion of live cells (stained fluorescent green by calcein AM) and dead cells (stained fluorescent red with ethidium homodimer-1). The green fluorescent calcein results from the hydrolisation of calcein AM by esterases present in the live cells. These cells retain the stain because of their complete membrane structures. The red fluorescent stain is ethidium homodimer-1 which enters cells with compromised cell membranes only and has a high affinity for nucleic acid.

2.11 Scanning Electron Microscopy (SEM)

To examine the attachment of hepatocytes on the coated glass channels, samples were scanned under an electron microscope. First, the samples were fixed in 3%

glutaraldehyde for at least 24 hours (Appendix 4.2). Then, the cells were washed three times with PBS and fixed in 1% v/v osmium tetroxide for 2 hours at room temperature (Appendix 4.3). After that, the samples were washed with distilled water and dehydrated through a series of ethanol concentrations (25%, 50%, 70%, 90%, 95% and 100% v/v in distilled water) and hexamethyldisilazane (HMDS). The samples were left to dry overnight at room temperature. Samples were sputter-coated with gold for 4 minutes (Blazers SCD030 Coater) resulting in a thickness of 20 to 25 nm. The SEM microscope was a Phillips SEM505 at a voltage of 25kV and the images were acquired using Semicaps 2000A® software package.

2.12 7-Ethoxyresorufin-O-deethylase (EROD) Activity

7-Ethoxyresorufin is reduced to its fluorescent product 7-hydroxyresorufin by 7-Ethoxyresorufin-O-deethylase (EROD). The reaction is mediated by cytochrome P450 enzymes (CYP1A1/2 and CYP1B1). Cells were incubated with 1 ml of 5 μM 7-ethoxyresorufin solution containing 10 μM dicoumarol in the dark at 37° C for 30 minutes (Appendix 5). Dicoumarol was added to prevent alternative metabolism of 7-ethoxyresorufin. The solution (200 μl) was then removed and incubated with β-glucuronidase enzyme (40 μl of 1600 units/ml) at 37° C overnight (Appendix 5). During this stage, any glucuronidated resorufin was deconjugated back to the original product. Before detecting fluorescence, sodium hydroxide (50 μl of 0.1 M) was added to the wells to create a pH in which resorufin is ionised and therefore optimally fluorescent. Fluorescence was detected using Microtiter® Plate Fluorometer with excitation at 530 nm and detection at 590 nm. A standard curve was created by measuring the fluorescence of a series of standards in the range 0,

6.25, 12.5, 25, 50 and 100 pmol/ml of 7-hydroxyresorufin. Background fluorescence was measured from cells, dicoumarol and 7-ethoxyresorufin as appropriate.

2.13 Rat albumin enzyme linked immunosorbent assay (ELISA)

Sandwich enzyme linked immunosorbent assay (ELISA) was carried out to measure the amount of albumin secreted by hepatocytes into the culture media. This was modified from the method supplied with the kit from Bethyl Laboratories (Appendix 6). Costar high binding 96-well plates were used. The surface of each well was coated with an albumin capture antibody (100 µL of 1 in 100) in carbonate-bicarbonate coating solution which was incubated at room temperature for 60 minutes or at 4° C overnight. The antibody was then removed and the wells washed three times with a washing solution. The free surface area was then blocked using a BSA (0.1%) based blocking solution (200 µL) for 30 minutes. The solution was removed and the wells were washed three times. Diluted purified albumin or samples were added and incubated for 60 minutes at room temperature. The following concentrations of rat albumin were used for the standard curve, 0, 7.8, 15.625, 31.25, 62.5, 125, 250, 500 ng/ml. The solution was removed and the wells were washed five times. Horse-radish peroxidase (HRP) conjugated anti-albumin antibody was then added at a concentration of 1:40,000 and incubated at room temperature for 60 minutes. The solution was then removed and the wells were washed five times. The final step was the development when the 3,3',5,5'- tetramethylbenzidine (TMB) was incubated in the wells at room temperature for 10 to 15 minutes. The development was stopped with 2 M H_2SO_4 and the absorbance was read at 450 nm. An MRX plate reader supplied by Dynex Technologies was used.

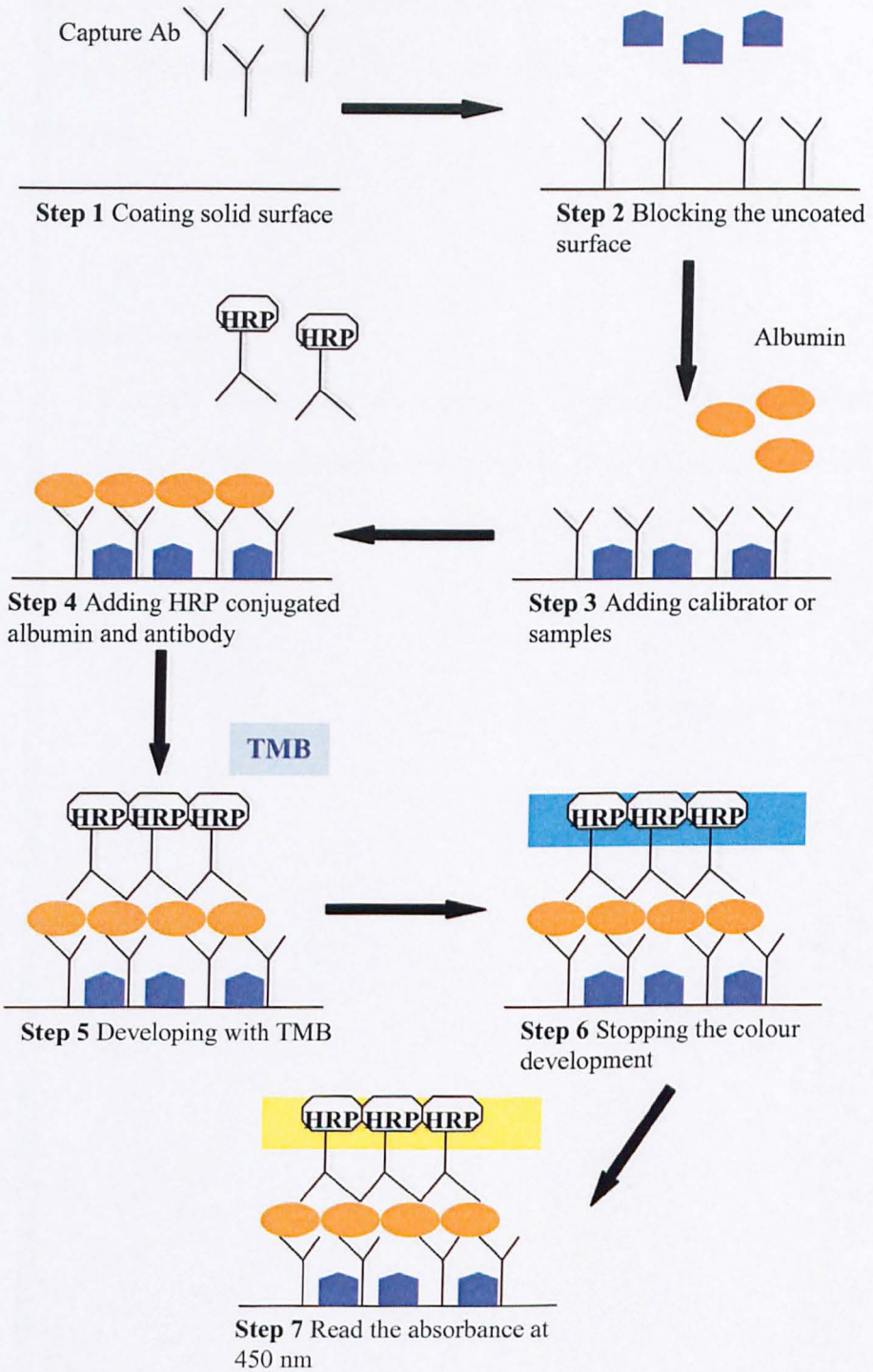

Figure 2.4 Diagram illustrating the various steps of albumin ELISA.

Media sampled from the culture was centrifuged at 13,000 rpm in a Micro Centaur Centrifuge for 5 minutes to remove any dead cells. The supernatant was collected and stored at -20° C until albumin ELISA assay. Samples were diluted appropriately before the assays.

2.14 Statistical analysis

All the results are presented as mean ± standard deviation (SD) or standard error of the mean (sem) and N is the number of multiple wells. The mean, SD and sem were calculated using statistical Microsoft Excel® 2000 software.

Chapter Three

Attachment and Functionality of Primary Rat Hepatocytes Plated onto Collagen and ppAAm coated Glass Coverslips

3.1 Introduction

The mechanism of cellular adhesion *in-vitro* is complex and is believed to comprise adsorption of media extra-cellular matrix (ECM) proteins onto the surface and subsequent cell-ECM interactions and attachment. The conventional method to use glass as the substrate is to pre-coat with poly(L-lysine) (PLL) prior to cell culture. The intentions of using PLL are to introduce positive charges onto the surface and promote electrostatic attraction between the surface and media ECM proteins which could be carrying the same negative charge at physiological pH. As a consequence, the proteins in the media adsorb onto the surface and subsequent cell-protein interactions and attachment occur. PLL coating alone is not sufficient for primary hepatocytes attachment and culture, and therefore, additional coating of the surface with ECM proteins is necessary to achieve optimal cell adhesion, survival rate and functionality (Guillouzo *et al.*, 1990; Pinske *et al.*, 2004). Collagen has been the most popular ECM protein for primary hepatocyte culture *in-vitro* and it can be used in numerous forms including thin adsorbed layers, gels and gel sandwiches (Guillouzo *et al.*, 1990; Guillouzo, 1998; LeCluyse *et al.*, 1996).

Nitrogen containing plasma polymer coatings, including plasma polymerised allylamine (Figure 3.1) (ppAAm), were demonstrated by various groups to encourage cellular attachment. These coatings were found to improve the attachment of 3T3 fibroblasts, human skin fibroblasts, human melanocytes and keratinocytes, neuronal cells, and bovine aortic endothelial cells (Barry *et al.*, 2005; Beck *et al.*, 2003; Eves *et al.*, 2005; Hamerli *et al.*, 2003; Harsch *et al.*, 2000; Tseng and Edelman, 1998). These various studies have reported that nitrogen rich plasma films embrace properties that encourage cellular attachment. These are the hydrophilicity of the surface with water contact angle measurements ranging between 50° and 70° (Hamerli *et al.*, 2003; Harsch *et al.*, 2000; Tseng and Edelman, 1998; Whittle *et al.*, 2002), improving the adhesion of the ECM proteins (Whittle *et al.*, 2002), low solubility in water, when autoclaved and under flow of media (Dehili *et al.*, 2006; Harsch *et al.*, 2000; Tseng and Edelman, 1998).

Most of the literature available around plasma coating for tissue culture involves the investigation of cell lines and exploring the behaviour of primary cells in this environment is important and could be very beneficial for the progress of some research areas. In this chapter, the attachment and functionality of primary rat hepatocytes (PRH) plated onto ppAAm and collagen coated glass coverslips were investigated.

3.2 Aims and Objectives

The aim of this chapter is to investigate the attachment and function of PRH on ppAAm in comparison with collagen gel. The following objectives were examined:

- ppAAm coating was characterised using X-ray photoelectron spectroscopy (XPS) analysis of ppAAm (before and after rinsing) and glass.
- The morphology of the cells on both surfaces was assessed with phase-contrast microscopy.
- Basic liver function, in terms of secreted albumin and cytochrome P450 (CYP1A1/2 and CYP1B1) enzyme activity, was measured to establish any side effects of ppAAm on the cells.

3.3 Materials and Methods

3.3.1 Cell Culture

The hepatocytes were isolated from the sacrificed animals using a two-step end of lobe collagenase perfusion technique as described in chapter 2. The cells were plated at 1 × 10^5 cells per cm^2 (Qiao *et al.*, 1999) in serum containing Leibovitz-15 (L-15) media. The cells were incubated under static conditions for 1 hour to allow them to attach. The cells were then washed with phosphate buffered saline (PBS) to remove any unattached dead cells and the media was replaced with serum-free L-15. The cells were incubated at 37° C on a shaker (IKA-Schutler MTS4, 50 rpm/minute) to prevent culture medium stagnation, and the medium was changed daily.

3.3.2 Functional Assessment of PRH

7-Ethoxyresorufin-O-deethylase (EROD) activity and albumin secretion were measured on a daily basis using the methods described in chapter 2. Media was collected daily to

measure albumin and then the cells were washed with PBS and used to measure EROD activity. After that, the cells were washed with PBS and fresh serum-free L-15 media was added.

After 48 hrs, the cells were lysed by incubation with 1 ml of 0.1 M sodium hydroxide at room temperature for approximately 48 hrs. The proteins were quantified using the Bradford protein assay. Bradford reagent (Sigma, UK) was incubated with the dissolved proteins for 15 minutes and absorbance detected at 595 nm using Labtech International plate reader. A standard curve (Appendix 7.1) was created with 0, 0.1, 0.2, 0.3, 0.4, 0.5, 0.6 mg/ml of bovine serum albumin (BSA) (Sigma, UK).

3.3.3 Phase Contrast Microscopy

An inverted Leica microscope (Leica model DMIRB) was used to visualise the cells by phase-contrast after 24 and 48 hrs from seeding, and the images were captured using a Leica DC200 digital imager.

3.3.4 Glass Preparation

Standard histological glass coverslips (Scientific Laboratory Supplies, UK) were cleaned with 7X detergent (ICN Biomedicals, UK) and distilled water. They were then sonicated twice in fresh distilled water. The coverslips were dried and used for plasma treatment or sterilised in 70% ethanol when used for untreated control glass or collagen type I gel attachment. ppAAm coated glass was rinsed with sterile distilled water by immersing the coverslip in 1 ml of water in a 24-well non-tissue culture treated plate (Corning Incorporated Costar®, UK) and shaking for 1 minute before aspirating the water off.

3.3.5 Plasma Treatment

The plasma reactor used in the experiments is shown in figure 3.2. The plasma reactor consisted of a cylindrical borosilicate glass T-piece sealed with stainless steel end-plates using Viton O-rings. A radiofrequency generator (13.56 MHz) was capacitively coupled to the glass deposition chamber via two external copper bands. The flow of allylamine vapour and oxygen into the glass chamber was adjusted using manual needle valves. The pressure in the chamber was maintained at 40 Pa before starting the deposition using a valve at the pumping line. A liquid nitrogen cold trap and alumina trap were used to prevent contamination of: the rotary pump with condensable plasma products and the plasma reactor by pump oil (Fomblin). The weight measurements of the deposited polymer were acquired using STM-100/MF vibrating quartz crystal microbalance (Sycon Instruments, New York). The crystal used was gold coated and the deposited film weight was established by measuring the resonance frequency of the exposed crystal. The samples were placed in a polystyrene Petri-dish as a support and introduced into the glass chamber. The allylamine monomer (Figure 3.1.) (Sigma, UK) was degassed using 3 freeze-thaw cycles. The plasma treatment was performed at a power of 20 W and the reflected power was reduced (< 1 W) by tuning a manual matching on the radiofrequency generator.

Cleaned coverslips were oxygen plasma etched first for 3 minutes and then coated immediately with ppAAm (approximately 3 minutes) (Figure 3.3) to a thickness of approximately 15 nm as estimated by XPS analysis. The coated coverslips were stored at room temperature and used within 24 hours of coating.

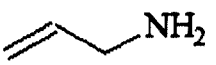

Figure 3.1 Chemical structure for allylamine (C_3H_7N).

(a)

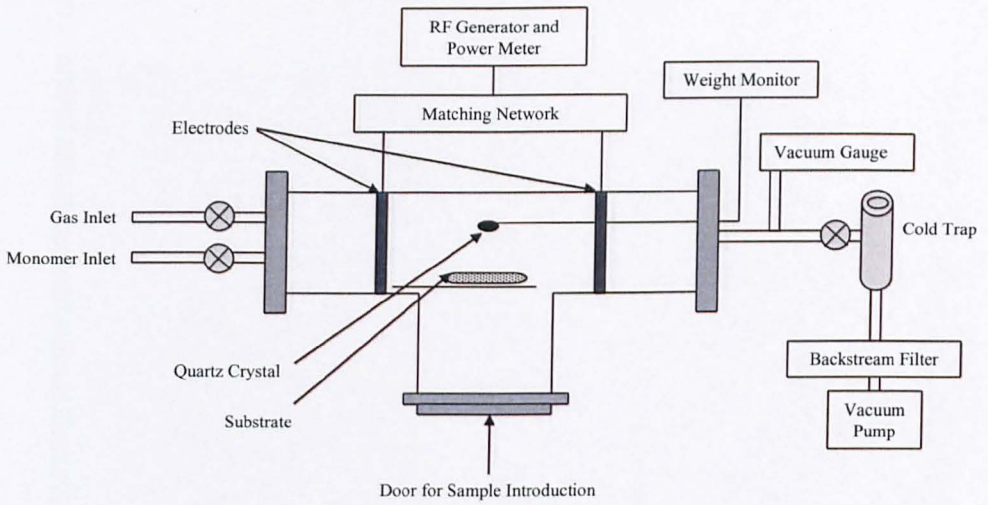

(b)

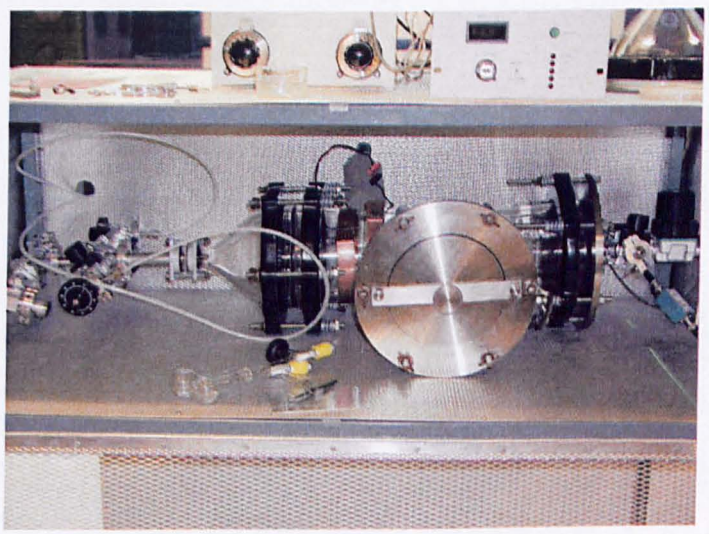

Figure 3.2 (a) Schematic diagram and (b) a photograph of the plasma reactor, the right electrode is grounded.

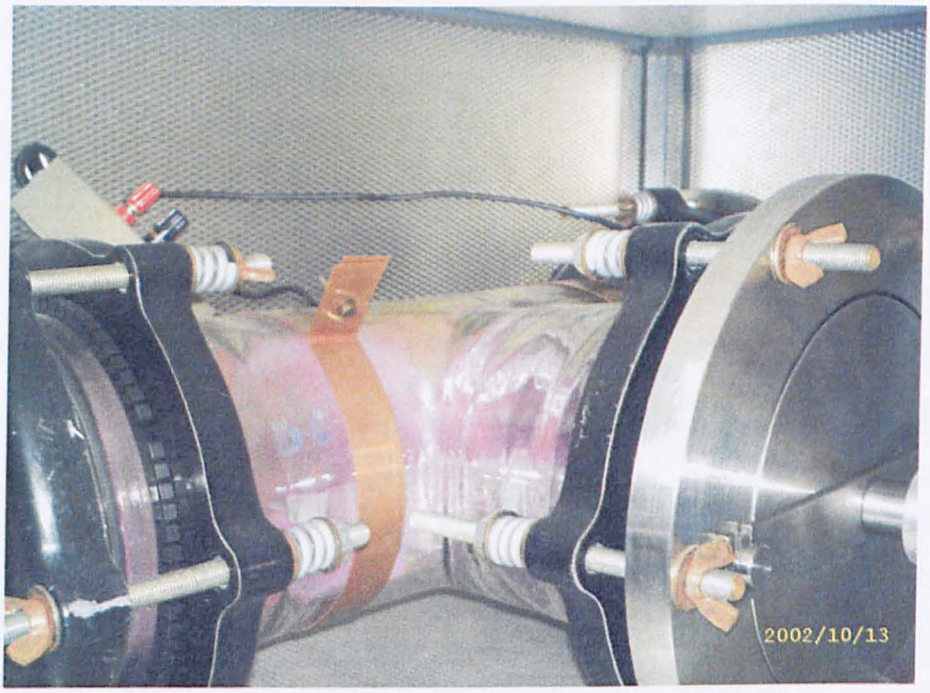

Figure 3.3 A photograph of the plasma reactor during ppAAm deposition.

3.3.6 Collagen Type I Gel Coating

First, the coverslips were placed in 24-well non-tissue culture treated plates (Corning Incorporated Costar®, UK). The method of collagen type I gel was adopted from the method reported by Pearson *et al.* (Pearson *et al.*, 2003). Bovine collagen type I (Cellagen solution AC-3 0.3% collagen type I, ICN Biomedicals, UK) was diluted to 0.02% using collagen buffer. Diluted collagen solution (0.5 ml) was added to the wells and shaken well for about 1 minute before removing the excess. The samples were incubated at 37° C for 30 minutes to allow the collagen to gel and then stored at 4° C until used. All materials used in the coating procedure were maintained cold during the process.

3.3.7 X-ray Photoelectron Spectroscopy (XPS)

X-ray photoelectron spectroscopy (XPS) analysis was carried out using a Kratos Axis Ultra instrument equipped with a source of monochromated AlKα radiation. The x-ray source was run at a power of 150 W, high resolution core levels were acquired either at a pass energy of 20 eV and survey scans at a pass energy of 160 eV. Charge neutralising electron flood was employed for all analyses. The X-ray spot is an ellipse of 0.5 mm × 1.0 mm (FWHM) oriented perpendicular to the energy dispersive axis. The photoelectrons were collected from a rectangle of dimensions 0.3 mm × 0.7 mm. Elemental and functional quantification was obtained using CASA XPS software (Neal Fairly, UK). Empirically modified sensitivity factors, supplied by the manufacturer, were used to calculate surface elemental compositions; the average from three separate areas on each sample is reported.

2.3.8 Contact Angle Measurements

Static contact angle measurements were quantified using CAM 200 Optical Contact Angle Meter purchased from KSV Instruments Ltd. For this purpose ultrapure water was used as test liquid. After contact of water with the surface, 15 images were captured at 1 second interval. The average contact angle of each image was calculated with the software provided with the meter. The first contact angle reading was discarded and the other values were used to plot a linear regression and estimate the contact angle at time zero.

3.4 Results

3.4.1 Surface Analysis of ppAAm

The surfaces were analysed by XPS before and after coating with ppAAm. The results obtained are summarised in table 3.1. The XPS analysis of uncoated glass established that the glass coverslip contained elements indicating a silica glass with soda, lime and borate (Figure 3.4). Figure 3.5 demonstrates an XPS survey scan of ppAAm coated glass showing that ppAAm almost totally attenuated core level peaks from elements exclusive to the glass and introduced new core levels peaks from other elements including nitrogen. There was still a small Si 2p core level picked up by the XPS analysis which resulted from the substrate signal just detected through the ppAAm coating. This indicated that the thickness of the ppAAm film was about 15 nm.

	Glass coverslip	ppAAm	Rinsed ppAAm
[C]	15	78	77
[N]	0.8	17	14
[O]	62	4.7	7.6
[Si]	16	0.3	1.7
[B]	2.0	-	-
[K]	2.2	-	-
[Zn]	0.8	-	-
[Na]	1.8	-	-
CH	-	60	61
C-N (1.0)	-	3	7
C=N/ C-O (1.5)	-	31	26
C=O (2.9)	-	5	5
N-C=O (3.1)	-	0	0
C(=O)OH/ C(=O)OR (4.1)	-	0	1

Table 3.1 Surface elemental composition as determined by XPS at % of glass coverslip, ppAAm, and rinsed ppAAm.

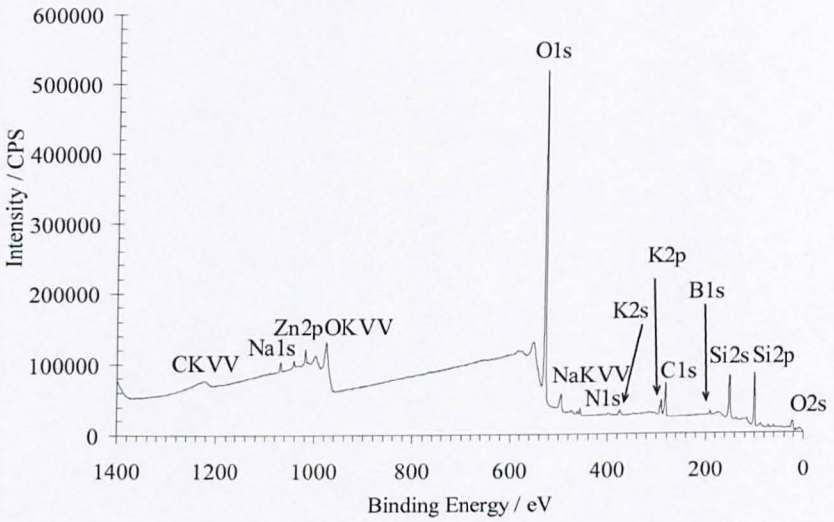

Figure 3.4 XPS survey scan of a glass coverslip.

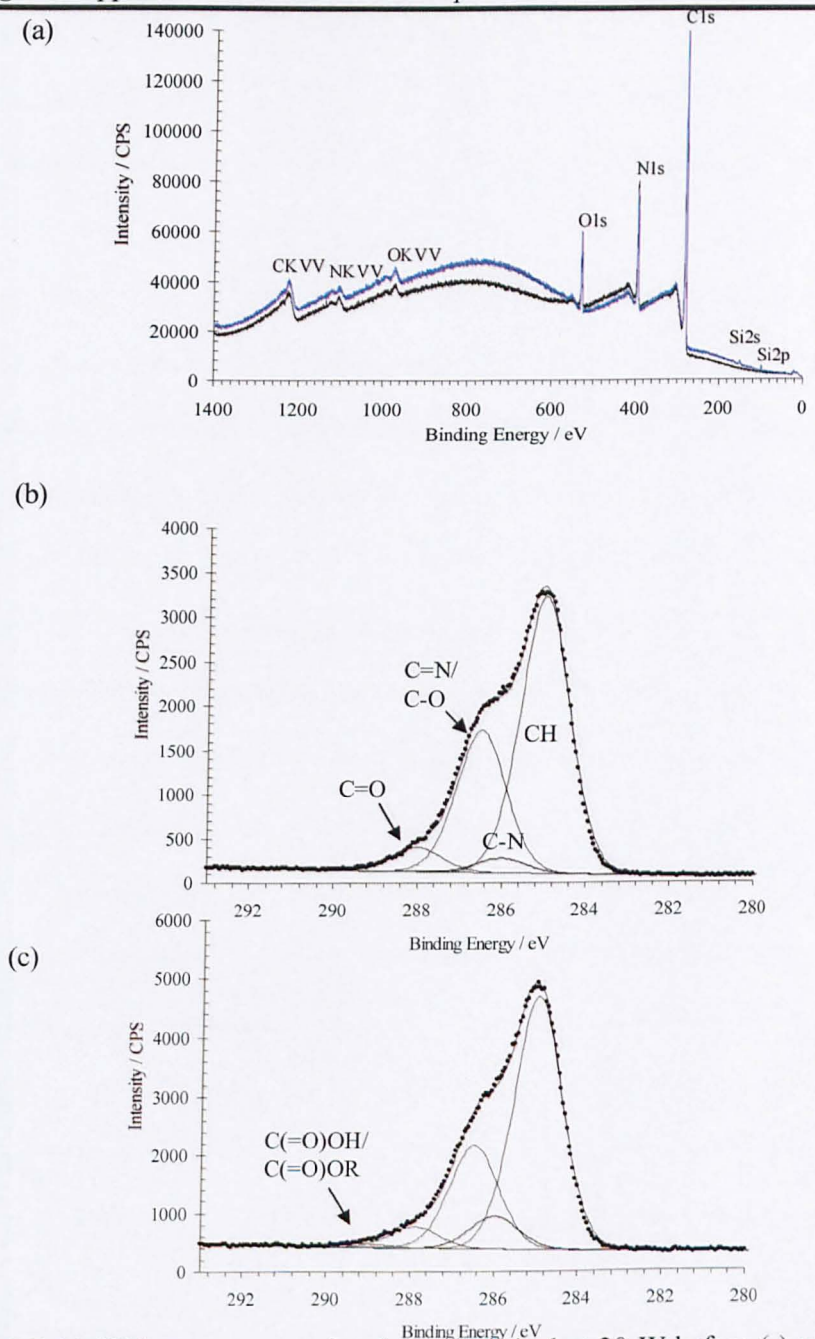

Figure 3.5 (a) XPS survey scan of ppAAm deposited at 20 W before (-) and after (-) rinsing in water. C1s narrow scan from ppAAm (b) before and (c) after rinsing, shown charge corrected to C-C at 285.0 eV. A single component peak position at 399.5 eV (relative to C-C at 285.0 eV) well fitted the ppAAm data after rinsing.

The XPS analysis (Table 3.1) indicated that rinsing the ppAAm coated glass with water did not significantly affect the elemental composition of the coating despite a slight thinning identified by the increase in the Si 2p signal intensity (Figure 3.5a).

Fitting the C1s core level from ppAAm coating with synthetic peaks representative of the functionalities taken from databases and other literature provided some information about the various functional groups present in the film. The C1s from ppAAm film was well fit by synthetic components representing hydrocarbon, amine (C-N), imine or alcohol/ester/ether environments (C=N/C-O), and carbonyl (C=O) functionalities (Figure 3.5b, Table 3.1). The possible presence of amides (shift 3.1 eV) could not be determined using XPS analysis alone as the carbonyl environment was very close in the C1s core level. The absence of an amide component was consistent with the NEXAFS data of Shard *et al.* (Shard *et al.*, 2004). Rinsing the ppAAm film resulted in the need of a low intensity component to fit the envelope which was assigned to acid/ester/ether functionalities (Figure 3.5c, Table 3.1). In addition, the imine concentration decreased which was possibly because of the loss of nitrogen as soluble deposit and some hydrolysis to form primary amines. The binding energy of the symmetric single component N1s core level, from both ppAAm deposits, was 399.5 eV (not shown). This was consistent with the prevalence of amines and imines proposed based on the C1s.

Water contact angle measurements of the cleaned glass coverslip and ppAAm were measured and found to be 40° and 70° respectively.

3.4.2 Cellular Attachment and Functionality

Phase-contrast microscopy showed that after 24 hours (Figure 3.6) very few cells attached to the untreated glass compared to the ppAAm, collagen type I gel, or collagen type I gel on ppAAm coated glass. The cell attachment to the glass was not significantly improved after 48 hours of culture (Figure 3.7). The number of hepatocytes attached onto ppAAm, collagen type I gel, and gel on ppAAm was similar for both culture periods. However, detachment of collagen type I gel from the surface was observed when the collagen type I gel was applied directly onto untreated glass (results not shown). This was not observed with the glass coated with ppAAm before coating with collagen type I gel. The cells on both treated and untreated glass had distinctive hepatocyte morphology with mono- and bi-nucleated cells both after 24 and 48 hours in culture.

The graph in Figure 3.8 illustrates total cellular proteins of hepatocytes on treated and untreated glass at 24 and 48 hours. The quantity of cellular proteins was lower at 48 hours compared to 24 hours in all the samples. The quantity of proteins of the cells plated on ppAAm, collagen type I gel and collagen type I gel on ppAAm (> 0.2 mg/ml at 24 and 48 hours) was significantly higher than the untreated control glass (< 0.12 mg/ml at 24 and 48 hours). This correlated with the number of attached cells in phase-contrast microscopy images.

Figure 3.9 shows that EROD activity normalised to proteins (expressed as resorufin pmol per minute per mg protein) was lowest in the untreated control glass. However, it was high in the treated glass samples and highest in the ppAAm coated glass. EROD

activity decreased after 48 hours compared to 24 hours in all the samples. EROD activity of hepatocytes on ppAAm, and gel on ppAAm was not statistically different from collagen type I gel.

Albumin normalised to total cellular protein (Figure 3.10) was low in the untreated control glass, while it was higher and comparable in the other 3 treatments at 24 hours as well as 48 hours. The albumin levels decreased after 48 hours. At both 24 and 48 hours in culture, there was no significant difference between the albumin secreted from hepatocytes plated on collagen type I gel and hepatocytes plated on ppAAm or collagen type gel on ppAAm.

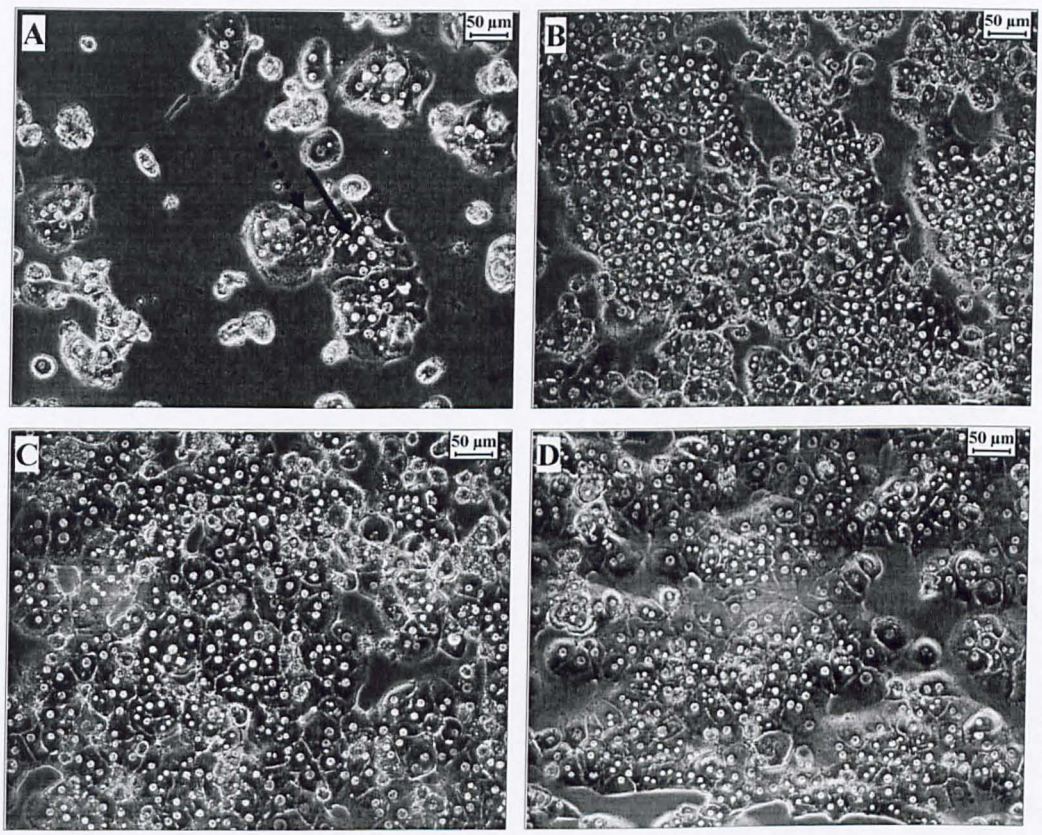

Figure 3.6 Phase-contrast microscopy of rat primary hepatocytes plated on (A) glass, (B) collagen type I gel coated glass, (C) ppAAm coated glass, (D) collagen type I gel on ppAAm coated glass, after 24 hours in culture. The black arrow indicates a bi-nucleated hepatocyte, and the dotted black arrow indicates a mono-nucleated hepatocyte.

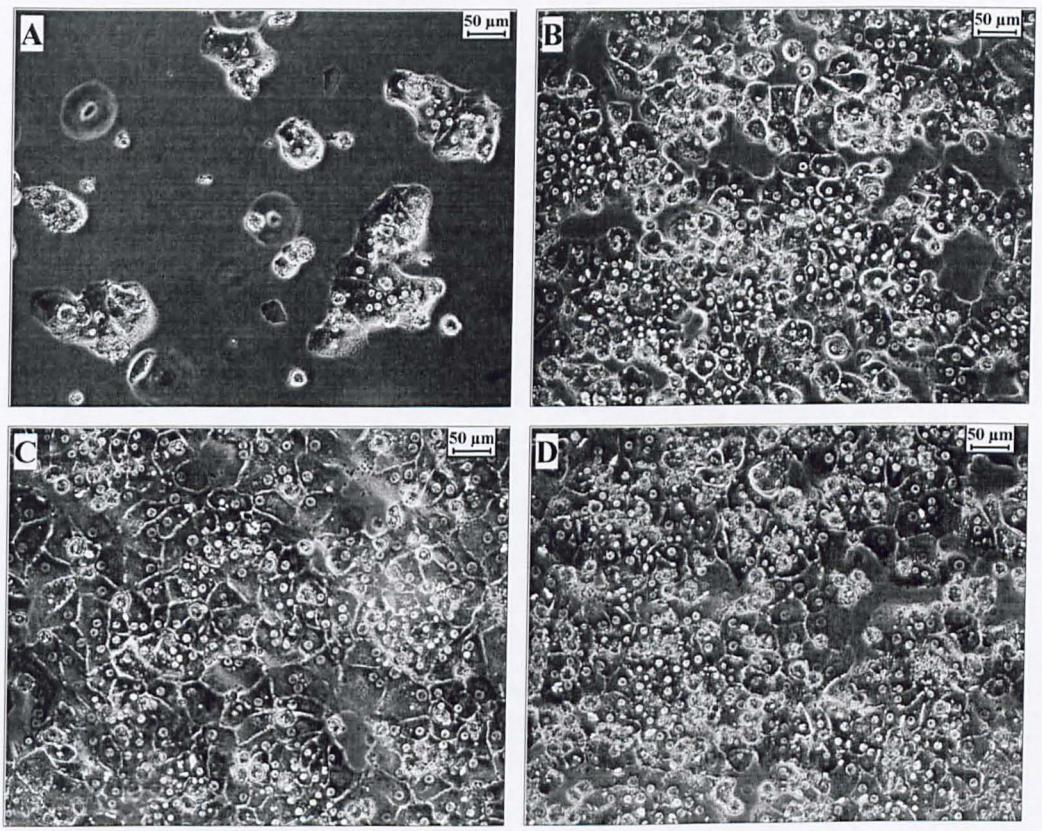

Figure 3.7 Phase-contrast microscopy of rat primary hepatocytes plated on (A) glass, (B) collagen type I gel coated glass, (C) ppAAm coated glass, (D) collagen type I gel on ppAAm coated glass, after 48 hours in culture.

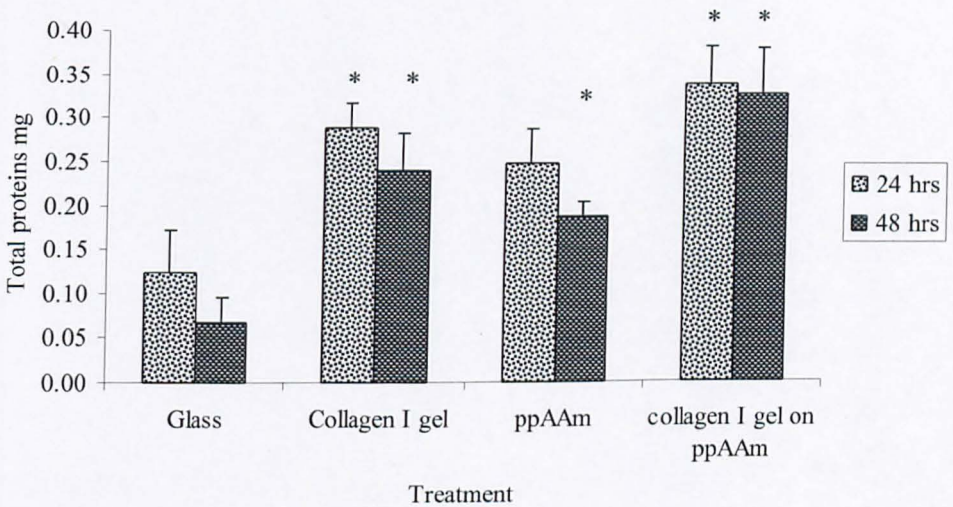

Figure 3.8. Total cellular proteins of primary rat hepatocytes plated on treated and untreated glass at 24 and 48 hours. Mean of 4 experiments (except for glass mean of 3 experiments), error bars indicating sem and results are marked * where data is statistically significant from untreated glass ($p<0.05$, 95% confidence).

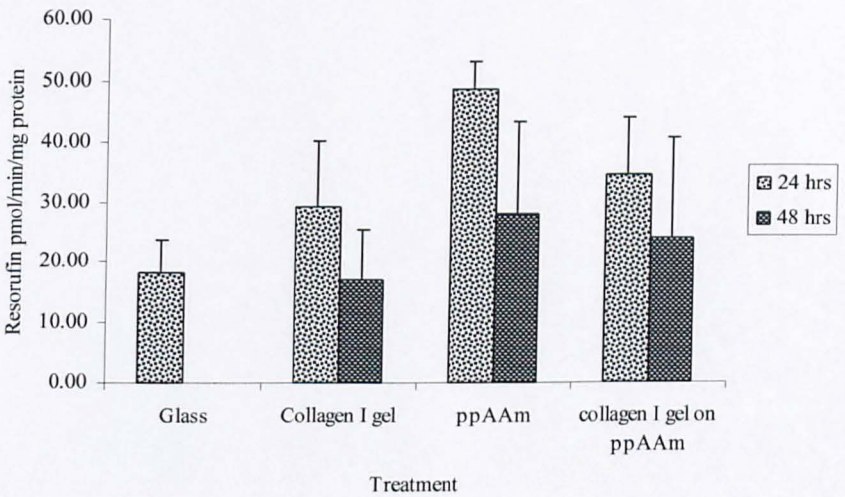

Figure 3.9 EROD activity of primary rat hepatocytes plated on treated and untreated glass after 24 and 48 hours in culture. Mean of 4 experiments (except for glass mean of 2 experiments), error bars indicating sem, ppAAm and collagen I gel on ppAAm are not statistically significant compared to collagen type I gel.

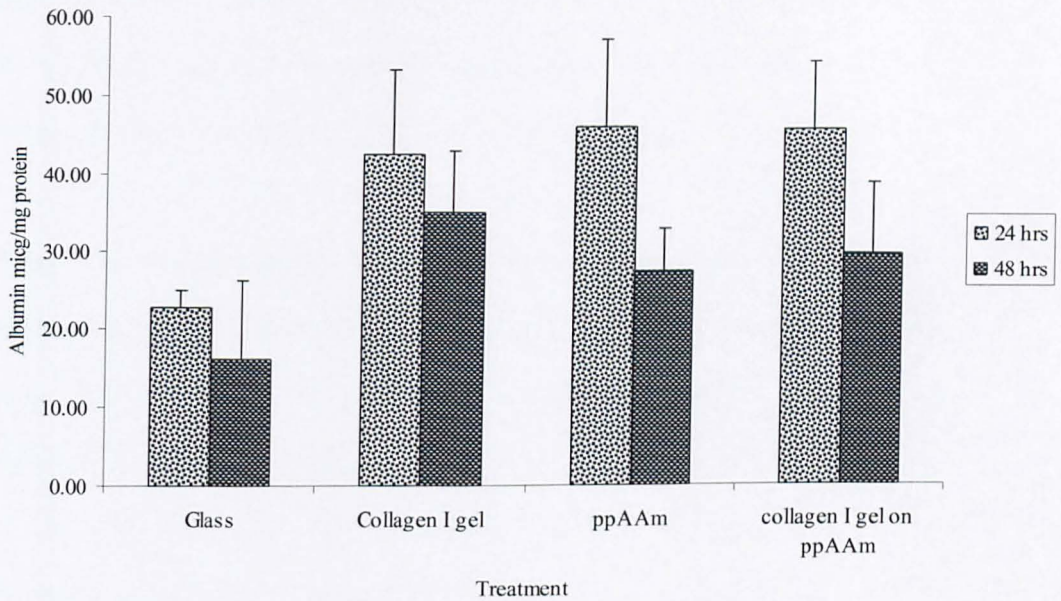

Figure 3.10 Rat hepatocyte albumin secretion on treated and untreated glass after 24 and 48 hours in culture. Mean of 4 experiments (except for glass mean of 2 experiments), error bars indicating sem, ppAAm and collagen I gel on ppAAm are not statistically significant compared to collagen type I gel.

3.5 Discussion

In this chapter, the study of ppAAm coating revealed that it contained nitrogen groups which affected the increase of hydrophilicity of the substrate and cellular attachment. The functional assessment found that the ppAAm film was comparable to collagen gel coating with regards to EROD activity and albumin secretion.

All the coatings used in these experiments showed similar attachment and functionality and were superior to untreated glass. Cellular attachment to substrata is dependent on a variety of factors including the physicochemical properties of the surface (hydrophilicity, surface charge, and the specific chemical functional groups), cell type and the composition of the culture medium. Hydrophilic surfaces have been demonstrated to promote cellular attachment and spreading of hepatocytes (Krasteva *et al.*, 2001), and fibroblasts (Webb *et al*, 1998; Yang *et al.*, 2002). Positively charged surfaces and specific functional groups have been linked with improved attachment of some cell types (Hamerli *et al.*, 2003; Harsch *et al.*, 2000). Using ppAAm or collagen type I gel in this work provided the surfaces with some of these physicochemical properties to achieve cellular adhesion.

The ppAAm coatings of approximately 15 nm introduced nitrogen functional groups to the surface which were not greatly affected by rinsing in water. The chemistry of ppAAm affects both surface hydrophilicity and surface charge in solution. This was confirmed by water contact angle measurements and previous published studies from other groups who reported a contact angle ranging between 50° and 70° for nitrogen rich

plasma films (Hamerli *et al.*, 2003; Harsch *et al.*, 2000; Tseng and Edelman, 1998; Whittle *et al.*, 2002). These nitrogen containing coatings have been found to promote the adhesion of various cell types under static and flowing media (Hamerli *et al.*, 2003; Tseng and Edelman, 1998). Other groups also demonstrated that the concentration of nitrogen groups correlated positively with cellular attachment (Hamerli *et al.*, 2003; France *et al.*, 1998). Tseng and Edelman reported that the seeding and attachment of bovine aortic endothelial cells on polytetrafluoroethylene (ePTFE) vascular grafts under constant or pulsatile flow was drastically enhanced when ePTFE was coated with butylamine plasma deposited films (Tseng and Edelman, 1998). Therefore, these surfaces could be ideal for fluidic bioreactor seeding and cell culture.

Curve fitting of the XPS C1s core level showed that the ppAAm coating contained a high concentration of imines with an increase in the proportion of amines, possibly primary, after rinsing. Similar chemical composition has been reported for ppAAm deposited at nominally the same power by Shard *et al.*; lower amine levels determined in this work probably arise from greater amount of actual power coupled into the plasma and the higher monomer pressure used in this work (Shard *et al.*, 2004).

The mechanism involved in cellular attachment onto ppAAm coated glass coverslips was not investigated, but it is believed that the cells adhere to ppAAm using the same mechanisms for cellular adhesion onto the collagen type I gel. The mechanisms mediating cellular adhesion have been studied extensively and it is widely accepted that protein adsorption, from the serum of the culture media or secreted by the cells, to be the initial step (Kleinman *et al.*, 1981; Lodish *et al.*, 2000; Pierschbacher and Ruoslahti,

1984; Yamamoto *et al.*, 1999). ECM proteins including vitronectin and fibronectin are thought to act as 'adhesive' proteins in this process. The cells recognise specific peptide sequences within these proteins, e.g. RGD, and bind to them via integrin receptors. Integrins transmit these chemical interactions to cytoskeleton proteins in the cells which results in cellular attachment and spreading.

The amount of total cellular proteins of the attached hepatocytes were highest in the samples treated with ppAAm before collagen type I gel coating and this was probably due to a better attachment of the gel to glass as a result of the ppAAm adhesion promotion layer. This is supported by optical observations of gel delamination when applied directly to the glass (data not shown). Furthermore, cells may attach to either collagen type I gel or ppAAm should the collagen type I gel coating be uneven.

The functionality of hepatocytes measured by EROD activity and albumin secretion was greater on the treated samples compared to the untreated control glass. This indicated that ppAAm did not have any obvious adverse effects on the hepatocytes especially as their function was similar to the function of the cells plated on collagen type I gel coated glass. The functionality in all the treatments decreased after 48 hours in culture and this is one of the characteristics of culturing primary hepatocytes. When the primary hepatocytes are isolated from the liver, they de-differentiate by modifying their morphology and functionality to adapt to the new *in-vitro* environment. In basic media, used in this work, the cells do not proliferate and their de-differentiation is followed by cell death (Guillouzo *et al.*, 1990; Guillouzo, 1998). The ppAAm coating did not prevent this *in-vitro* adaptation during the 48 hour culture period, however, it produced a good

attachment that can allow the further investigation of factors involved in *in-vitro* hepatocyte culture.

3.6 Conclusions

In conclusion, ppAAm coating produced a nitrogen containing film on the glass which promoted cellular adhesion similar to the one obtained with collagen type I gel. The ppAAm film contained nitrogen groups which were minimally affected by water during the rinsing method employed. The mechanism mediating the attachment and spreading of the cells are believed to be the same on both surfaces and to be initiated by protein adsorption. The functionality of the hepatocytes was comparable on both ppAAm and collagen type I gel when measured using EROD assay and albumin secretion. Therefore, ppAAm did not induce any unwanted effects on the cells which could alter their functionality and cause toxic effects.

Chapter Four

Hexagonal Glass Etched Bioreactor for *In-vitro* Culture of Hepatocytes

4.1 Introduction

Various bioreactors have been developed to culture rat hepatocytes *in-vitro*. Because of the complexity of the liver, none of these bioreactors encompass all of the liver features. Flat plate bioreactors have been employed to investigate the zonation of liver as the one developed by Bhatia's group, or to investigate the use of liver cells for *ex-vivo* organ replacement as the system developed by Bader's group (Bader *et al.*, 2000; Langsch and Bader, 2001). In addition to the flat plate system, other fluidic bioreactors have been based on culturing the cells in a 2-D monolayer. This includes the multi-channel micro-fluidic system developed by Bettinger and co-workers using poly(glycerol sebacate) (PGS), a novel flexible biodegradable polymer, or the poly(dimethysiloxane) (PDMS) micro-fluidic bioreactor developed by Leclerc and colleagues (Bettinger *et al.*, 2006; Leclerc *et al.*, 2004). Both of these bioreactors aimed to increase the number of cells populating the bioreactor in order to achieve a functional device for *in-* or *ex-vivo* liver replacement tool.

On the other hand, some fluidic bioreactors have been developed with the aim to maintain the 3-D morphology of the liver cells. These include bioreactors culturing cell aggregates such as the one Griffiths and researchers have investigated. The aggregates

can be formed with the support of a scaffold or pre-formed in spinner flasks and then seeded into the bioreactor (Powers *et al.*, 2002a; Powers *et al.*, 2002b; Sivaraman *et al.*, 2005).

Other strategies to maintain the 3-D morphology of the cells was to use extracellular matrix proteins gels in the form of ECM sandwiches (Bader *et al.*, 2000; Langsch and Bader, 2001) or in the form of cells entrapped in gels (Toh *et al.*, 2005).

The substrates that have been used to seed the cells in the different bioreactors reported here varied from glass slides, polycarbonate plates, membranes, silicon, to PDMS and PGS polymers (Bader *et al.*, 2000; Bettinger *et al.*, 2006; Langsch and Bader, 2001; Leclerc *et al.*, 2004; Powers, *et al.*, 2002). Nevertheless, most of these surfaces were coated with collagen to enhance cell attachment especially when seeded with primary hepatocytes.

In this chapter, a novel bioreactor (Figure 4.1-4.3) for *in-vitro* hepatocyte culture was developed and assessed. The design of the bioreactor was inspired from the hexagonal primary structure of the liver. The structure was etched into glass wafers (Figure 4.4) and it comprised a hexagon with 6 internal channels corresponding to sinusoids supplying media into seeded cells. The bioreactor will be described, in this chapter, together with the assessment and the optimisation procedures performed.

4.2 Aims and Objectives

The aim of this study was to develop, assess and optimise a hexagonal bioreactor for potential use as *in-vitro* liver model. The following objectives were set to achieve:

- Assess the viability of liver primary cells and cell lines in the glass etched channels.
- Optimise cell attachment to the etched glass system by coating the glass using various coating techniques including collagen and plasma polymerised allylamine (ppAAm).
- Examine the bioreactor in terms of its utilization and the flow of media through the channels.
- Investigate the survival of both primary liver cells and cell lines in the bioreactor under the following conditions: static media and media flow for varying incubation periods.

4.3 Materials and Methods

4.3.1 The Bioreactor

The main unit of the bioreactor was the medium chamber (Figure 4.1). The chamber had a top lid containing inlets which supplied the medium to the chamber (Figure 4.1). The bottom lid contained a precisely fabricated compartment to position the square glass wafers (Figure 4.2). This also allowed the attachment of outlet part (Figure 4.1 and 4.2). The medium was supplied using a syringe pump purchased from Harvard Apparatus, UK, and the bioreactor was placed in a bench top incubator (Scientific Laboratory supplies, UK) to maintain the temperature at 37° C (Figure 4.3).

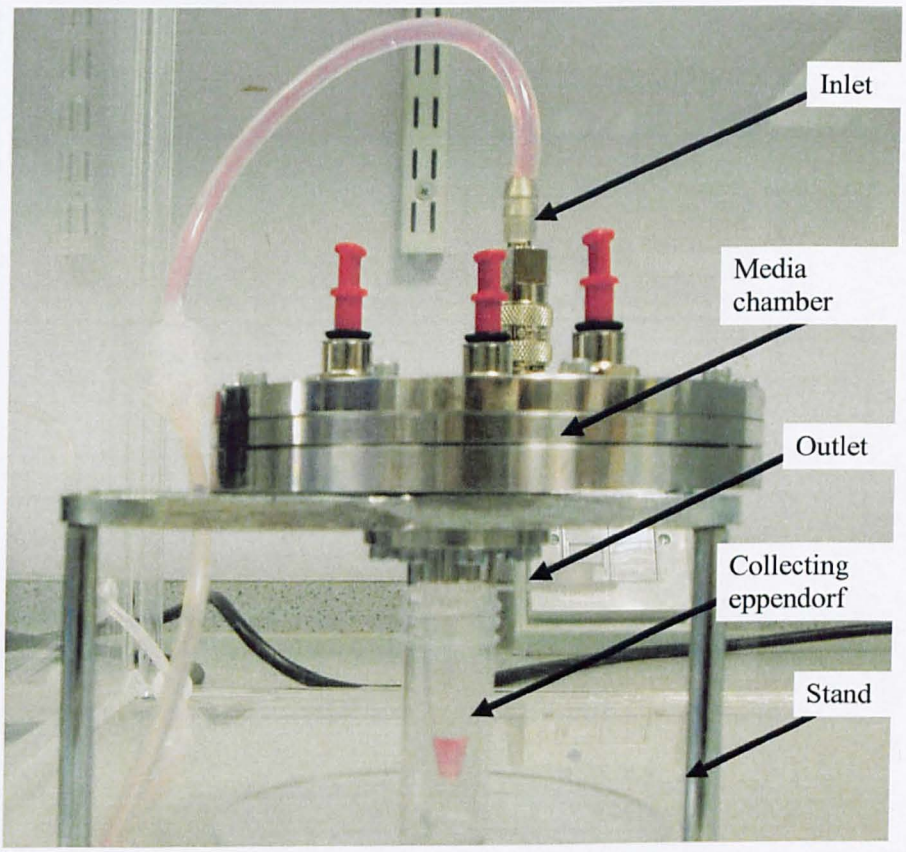

Figure 4.1 A digital image of the hexagonal glass bioreactor labelled with the different parts.

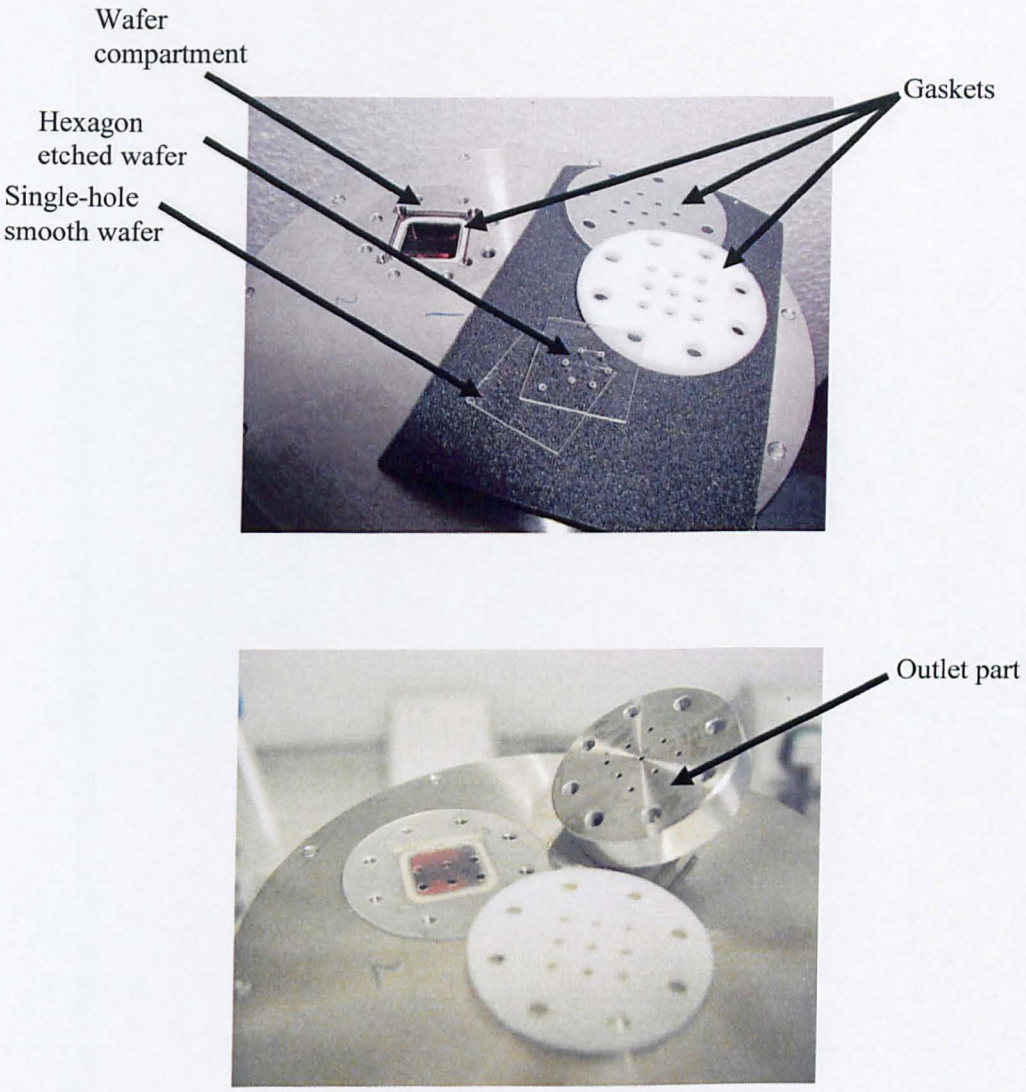

Figure 4.2 Bioreactor parts showing the wafer compartment, glass wafers, various gaskets and the outlet part.

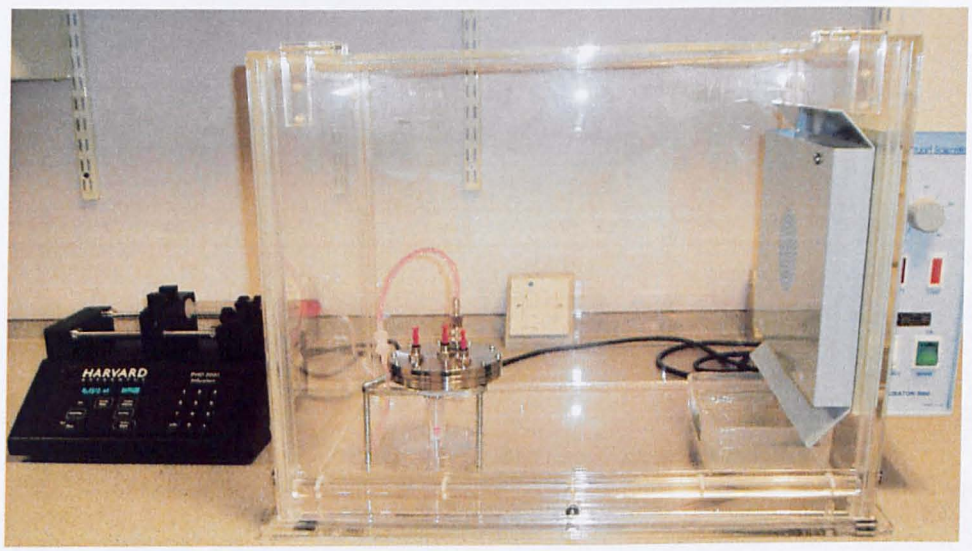

Figure 4.3 A photograph of the hexagonal glass bioreactor in the incubator showing the connections with the syringe pump.

(a)

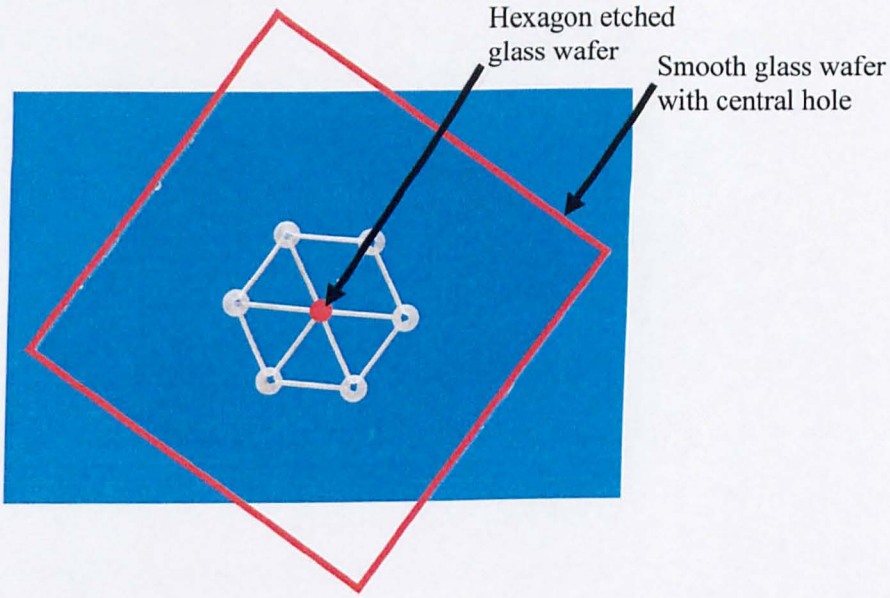

(b)

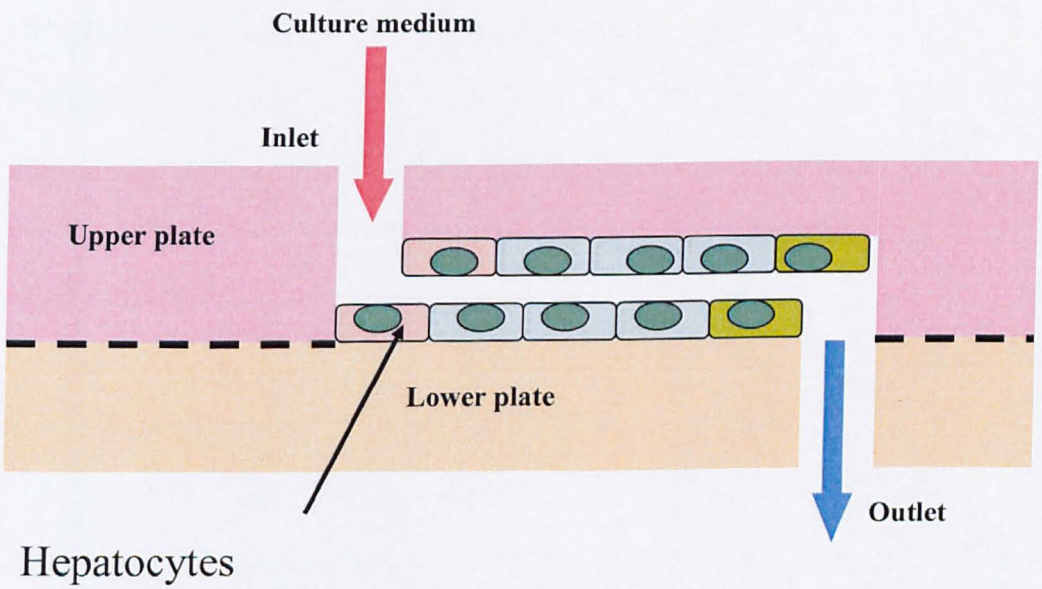

Figure 4.4 (a) An image of the hexagon etched glass wafer with a schematic of the single-hole smooth glass wafer, (b) schematic diagram of a cross section into the cells sandwiched between the two glass wafers.

The square glass wafers had a hexagonal etched pattern of channels which were produced using powder blasting techniques (RAL, Oxfordshire). Two wafers were superimposed in the square compartment of the bottom lid (Figure 4.2 and 4.4). The top wafer was the etched channels with inlet holes at the peripheries and the bottom wafer was smooth and only contained one hole in the centre, forming the outlet (Figure 4.2 and 4.4). The medium entered the inlets and flowed through the channels to leave the hexagonal structure at the central hole.

4.3.2 Processing of Glass for Cell Culture

a) Coating of the Etched Glass Channels for Cell Culture

The glass etched channels were coated for cell culture using various methods. These include: adsorbed collagen on poly(L-lysine) (PLL) coated channels, adsorbed collagen on PLL and poly(DL-lactic acid) (PLA) coated channels, collagen gel on PLL and PLA coated channels, and ppAAm coated channels. ppAAm coating was performed as described in chapter 3.

PLA coating was performed using dip-coating of the glass pieces in 1 mg/ml solution of PLA in chloroform and air dried. When coating with PLL, the appropriate quantity of PLL solution was incubated on the surfaces for 2 hours at room temperature. After the adsorption of PLL on the glass channels, the solution was removed and coating with collagen followed. To adsorb collagen onto the glass, it was incubated with appropriate 0.05 mg/ml solution of collagen in PBS for 2 hours at room temperature or over night at 4° C. The solution was then removed and the glass channels rinsed with fresh PBS. To form collagen gel onto the glass, collagen stock (Cellagen solution AC-3 0.3% collagen)

was diluted using collagen buffer to a concentration of 0.02% and added to the wells containing the glass channels. The collagen solution was shaken well for about 1 minute and the excess removed (all materials used in this coating procedure were maintained cold). The collagen solution was gelled by incubating for 30 minutes at 37° C and then stored at 4° C until used.

Glass wafers containing etched channels were placed in 24- or 6-well plates and cells (PRH, Huh-7) were plated at 1×10^5 cells per cm^2 and FGC4 cells were seeded at 5×10^5 cells per cm^2. When PRH were used, the serum containing media was removed after 1 hr of attachment and the cells were rinsed and incubated overnight in serum-free media. The primary cells were incubated on a shaker (IKA-Schutler MTS4, 50 rpm/min) to prevent culture media stagnation and prolong the longevity of the cells. The cell lines were incubated in serum containing media and under static conditions for 24 hrs. The attached cells were then stained with live/dead stain, for fluorescent and confocal microscopy, or prepared for SEM imaging. The cells were also visualised with phase-contrast microscopy.

b) Cleaning Procedures of the Glass Etched Channels

After cell culture, the glass wafers were incubated in diluted trigene overnight to destroy biological materials. The glass was then cleaned with 7X detergent and sonicated twice in distilled water. After that, the glass wafers were air dried in class I laminar flow cabinet. Because the glass wafers coated with ppAAm were re-used, they were further cleaned by exposing them to oxygen plasma for 10 minutes at 20 W. All the glass wafers

were cleaned using the same method with the exception of trigene incubation on their first use.

c) XPS Analysis

XPS was performed to determine the extent of ppAAm in the channels and compare it to the smooth glass on their side.

d) Confocal Microscopy

To determine the extent of the penetration of collagen coating into the etched glass channels, collagen was stained using an immunostaining method and visualised using a confocal microscope. The proteins in the collagen gel samples were blocked by incubating the samples with a serum-free protein block solution (DAKO-Cytomation, UK) for 10 minutes at room temperature. This was followed by the incubation with the primary antibody, mouse anti-collagen type I monoclonal antibody (1:2,000) (Sigma, UK), for 60 mins. The samples were washed with PBS and incubated with FITC conjugated anti-mouse antibody (10 μg/ml) (Vector, UK) for 60 mins. Finally, the samples were washed in PBS and visualised with confocal microscopy. Confocal microscopy was also employed to assess the efficacy of cell attachment into etched glass channels after staining the cells with live/dead staining kit.

4.3.3 Avidin-biotin Seeding Technique

a) Glass Surface Treatment (Figure 4.5)

The ppAAm coated glass channels were incubated with 6 ml of Biotin-X-NHS (Calbiochem, UK) at a concentration of 50 μg/ml in sterile distilled water in a 6-well

plate for 6 hrs at room temperature. The channels were then rinsed twice in sterile distilled water. After which they were incubated with 5 ml of avidin (Sigma, UK) at a concentration of 80 μg/ml in avidin buffer (Appendix 8.1) for 1 hr at room temperature. FTIC-avidin (Sigma, UK) was used to determine the efficacy of the above reaction. The channels were rinsed with PBS, and kept in PBS until cell seeding (same day).

b) Cell Surface Modification (Figure 4.6)

Huh-7 cells were trypsinised and counted. Then, they were incubated 1mM sodium periodate (Sigma, UK) in PBS (1 ml/million of cells) for 5 min at 4° C. The cells were centrifuged and washed with avidin buffer and then washed with biotin buffer (Appendix 8.2). After that, the cells were incubated with 5 mM biotin hydrazide in biotin buffer for 15 mins on a shaker at 37° C (slow shaking to prevent cell damage). The cells were centrifuged and washed twice in avidin buffer (Appendix 8.1) before suspending them in media. The cells were counted and then seeded at the desired density (Figure 4.7). To determine the efficacy of the procedure, some cells were plated in a tissue culture treated 6-well plate overnight and incubated in 2 ml of FITC-avidin at a concentration of 10 μg/ml in avidin buffer for 15 mins at 37° C. These cells were then visualised using fluorescent microscopy.

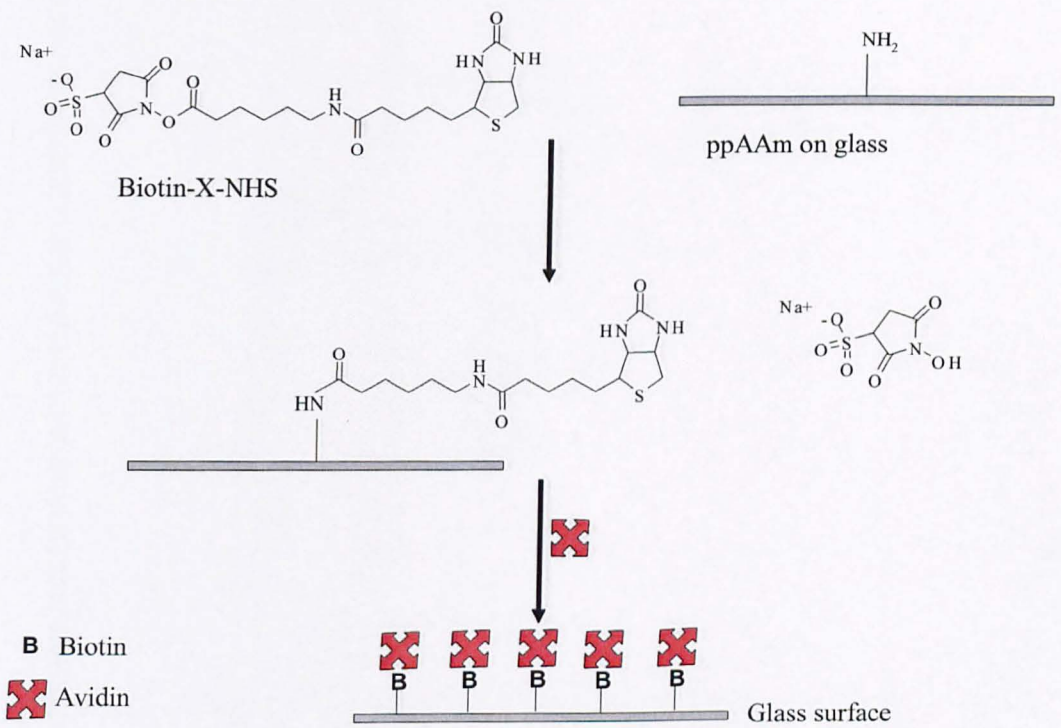

Figure 4.5 Schematic diagram demonstrating surface treatment of the glass channels using biotin-avidin technique.

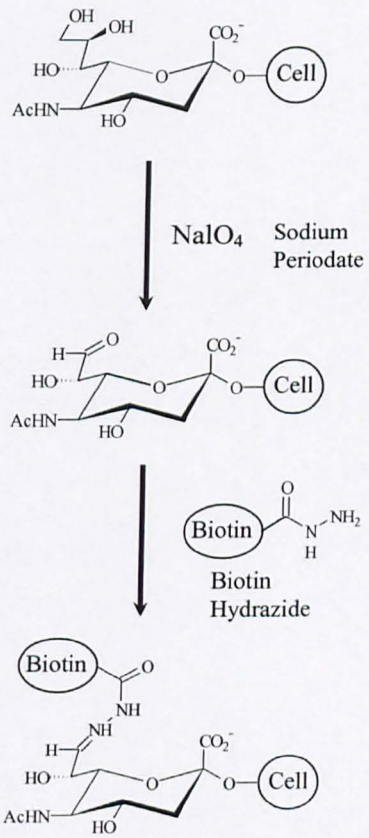

Figure 4.6 Schematic diagram illustrating the biotinylation of the cells through the two-step sodium periodate/ biotin hydrazide method (De Bank *et al.*, 2003).

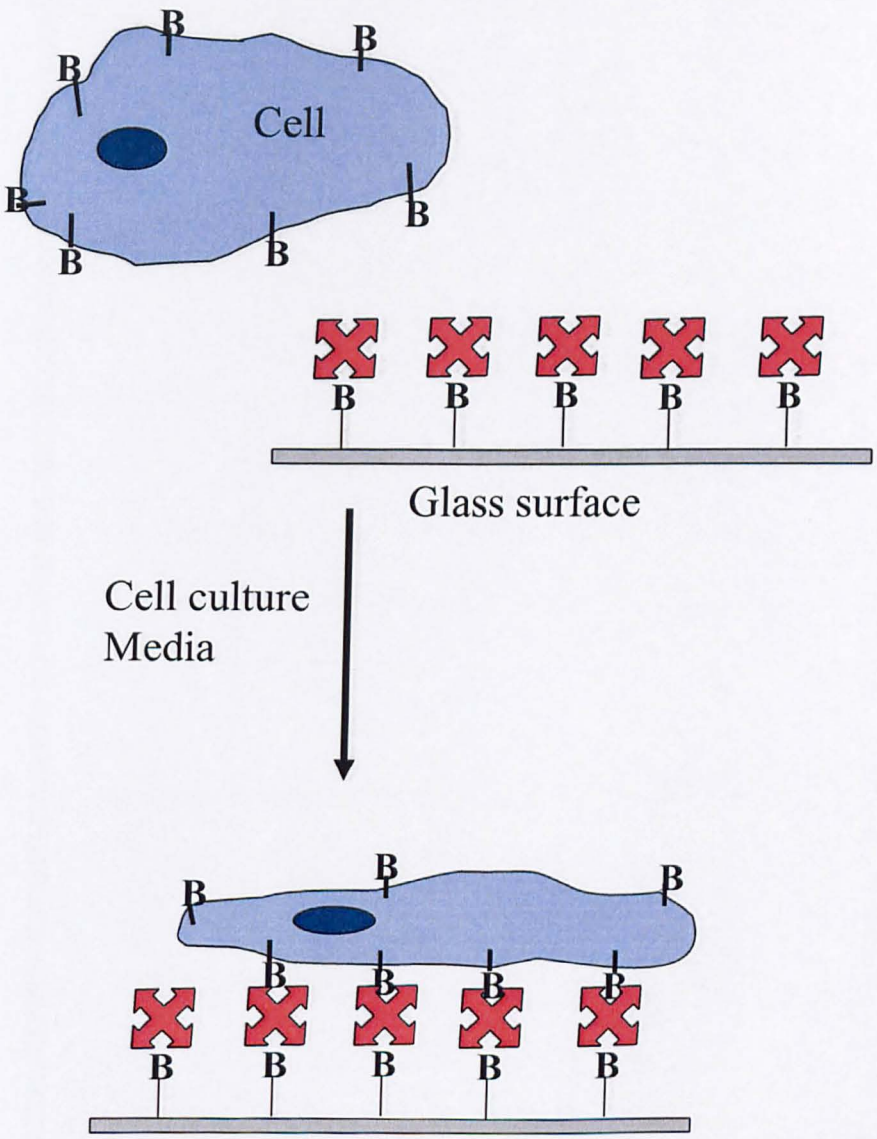

Figure 4.7 Schematic diagram of the engineered cell-substrate attachment through biotin-avidin technique (B: biotin, red shape: avidin).

4.3.4 Flow Experiments

The volume of the channels was calculated using the half-cylinder equation as follows:

$$\text{Volume} = (\pi \times \text{radius}^2 \times \text{height}) / 2.$$

For example: volume of media flowing through the hexagon

Volume inner channels = $[(3.14 \times 0.15^2 \times 3)/2] \times 6 = 0.63\ mm^3 = 0.63\ \mu l$

In the case of the hexagons, there were 6 channels with flowing media (inner channels) and 6 channels filled with static media (outer channels). The flow rate was calculated with respect to the inner channels only. The flow rate was set so that the medium filling the inner channels changed at least once per minute. Therefore, these flow rates were used 60, 100, 200 and 400 μl/hr respectively. The output media was collected in an eppendorf and weighed to determine the volume of the media and compare it to the theoretical expected volume.

The medium was set to flow through the system for 1, 3 and 6 hrs and the attachment of the cells before and after the experiments was assessed by staining the cells with live/dead staining kit. The cells used for flow experiments were incubated under static conditions for 24 hrs after seeding into the channels before their placement in the bioreactor. After the flow experiment, the wafers were removed from the bioreactor, placed in a well plate. The cells were washed three times with PBS and stained and visualised for live/dead using fluorescent microscopy (Chapter 2). For these flow experiments, ppAAm coating and biotin-avidin seeding technique were examined.

4.4 Results

4.4.1 Cellular Attachment into Glass Etched Channels

PRH attachment to glass etched channels was promoted with various coating procedures including adsorbed collagen on PLL, adsorbed collagen on PLA and PLL, collagen gel on PLA and PLL and ppAAm. When PRH were seeded into channels coated with PLL and adsorbed collagen, the cells died after 24 hrs as indicated with live/dead stain (Figure 4.8 C). Phase-contrast microscopy, SEM analysis and the fluorescent microscopy of the live/dead stain in these cells in figure 4.8 showed that their morphology was round which was due to absence of attachment and spreading of the cells. The pre-coating of the channels with PLA improved the survival of the cell on both adsorbed collagen and collagen gel (Figure 4.9). However, SEM analysis of PRH (Figure 4.9 A-D) seeded onto collagen gel showed that PRH had more 3-D like morphology than the cells plated onto adsorbed collagen coating. PRH were also seeded into ppAAm coated channel (Figure 4.9) and their survival and morphology after 24 hrs incubation was similar to the PLA, PLL and adsorbed collagen. Figure 4.10 illustrates some disadvantages observed when coating the channels with PLA, PLL and adsorbed collagen or collagen gel. These drawbacks include the gel blocking the channels during the coating process, the gel or the PLA layer detaching form the glass at any stage of the experiments. Various hepatoma cell lines, Huh-7, Hep G2 and FGC4 cells, were assessed for their adhesion and survival into ppAAm coated glass etched channels. They all showed good attachment, distribution in the channels and viability as indicated in figure 4.11 (Hep G2 cells not shown).

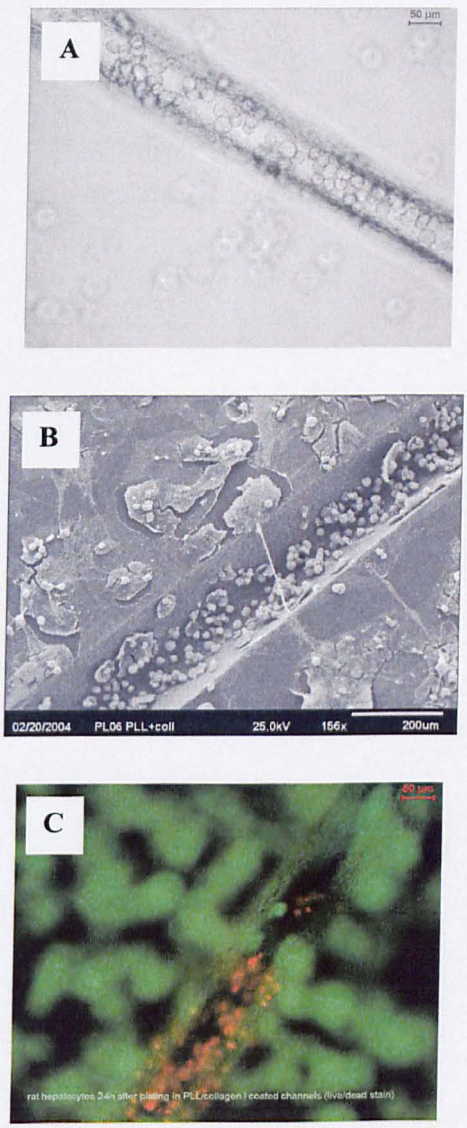

Figure 4.8 (A) Phase-contrast image, (B) SEM image and (C) live/dead stain of PRH plated on adsorbed collagen on PLL coated etched glass channels.

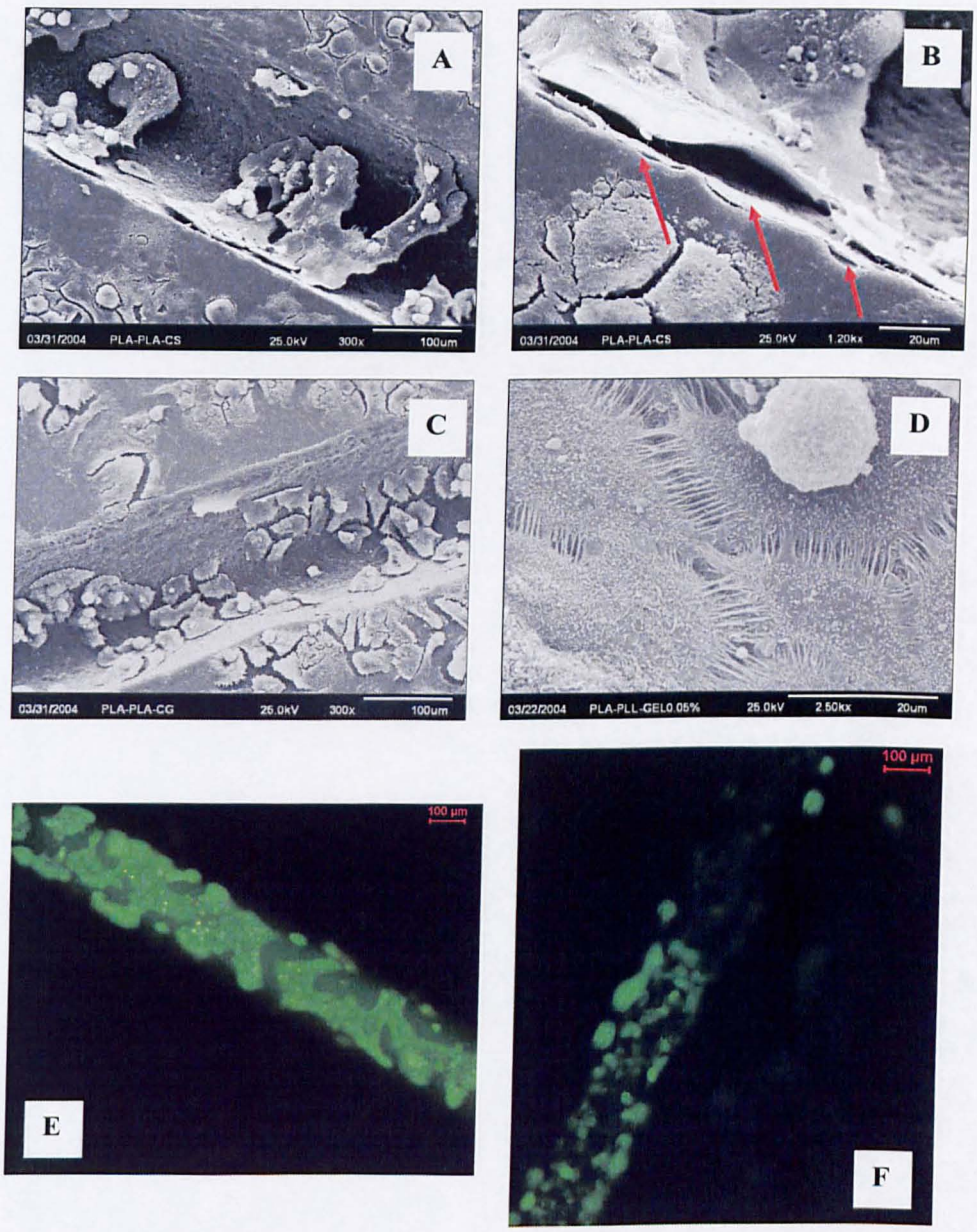

Figure 4.9 (A,B) SEM images of PRH plated on PLA, PLL and adsorbed collagen coated channels, (C, D) SEM images of PRH seeded on PLA, PLL and collagen gel coated channels, (E) live/dead stain in PRH plated on PLA, PLL and collagen gel coated channels, (F) live/dead stain in PRH plated on ppAAm coated channels.

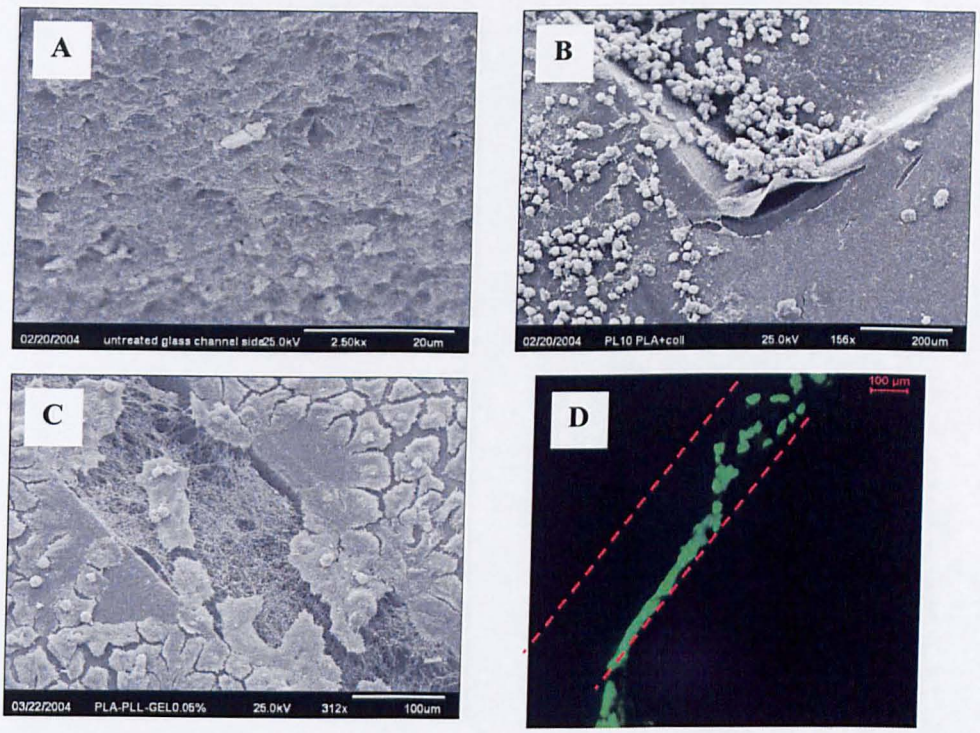

Figure 4.10 (A) SEM image of the etched glass, (B) SEM image of PRH plated into etched glass channels coated with PLA and adsorbed collagen, (C) PRH seeded into glass etched channels coated with collagen gel on PLA and PLL and (D) live/dead stain in PRH plated into glass etched channels coated with collagen gel on PLA and PLL.

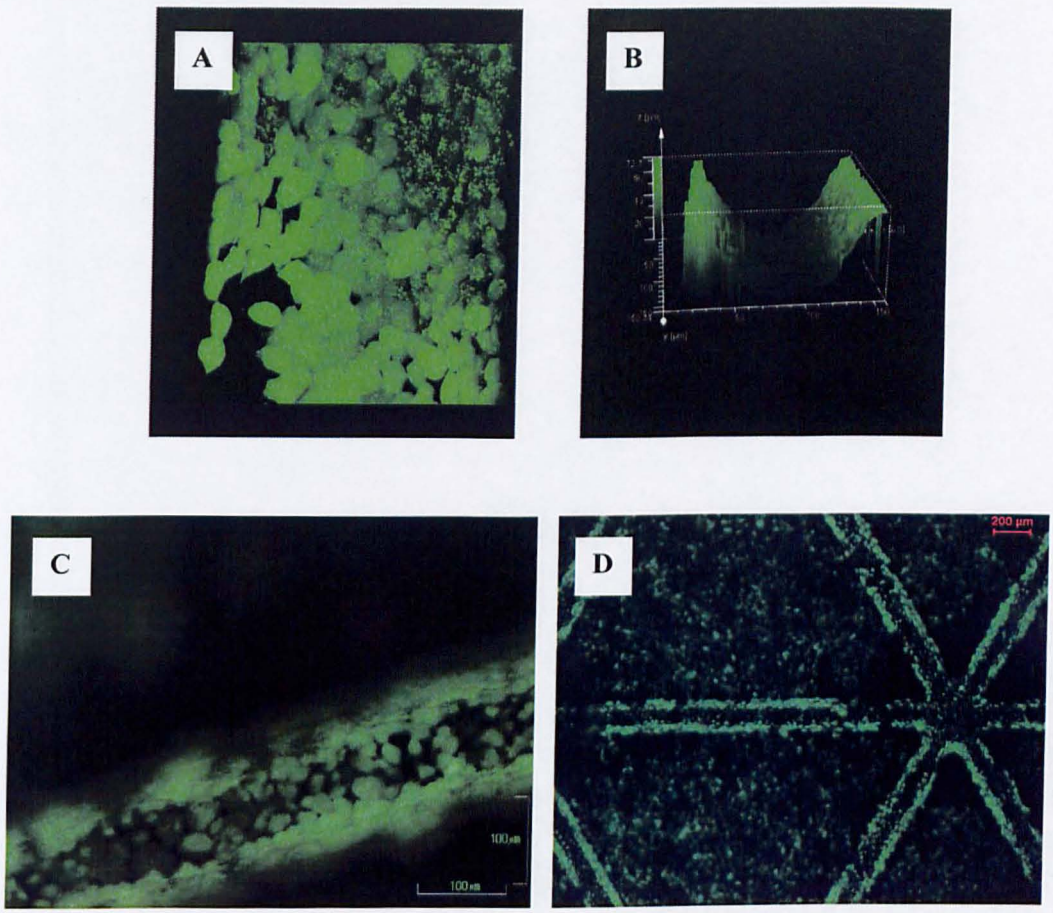

Figure 4.11 Distribution of (A, B) FGC4 cells into glass etched channels coated with ppAAm when a live/dead stain was analysed with confocal microscopy, (C) Huh7 cells plated into ppAAm coated channels and (D) hexagons when a live/dead stain was captured using a fluorescent microscopy. All images were taken 24 hrs after seeding and incubation under static conditions in a 6-well plate.

4.4.2 Analysis of Collagen Coating and ppAAm

Confocal microscopy analysis was employed as a tool to determine the efficiency of collagen coating. Figure 4.12 shows that the coating penetrated the channels and covered the smooth part of the glass wafers as well. Nevertheless, there was a stronger signal from collagen gel and both the gel and adsorbed collagen were not evenly distributed with stronger signal observed in some areas.

The XPS analysis of untreated smooth glass surrounding the channels and untreated etched glass channels revealed the same elemental composition of silica based glass (Figure 4.13). The percentage elemental composition of the smooth glass surrounding the channels/etched glass channel was respectively: O (60/60), C (13/15), and Si (26/26). After ppAAm coating, XPS analysis demonstrated that the coating of ppAAm on the etched glass channel and the smooth glass surrounding the channels attenuated the core level peaks originating from elements representing the glass, which was mainly silica (Figure 4.14). The XPS results obtained for both the smooth glass surrounding the channels and the etched glass channel showed similar elemental composition after the ppAAm treatment. This was represented as smooth glass surrounding the channels/etched glass channel: O (10/10), C (71/71), and N (20/19). The best fitting achieved of the C1s core level with synthetic peaks taken from databases and other literature of both spectra indicated the presence of four functionalities (Figure 4.15). These components were hydrocarbon, amine, imine or alcohol/ester/ether and carbonyl as indicated in Figure 4.15. These were fitted at shifts of 1, 1.5 and 2.9 eV respectively from the hydrocarbon (285 eV).

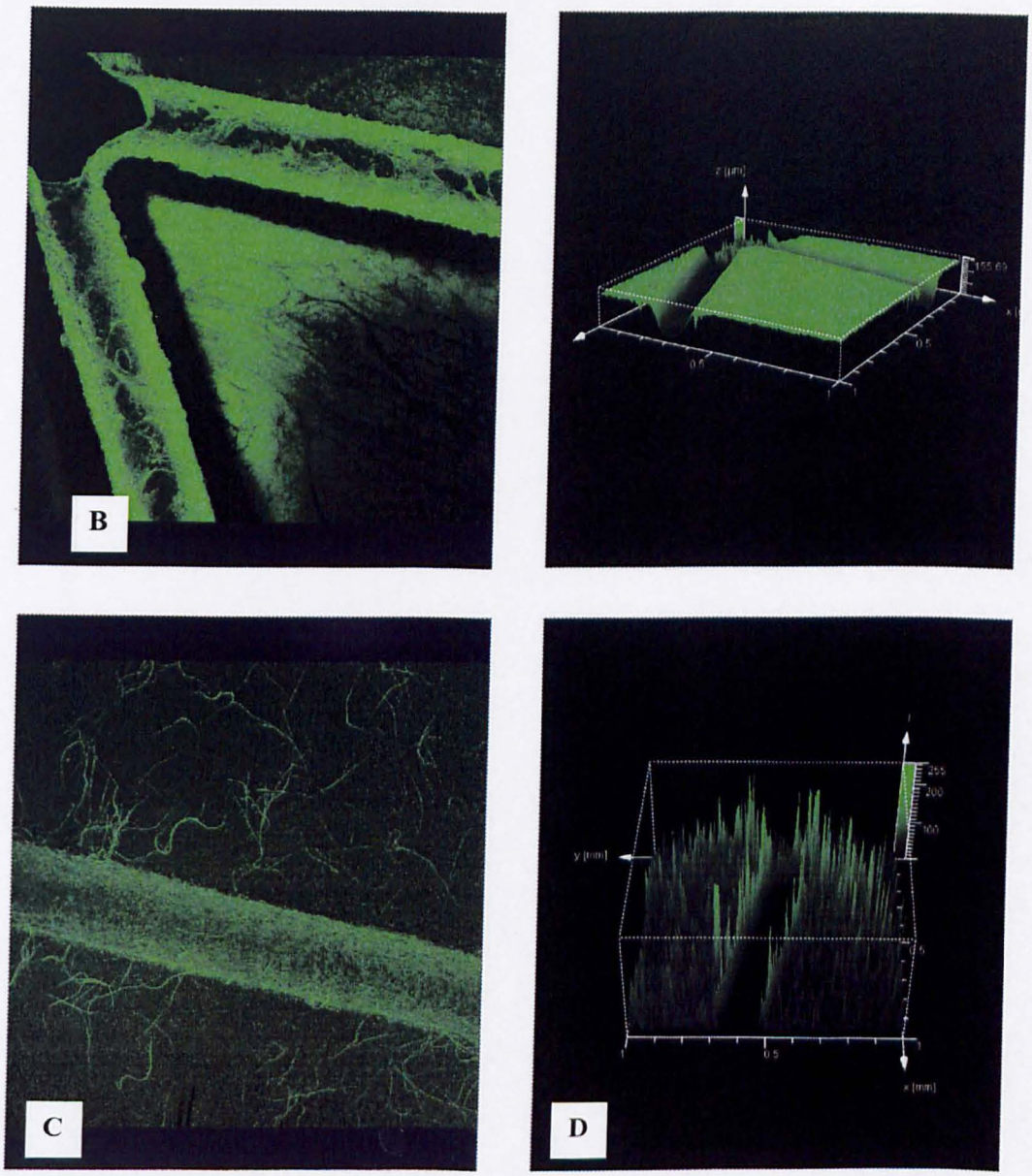

Figure 4.12 Confocal microscopy analysis of collagen coating into glass etched channels. (A) A composite and (B) a 3-D view of collagen gel coated channel, (C) a composite and (D) a 3-D view of collagen adsorbed into etched glass channels.

(a)

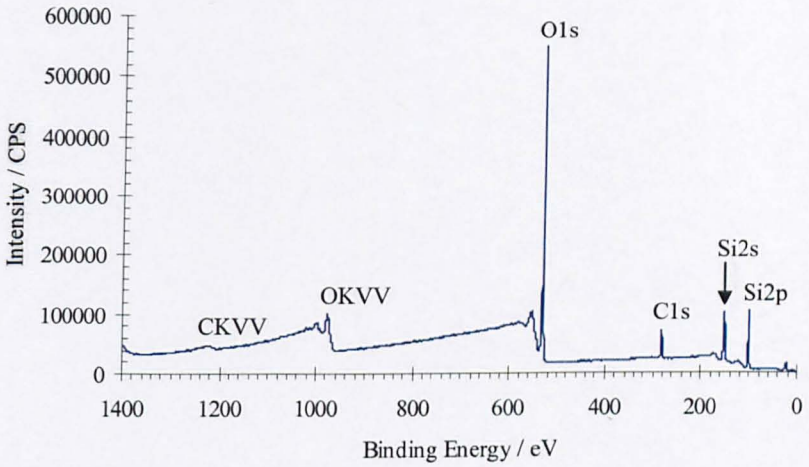

(b)

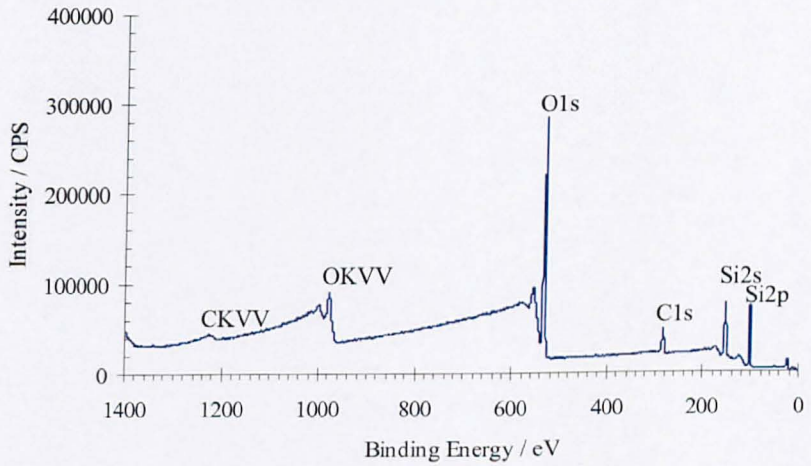

Figure 4.13 XPS survey scan from uncoated (a) smooth glass surrounding the channels and (b) etched glass channels.

(a)

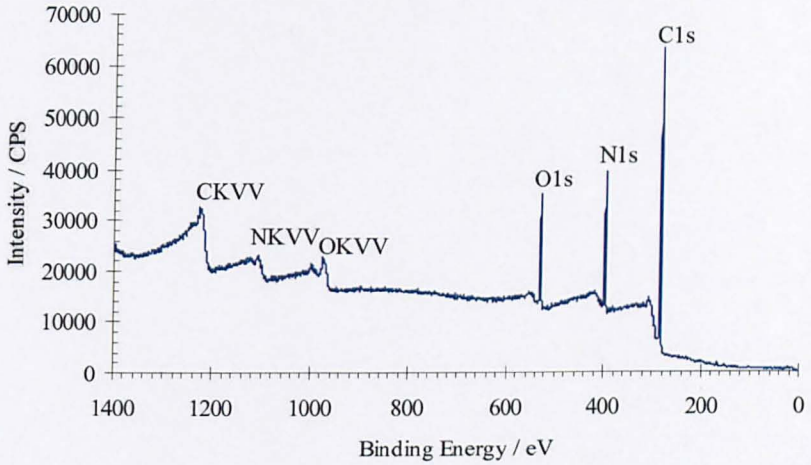

(b)

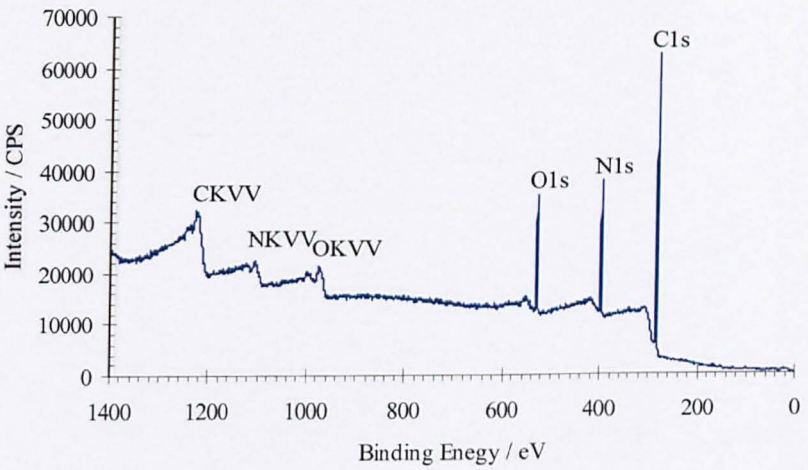

Figure 4.14 XPS survey scan from ppAAm film on (a) smooth glass surrounding the channels and (b) glass etched channel.

(a)

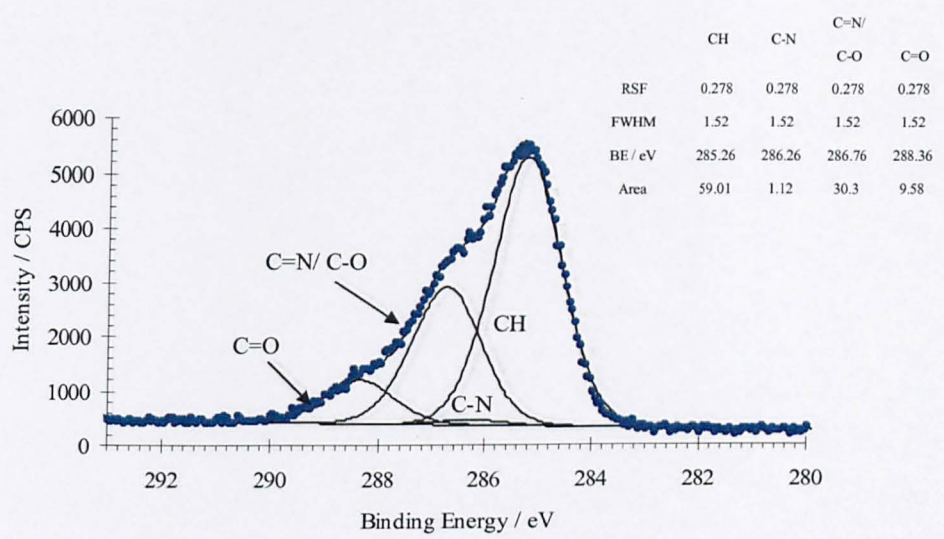

(b)

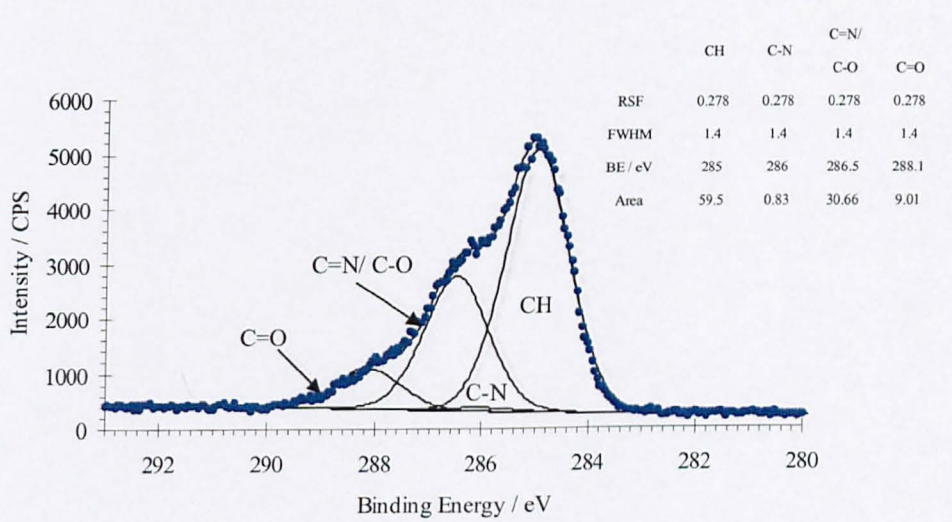

Figure 4.15 C1s narrow scan from the ppAAm on (a) smooth glass surrounding channels and (b) glass etched channel.

4.4.3 Assessment of the Survival of Huh-7 Cells in the Bioreactor

In the absence of media flow, Huh-7 cells survived an incubation period of 5 hrs in the bioreactor and few dead cells were observed at the edges of the channels and the inlets/ outlets (Figure 4.16). After 24 hr, all the cells were detected dead with the live/dead stain (Figure 4.16). This was observed using both ppAAm coated channels and the avidin-biotin method.

Using media flow, apparent differences were observed with the ppAAm coated glass. These were detachment of the cells after 24 hrs incubation and cell death and detachment over shorter incubation times at higher flow rates. Media flow rate and the duration of the incubation were inversely related to the survival and attachment of the Huh-7 cells. The lowest flow rate used was 60 µl/hr and 5 hrs incubation resulted in the observation of viable cells as shown in figure 4.17. When the flow rate was increased, the cells died quicker and detached from the surface as can be observed from figure 4.18 when a flow rate of 200 µl/hr was used. When the time of incubation was extended to 24 hrs, the cells died and detached from the surface of the channels even at the lowest flow rate employed (60 µl/hr) (Figure 4.17).

The avidin-biotin seeding technique, improved the attachment of the cells to the glass etched channels and it was observed that the cells died but did not detach at high flow rates (100 and 200 µl/hr) over 24 hrs incubation (Figure 4.19). The avidin-biotin seeding technique reduced cell viability prior to seeding (Figure 4.19 A), but batches having a viability of less than 80%, as calculated with trypan blue stain, were excluded from the experiments.

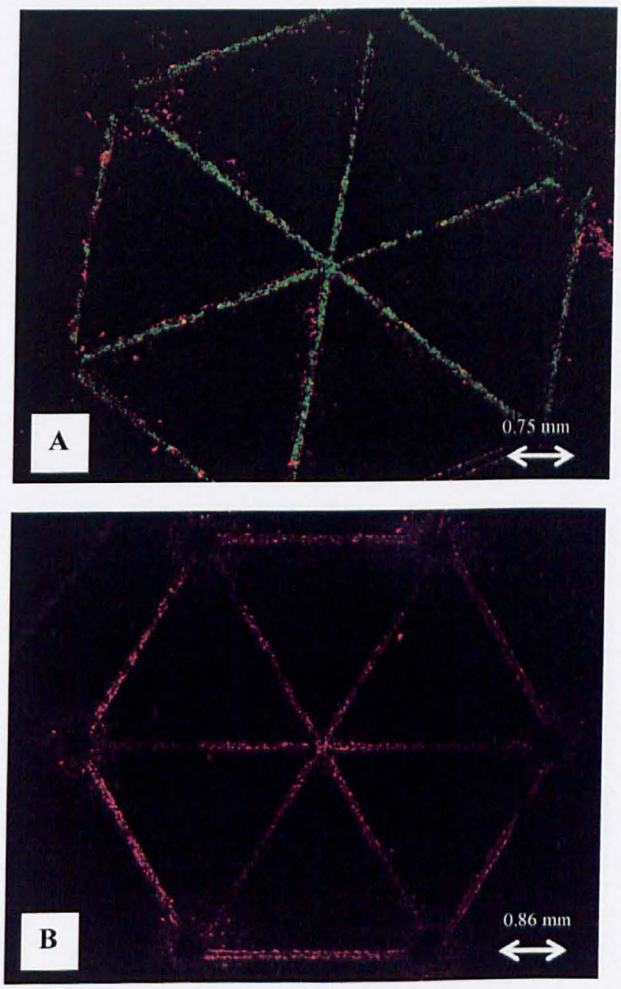

Figure 4.16 Live/dead stain in Huh-7 cells plated into ppAAm coated glass etched hexagons after (A) 5 hrs and (B) 24 hrs incubation in the bioreactor with no flow of media. The images were taken with Nikon stereo-microscope.

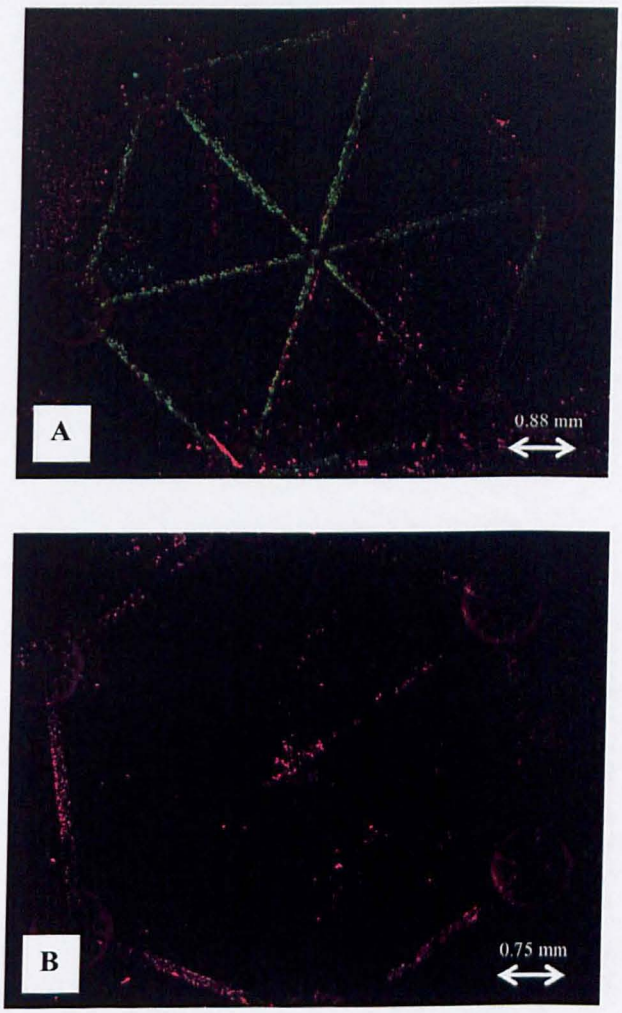

Figure 4.17 Live/dead stain in Huh-7 cells plated into ppAAm coated glass etched hexagons after (A) 5 hrs and (B) 24 hrs incubation in the bioreactor with media flow at a flow rate of 60 µl/hr. The images were taken with Nikon stereo-microscope.

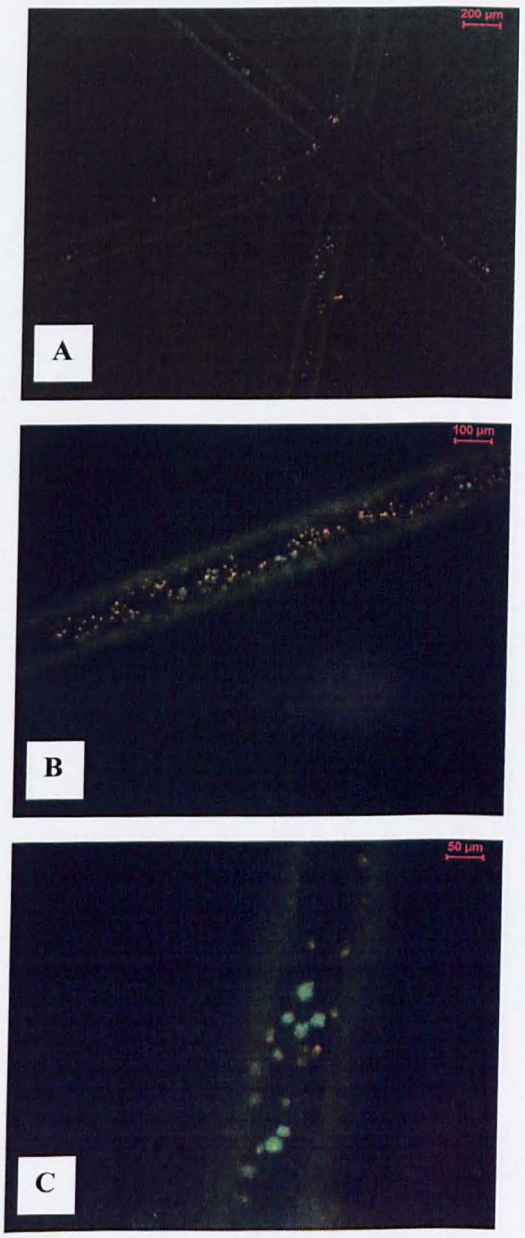

Figure 4.18 Huh-7 cells plated into ppAAm coated hexagons (A) after flow of media at a flow rate of 200 µl/hr for 5 hrs; (B) represents a channel at the peripheries of the hexagon and (C) represents an inner channel.

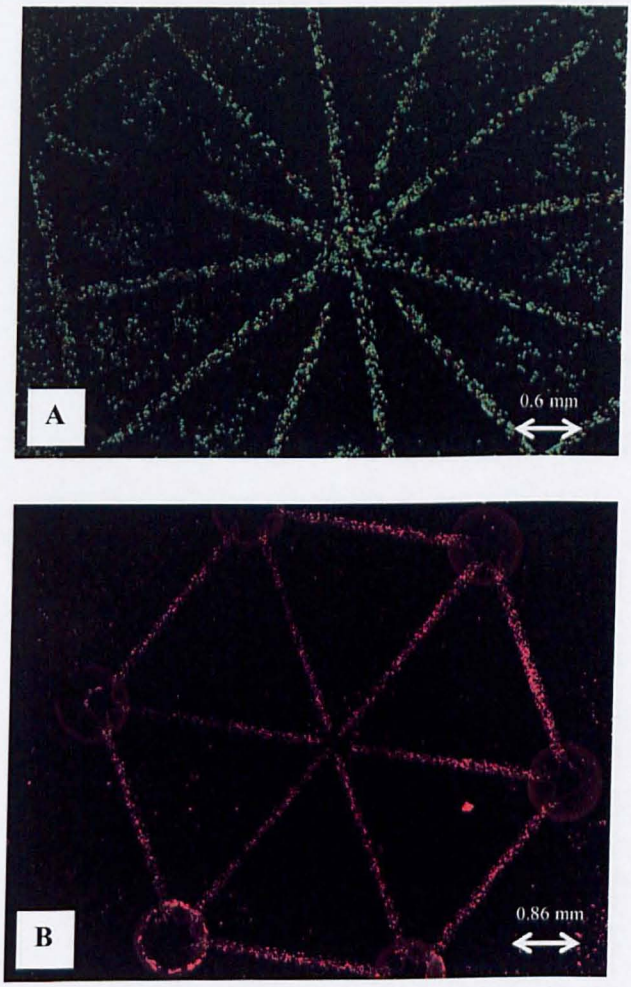

Figure 4.19 Live/dead stain in Huh-7 cells plated into glass etched hexagons using avidin-biotin technique (A) 24 hrs after seeding into a different shape of hexagons under static conditions in a well-plate and (B) after 24 hrs incubation in the bioreactor with media flow at a flow rate 200 µl/hr. The same results were obtained with flow rates of 60 and 100 µl/hr for 24 hrs. The image was taken with Nikon stereo-microscope.

Under media flow using both seeding methods, the cells attached at the edges of the channels died and detached quicker than the cell in the channels (Figure 4.20). This was also observed near the outlet as represented in figure 4.21.

Other observations from the analysis of various microscopy images were: the alignment of the outlet with the hexagon (Figure 4.21); the detachment of confluent cell mono-layers from the smooth glass surrounding the channels (Figure 4.22); air bubbles at the inlets (Figure 4.22).

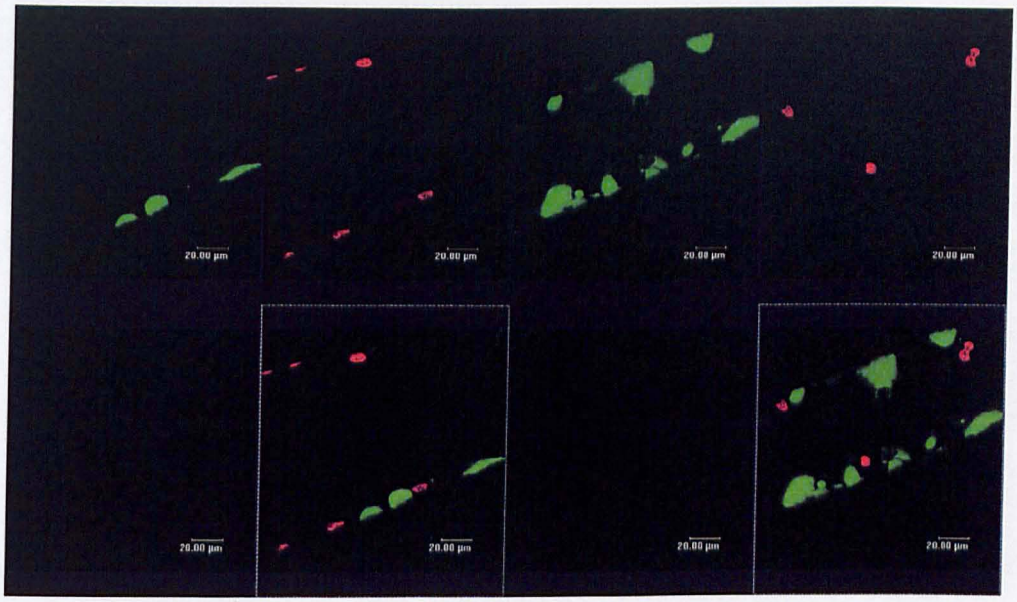

Figure 4.20 Confocal microscopy images of live/dead stain in Huh-7 cells seeded into ppAAm coated hexagons after an incubation in the bioreactor for 2 hrs at a flow rate of 100µl/hr. The images illustrate the effects of the flow on the cell attached to the top edges of the channels.

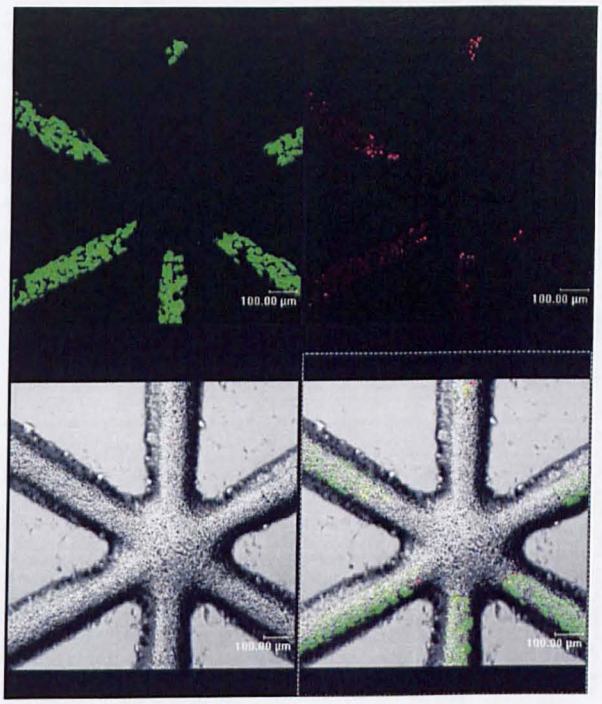

Figure 4.21 Confocal microscopy images of live/dead stain in Huh-7 cells seeded into ppAAm coated hexagons after an incubation in the bioreactor for 2 hrs at a flow rate of 100µl/hr. The images illustrate the distribution of the cells at the outlet of the hexagon.

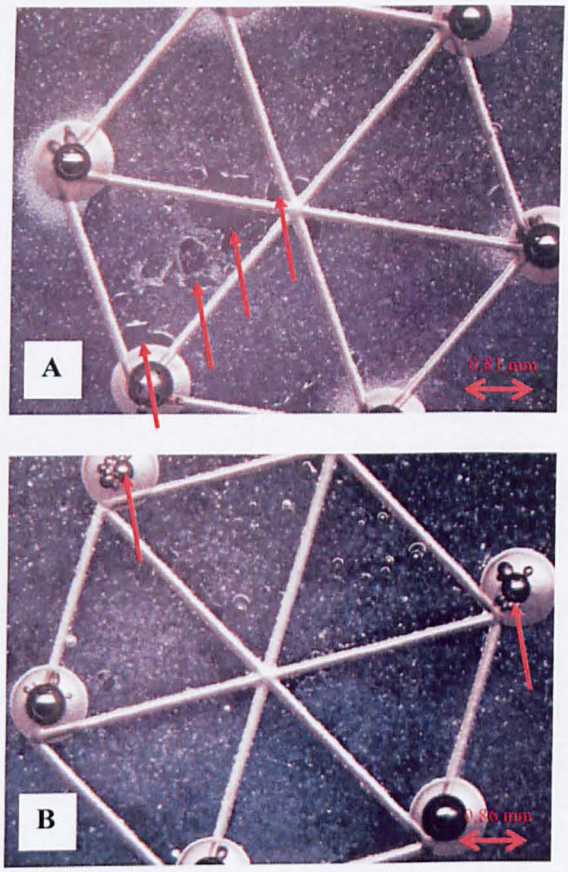

Figure 4.22 Light stereo-microscope images of Huh-7 cells seeded into (A) uncoated glass etched hexagons and (B) ppAAm coated glass etched hexagons.

4.5 Discussion

In this chapter, various substrate coating techniques, including ppAAm, were demonstrated to improve the adhesion of cells into the glass etched channels of the hexagonal bioreactor. Seeding the cells into the glass etched channels after ppAAm coating or via avidin-biotin seeding method was established to be the most appropriate procedures for use in the flow through bioreactor. The avidin-biotin technique was found to provide a better adhesion during the flow experiments. However, the cells incubated in the flow through bioreactor were shown to have a limited survival time.

4.5.1 Cellular Attachment into Glass Etched Channels

PRH cells were round in shape and died when seeded into glass etched channels coated with PLL and adsorbed collagen because of poor attachment and spreading into the rough glass. Lack of oxygen and nutrients in the channels was not considered to be a cause of cell death as there was enough media in the well-plates to cover the glass wafers. Various modifications of the coating technique were examined. Pre-coating the channels with PLA aimed to reduce the roughness of the glass and therefore improve cellular adhesion. The smoothing effect of PLA was primarily observed in SEM imaging of the different samples of the tested coatings. Figure 4.9 B (red arrows) illustrates that PLA filled the groves of the etched glass and decreased its roughness. On the top of the PLA and PLL, a collagen layer was added in the form of gel or a thin adsorbed ECM layer. This influenced the spreading of PRH cells which maintained a more 3-D like morphology on the collagen gel compared to adsorbed collagen (Figure 4.9). The morphology of primary hepatocytes has been extensively studied and the morphology

observed in this work on the two collagen surfaces agreed with the literature (Kaufmann *et al.*, 1997; Michalopoulos and Pitot, 1975; Talamini *et al.*, 1997; Wang *et al.*, 2004)

Despite the improvement achieved in the coating procedures, there were concerns that the coatings could affect the performance of the bioreactor during media flow experiments. The two main problems were the coatings detaching from the glass substrate and the collagen gel filling the channels. The detachment of PLA, PLL and collagen coating was not only detected during SEM imaging, but was also observed during phase-contrast and fluorescent microscopy (Figure 4.10). Some of the visible detachment could be attributed to the drying processing of the samples prior to SEM microscopy. The collagen coating was effective for both collagen gel and adsorbed collagen in coating the glass etched channels (Figure 4.12). However, results obtained with the coating procedures employed were not consistent as the collagen gel was uneven in thickness (Figure 4.12). This led, in some experiments, to filling the channels with gel which resulted in the loss of the channel shape (Figure 4.10).

For these reasons, ppAAm was chosen as an alternative coating method especially when the cell attachment and viability in ppAAm coated channels was similar to the results obtained on PLA, PLL and adsorbed collagen. The morphology was not investigated but it was believed to be similar to PRH plated on adsorbed collagen. Various cell lines, including HepG2, FGC4 and Huh-7 cells, showed good adhesion and spreading into ppAAm coated channels (Figure 4.11).

4.5.2 Analysis of ppAAm Films

The analysis of the ppAAm coating with XPS revealed that the elemental composition of the smooth glass surrounding the channels and etched glass channels was similar before and after coating with ppAAm. The analysis also determined that ppAAm on smooth glass and glass etched channels had similar functionalities with similar percentages. These results concluded that the rough surface of the channels did not affect the ppAAm film produced and the functionalities introduced. These XPS results were similar to the results obtained from the XPS analysis of the ppAAm films on the coverslips reported in chapter 3.

There are numerous studies showing the use of plasma films in coating 2-D surfaces and 3-D scaffold. As reported by Barry and collaborators, the plasma penetrated the scaffolds and a gradient of intensity of the film was formed from the surface of the scaffold to its centre (Barry *et al.*, 2005; Barry *et al.*, 2006). The glass etched channel was not a smooth surface, a flat surface or a scaffold. However, it was a rough curved surface which could be compared to the surface of porous 3-D scaffolds. The roughness of the surface of the glass was similar to the roughness of the surface of the scaffolds created by the presence of pores. On these surfaces, a similar result to coating a flat smooth surface was obtained during plasma polymer coating.

4.5.3 Assessment of the Survival of Huh-7 Cells in the Bioreactor

When the Huh-7 cells seeded glass wafers were placed in the bioreactor and incubated under no media flow, the cells stained fluorescent green with live/dead stain after 5 hrs incubation which concluded that they were alive (Figure 4.16). However, a 24 hrs

incubation under the same conditions resulted in red stained cells which revealed the death of the cells and this was probably due to diminishing nutrients and oxygen in the channels of the hexagon. When there was no continuous flow of media in the channels, the cells consumed the nutrients and oxygen in the media filling the channels and over a period of time this decreased gradually until the starvation of the cells and their death occurred. With continuous media flow, the nutrients and oxygen in the media filling the channels were replenished by changing the media in the channels of the hexagon. Therefore, with media flow the cells received constantly fresh media and were expected to survive longer in the channels.

Media flow rate was varied in the experiments performed. Increasing the flow rate inversely correlated to cell survival in the channels. As a result of increasing the flow rate of media, the duration of cell incubation in the bioreactor was limited because the cells died and detached. The main reason for this was probably shear stress of media flow. Other contributing reasons include the bioreactor and the general set up, air bubbles blocking the flow of media into the channel (Figure 4.22), ppAAm did not achieve adequate attachment for a fluidic system.

Introducing the biotin-avidin seeding method improved the attachment of the cells for the media flow experiments. Nevertheless, the cells still died after 24 hrs incubation period in the bioreactor (Figure 4.19). The reasons for this were unclear especially when the blockage of the media flow by air bubbles in the system was unlikely. The assessment of the volume of the collected media from the outlet of the bioreactor

revealed the same volumes as theoretically calculated using flow rate and duration of incubation (Results not shown).

Avidin could adsorb onto the ppAAm coated glass surface. In this work, no blocking steps were used in the experiments to prevent non-specific adsorption of avidin in order to maximise the number of avidin groups on the surface. The purpose was to increase the number of avidin-biotin bonds linking the cells and the glass substrate. The method of the avidin-biotin technique employed in this chapter was adapted from the study published by De Bank and associates and other unpublished research by the group. The avidin-biotin bond was employed by various groups to seed scaffolds (Kojima *et al.*, 2006) or to form homo- and heterogeneous aggregates (De Bank *et al.*, 2003; De Bank *et al.*, 2007).

In a study where HepG2 cells were seeded onto porous poly(L-lactic acid) (PLLA) scaffolds using the avidin-biotin method, the cells proliferated and their functionality was minimally altered (Kojima *et al.*, 2006). However, the technique was different from the one reported in this chapter and it involved the adsorption of avidin onto the surface and the use of EZ-Link®Sulfo-NHS-LC-LC-Biotin reagent to add Biotin onto the cell surface (Kojima *et al.*, 2006). The work published by De Bank and the tissue engineering group demonstrated that the avidin-biotin linking method potentiated control over cell aggregation and accelerated aggregate formation with maintaining the functional and differentiation abilities of the cells including embryonic stem cells (De Bank *et al.*, 2003; De Bank *et al.*, 2007). There is a high affinity binding between avidin and biotin with four biotin binding sites for each avidin molecule. This receptor-ligand

interaction is similar to interactions occurring during cellular adhesion such as integrin-fibronectin. Studies investigating affinity constant of such binging interactions between the ligand and the receptor have demonstrated that avidin-biotin interaction has an affinity constant of 10^{15} M^{-1} while integrin-fibronectin interaction has an affinity of 10^{6} M^{-1} (Akiyama *et al.*, 1985; Codogno *et al.*, 1987; Green, 1975; Terranova *et al.*, 1983).

The cells, attached to the channels at the peripheries of the hexagons, did not detach in most of the experiments, even at high flow rates. These cells died but were still attached when visualised using fluorescent microscopy. This emphasised that the media flowed through inner channels only and there was a stagnation of media in the channels at the peripheries of the hexagons. In the experiments that resulted in cell death and detachment in the inner channels of the hexagons, the order of these events was unclear. The cells at the edges of the channels detached quicker than the cells in the middle of the channels and this was probably due to the set up and the way the bioreactor was assembled together. At the centre of the hexagons (outlet), the cells detached quicker and the main reason was probably the flow of media and the shear stress.

The concerns about the bioreactor that need to be addressed were the alignment of the glass wafers (hexagon and outlet), media chamber and its size, visualisation of the channels and the media flow without having to stop the experiment and open the bioreactor.

4.6 Conclusions

Finally, the ppAAm coating improved the attachment of the cells to the glass and it was comparable to other coating techniques used. In addition, the ppAAm was simpler to perform and quicker than the multiple coating procedures involving collagen coating. However, ppAAm coating was not sufficient to keep the cells attached during flow experiments. Other methods, including biotin-avidin seeding technique showed more promising results in the bioreactor.

This bioreactor for liver *in-vitro* engineering was a new concept. The glass, despite being widely used in tissue culture, demonstrated some disadvantages in this hexagonal system. These were primarily related to cellular-substrate attachment. This could be overcome in the future as the aim was to use the glass as prototype ahead of the fabrication of plastic based hexagons. In addition, some parts of the bioreactor could benefit from change of material from stainless steel to clear material, such as Perspex®, to be able to view the glass channels during the flow experiments.

Chapter Five

Attachment of Huh-7 and Primary Rat Hepatocytes into Uncoated, Collagen and ppAAm Coated Ibidi Channels

5.1 Introduction

Various flat plate bioreactors have been used for *in-vitro* cell culture and specifically for PRH culture and toxicology studies. However, the majority of these systems are seeded with cells before the assembly of the bioreactor. The system developed by Bhatia and colleagues consisted of a glass slide that was seeded and incubated for attachment for a few days before assembly into a flow through chamber (Allen and Bhatia, 2003; Allen *et al.*, 2005). Other materials have been used in the fabrication of flat plate bioreactors and these include gas-permeable membranes such as the one developed by Bader's research group (Bader *et al.*, 2000; Langsch and Bader, 2001), and poly(dimethylsiloxane) such as the bioreactors investigated by Fujii and colleagues (Leclerc *et al.*, 2004).

Most of these fluidic systems employ ECM coating, predominantly collagen in 2-D and 3-D geometries in the form of thin coatings, gel layers and gel sandwiches to promote cellular adhesion and achieve the desired cell morphology (Allen and Bhatia, 2003; Allen *et al.*, 2005; Bader *et al.*, 2000; Langsch and Bader; 2001; Leclerc *et al.*, 2004).

Plasma polymers, including plasma polymerised allylamine (ppAAm), have been reported to promote cellular attachment in static and flow through cultures (Barry *et al.*, 2005 and 2006; Dehili *et al.*, 2006; Tseng and Edelman, 1998). Plasma polymerised allylamine coating was also demonstrated to penetrate complex structures such as porous scaffolds (Barry *et al.*, 2005 and 2006) leading to enhanced cellular diffusion and adhesion. In addition, these polymers did not display any toxic or undesirable effects on hepatocytes according to the research carried out in our laboratories and the available literature.

Ibidi channel (http://www.ibidi.de/products/slidel.html) consists of a gas permeable thin base plastic of a thickness of 0.18 mm. The channel dimensions are 50×5×0.4 mm which results in a surface area of 2.5 cm^2 and a volume of 100 µl. Each end of the channel is equipped with a well to supply media to the channel. These wells also act as air bubble traps once the channel was inserted in the flow through set-ups used in the study. As the channels are pre-assembled, the cells have to be seeded in-situ. Moreover, the surface of Ibidi channels is hydrophobic with a contact angle of 89° which does not favour cell attachment. Therefore surface coating was necessary prior to cell seeding of both primary cells and cell lines.

5. 2 Aims and Objectives

The aim of this chapter was to seed collagen and ppAAm coated Ibidi channels with a confluent mono-layer of Huh-7 or PRH cells in order to start media flow incubation. These aims were reached through the achievement of the following objectives:

- Three different surfaces were assessed for cell seeding and attachment. These were uncoated channel, collagen coated channel and ppAAm coated channel.
- The seeding density of the cells was optimised for both Huh-7 cells and PRH by seeding various densities varying between 2.5×10^5 and 1×10^6 cells per channel.
- The appropriate time to start the flow of media after seeding was examined for both cell types.
- For PRH, various ppAAm coatings were assessed by investigating the attachment of PRH to ppAAm of increasing deposition time of the polymer.
- Characterisation of ppAAm by X-ray photo-electron spectroscopy (XPS) and contact angle measurements to determine the nature of the surface.
- The morphology of the cells was examined and compared between static media and media flow incubations at 24 hrs to determine the survival of the cells in the micro-environment of the channels.
- The effects of flow shear stress on Huh-7 cells were investigated by incubating Huh-7 seeded into uncoated, collagen coated and ppAAm coated channels with media flow at various flow rates.

5.3 Materials and Methods

5.3.1 Surface Coating

Uncoated Ibidi (Figure 5.1) channels were purchased from Ibidi, Germany (Thistle Scientific, UK). The channels were used for cell culture as uncoated or they were coated with plasma polymerised allylamine (ppAAm) or adsorbed rat tail collagen type I.

a) ppAAm Coating

The channels were placed in the plasma chamber and coated as described in Chapter 3. The channels were coated for 7, 10 and 20 mins. For comparison, Ibidi sheets were also coated with ppAAm for 10 mins, which was the same duration of coating of the coverslips in Chapter 3. The ppAAm coated materials were stored in a desiccator overnight before cell culture.

b) Collagen Coating

Collagen (Upstate, UK) was dissolved in PBS to a final concentration of 0.05 mg/ml. The channels were filled (100 µl) with the collagen solution and incubated at 37° C for 2 hrs. The collagen was removed by adding PBS to one end of the channel and aspirating it from the second end. The channels were further washed with PBS. The collagen coated channels were used immediately or stored at 4° C overnight.

5.3.2 Characterisation of ppAAm Coating

The properties of ppAAm film in the coated channels were assessed with XPS and contact angle measurements. Ibidi sheets were also examined with XPS and contact angle before and after coating with ppAAm as described in Chapter 3.

(a)

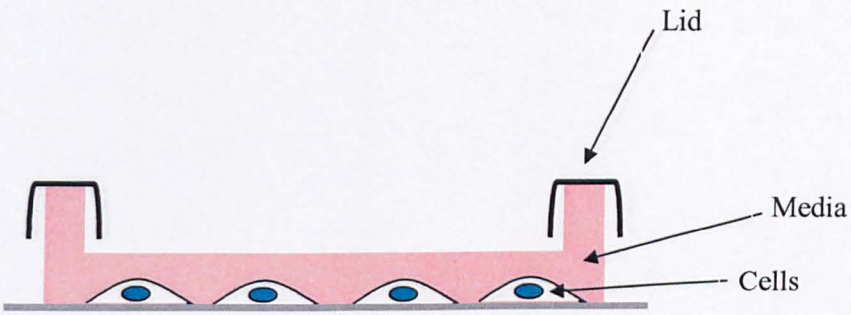

(b)

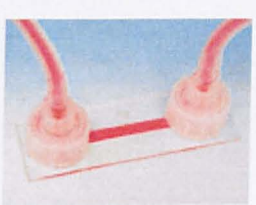

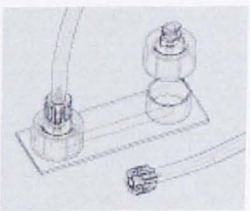

Figure 5.1 (a) Schematic diagram of the flat plate (Ibidi) channel, (b) images of the flat plate channel (http://www.ibidi.de/products/slideI.html).

a) XPS Analysis

After plasma coating the channels, the surface was analysed by XPS within 24 hrs. The bottom of the channel was gently cut and removed with scalpel blade and tweezers. This sheet of Ibidi polymer was divided into 10 areas of 5 mm width and then 3 spots were scanned in each area.

b) Contact Angle Measurements

The bottom of the channel was removed as describe earlier and divided into an average of 10 areas. The contact angle was measured an average of two contact angle measurements was taken for each area.

5.3.3 Cell Culture

The channels were placed in large petri-dishes (Scientific Laboratory Supplies, UK) during all the procedures.

a) Huh-7 Cell Culture

After trypsinising and counting the cells, they were plated at 2.5×10^5 cells per channel (100 µl, surface area of 2.5 cm^2). The channels were placed in an incubator at 37° C for about 2 hrs before cell seeding and the media was kept warm until cell seeding to prevent air bubble formation. The cells were incubated to attach for 1 hr and then media was changed and the reservoirs at both ends of the channels were filled with 1 ml of media. The cells were incubated for another 2 hrs until assembled in the flow through set-up with a flow rate of 100 µl/min or static as control. With the exception of media flow in the bioreactor flow set-up, the cells were kept under static conditions at all times. The channels supplied with static media were fixed in

the form of bridges in order to provide the cells with adequate gas supply through the gas-permeable bottom sheet of the channels.

In flow through circuits, Huh-7 were maintained in Leibovitz (L)-15 media supplemented with antibiotic/antimycotic cocktail (100 U/ml penicillin, 100 µg/ml streptomycin and 250 ng/ml amphotericin B) and L-glutamine (2 mM).

b) PRH Cell Culture

PRH were isolated as described in chapter 2 and maintained in (L)-15 media supplemented with 10 % FCS and antibiotic/antimycotic cocktail (100 U/ml penicillin, 100 µg/ml streptomycin and 250 ng/ml amphotericin B) and L-glutamine (2 mM) until seeded into the channels. The channels were placed in an incubator at 37° C for about 2 hrs before cell seeding and the media was kept warm until cell seeding to prevent air bubble formation. Various cell seeding densities were examined to seed PRH. These were 2.5×10^5, 5×10^5, 7.5×10^5 and 10×10^5 cells per channel. The cells were incubated under static conditions to attach for 1 hr and then they were washed with serum-free L-15 media. After that, the reservoirs at both ends of the channels were filled with 1 ml of serum-free L-15 media. The channels were tilted a few times to change the media in the channels. This enabled the cells to receive enough oxygen and nutrients for survival while the flow through set-up was being prepared. The cells were imaged using phase microscopy and then introduced in the flow through set-up with a flow rate of 50 µl/min overnight, or kept static as control. The following day, the cells were imaged using phase-contrast microscopy as described in chapter 2. Media reservoirs in the flow through set-up contained 50 mls of serum-free PRH media.

5.3.4 Flow through Media Circuit

The flow through set-up (Figure 5.2) was a closed circuit that comprised a media reservoir connected with silicone and Marprene tubing (Scientific Laboratory Supplies, UK) to a peristaltic pump (Watson-Marlow, UK). The media reservoir had an opening to allow an exchange of gases.

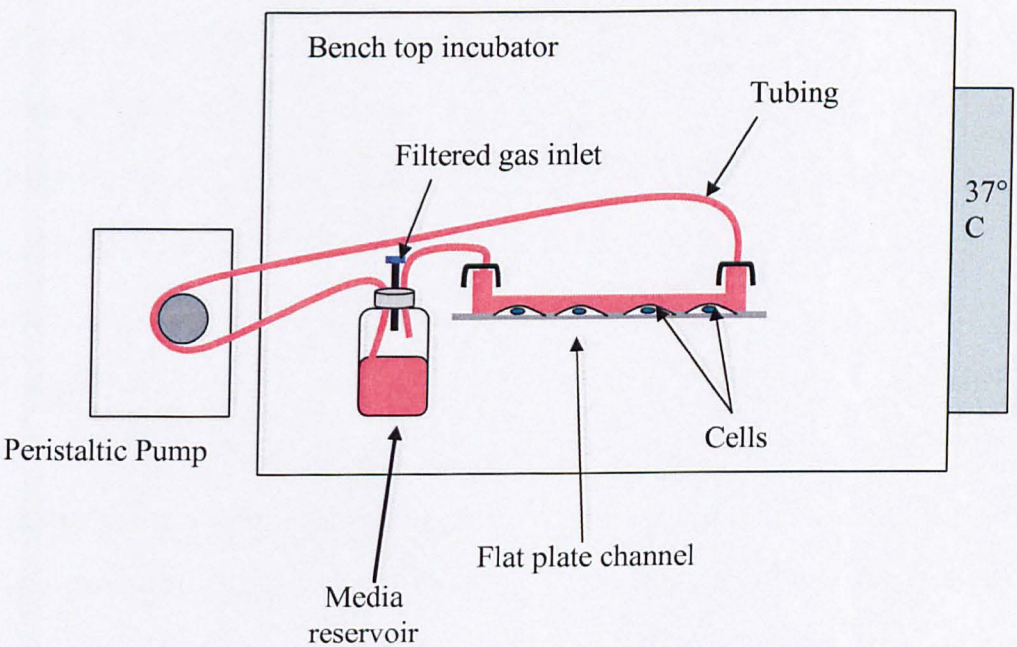

Figure 5.2 Schematic diagram of the fluidic bioreactor.

5.4 Results

5.4.1 Surface Analysis

a) XPS

XPS analysis results are summarised in table 5.1 which reports the elemental composition of uncoated Ibidi sheets, oxygen etched and ppAAm coated Ibidi sheets and various areas of the channels. The XPS analysis of uncoated channels revealed that they comprised 3.3 at % oxygen and no nitrogen (Figure 5.4a). After oxygen etching of samples in the plasma reactor, the surface contained mainly carbon and oxygen with a small amount of nitrogen contamination [N] = 1.6 at %. Coating the channels with ppAAm for different periods resulted in the appearance of nitrogen peaks in the XPS spectra (Figure 5.8a to 5.11a). The ppAAm coated channels contained varying concentrations of nitrogen depending on the ppAAm deposition time, indicating that this represents a thickening of the ppAAm coating on the oxygen plasma treated Ibidi surface. Figure 5.3 summarises XPS analysis of nitrogen elemental composition changes through the channel after depositing ppAAm for varying periods of time. The figure shows that nitrogen composition was highest at the ends and decreased through the channel to reach the lowest in the middle. This pattern was observed in all the different ppAAm depositions examined. The ratio of nitrogen concentration at the ends of the channel over the middle and the distance over which the nitrogen variation was observed decreased with increasing the time of ppAAm deposition. For illustration, the difference after 20 mins was half the one measured after 7 mins coating.

Area (mm)	Time of deposition of ppAAm (mins)	[C]	[N]	[O]
Uncoated Ibidi sheet		97	-	3.3
0 to 5	O2	82	1	17
	7	80	15	4.5
	10	80	18	2.0
	20	80	18	1.8
5 to 10	O2	85	0.99	15
	7	81	12	7.2
	10	80	16	4.1
	20	80	19	1.5
10 to 15	O2	85	0.81	14
	7	81	10	8.6
	10	81	13	6.4
	20	80	18	2.2
15 to 20	O2	85	0.78	14
	7	82	9.4	9.1
	10	82	11	7.6
	20	81	16	3.7
20 to 25	O2	85	0.47	14
	7	84	6.8	9.5
	10	81	10	8.4
	20	81	15	4.1
25 to 30	O2	85	1.5	14
	7	83	7.2	9.9
	10	82	9.5	8.8
	20	80	15	5
30 to 35	O2	85	1.1	14
	7	93	8.9	7.9
	10	81	10	8.5
	20	80	16	3.4
35 to 40	O2	85	0.7	14
	7	83	9.5	7.5
	10	81	11	7.9
	20	80	17	2.6
40 to 45	O2	84	1.5	14
	7	82	12	5.8
	10	81	15	5
	20	80	18	1.8
45 to 50	O2	83	0.8	16
	7	81	16	3.1
	10	79	18	2.2
	20	80	19	1.5
O2 on Ibidi sheets	O2	80	1.6	18
ppAAm on Ibidi sheets	3	79	19	2

Table 5.1 Surface elemental composition as determined by XPS at % of uncoated, O_2 etched and ppAAm coated Ibidi sheets, O2 etched Ibidi channel surface and ppAAm coated Ibidi channel surface at various ppAAm thicknesses and different positions.

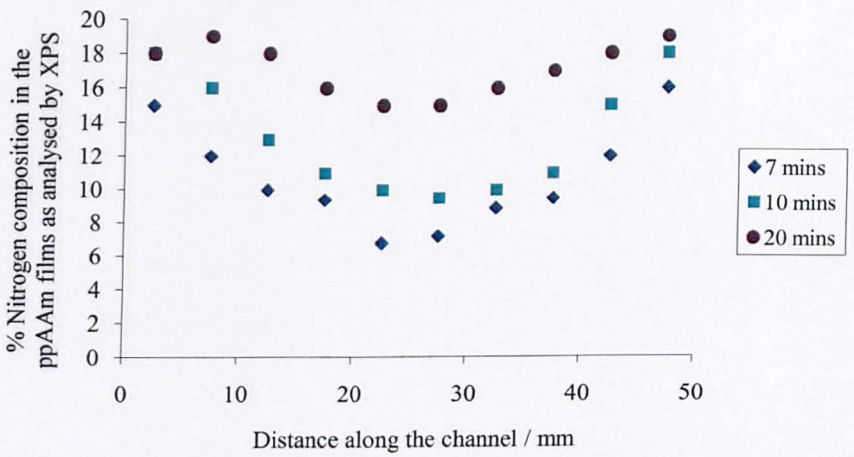

Figure 5.3 Distribution of nitrogen elemental concentration in the ppAAm films along the Ibidi channels as determined by XPS analysis. The ppAAm was deposited for time periods of 7, 10 or 20 mins. XPS of 20 mins channels was performed separately.

Some functional group information on the ppAAm deposit formed can be obtained by fitting the C1s core level with synthetic peaks representing functionalities using binding energy values acquired from databases and available literature (Beamson and Briggs, 1992). The C1s core level from the uncoated Ibidi sheet was well fit by synthetic peaks representing hydrocarbon (asymmetric peak of poly(ethylene), alcohol/ester/ether (C-O) and carbonyl (C=O) functionalities at shifts of 1.5 eV and 2.9 eV respectively (Figure 5.4b). This was consistent with the O1s core level components represented in figure 5.4c.

The C1s core level from the oxygen treated channel surface was fit with synthetic peaks corresponding to hydrocarbon, amine/carbon-oxygen-carbon bridges (C-O-C/C-N) at shift of 1 eV, cyclic carbon-oxygen-carbon structures (cyclic C-O-C) at shift of 2 eV, carbonyl/amide (C=O/N-C=O) at shift of 3 eV and acid/ester (C=(O)OH/C=(O)OR) functionalities at a shift of 4.1 eV. This was the best fit obtained at the edges as well as the centre (Figure 5.6a, b) of the channels coated with oxygen only. A more profound understanding and fitting of the synthetic functionalities was limited by the poor knowledge of the detailed chemical structure of the plastic used. The presence of nitrogen was due to contamination occurring in the plasma reactor during oxygen etching or on exposure to the atmosphere afterwards.

The C1s core level fitting from ppAAm coated channels for 7 or 20 mins was different at the centre of the channels but was similar at the edges and this is summarised in figures 5.9 and 5.12.

(a)

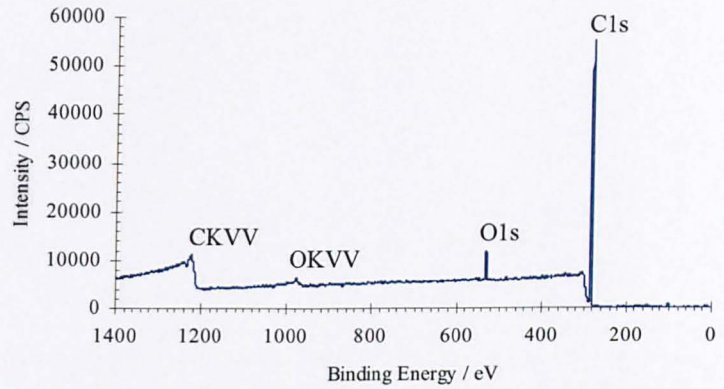

(b)

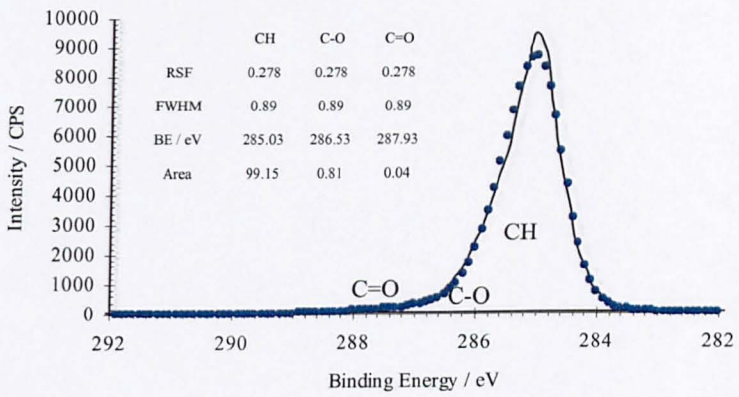

(c)

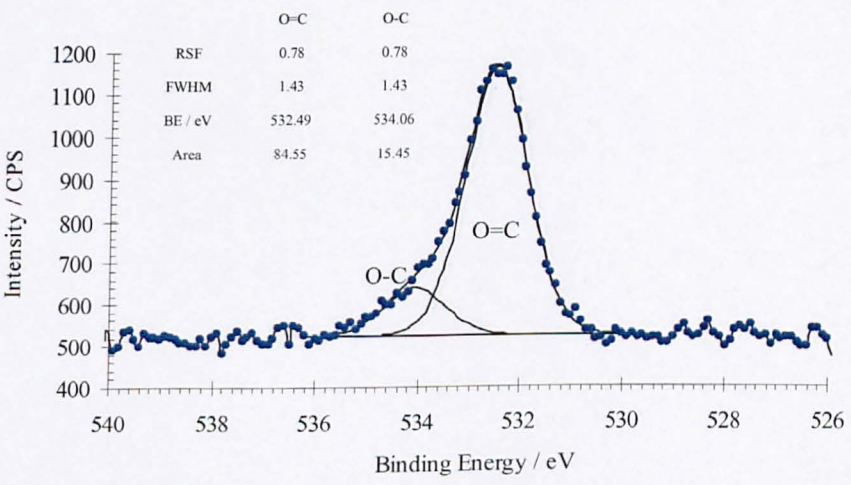

Figure 5.4 (a) XPS wide scan, (b) C1s narrow scan and (c) O1s narrow scan of uncoated Ibidi channel surface.

(a)

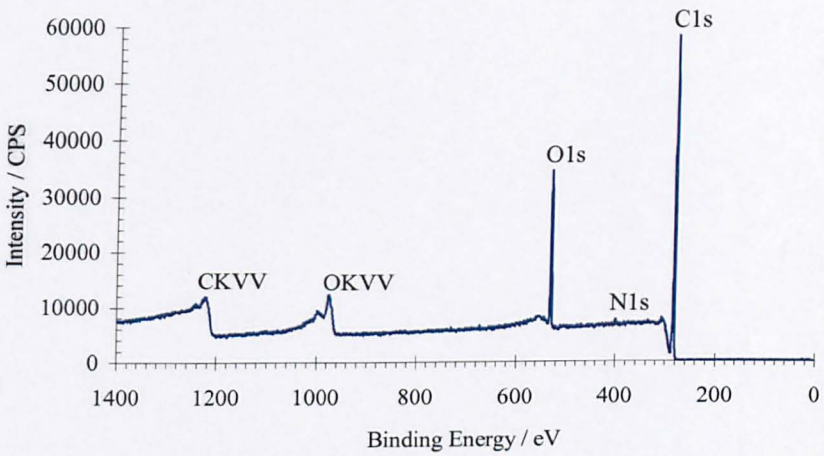

(b)

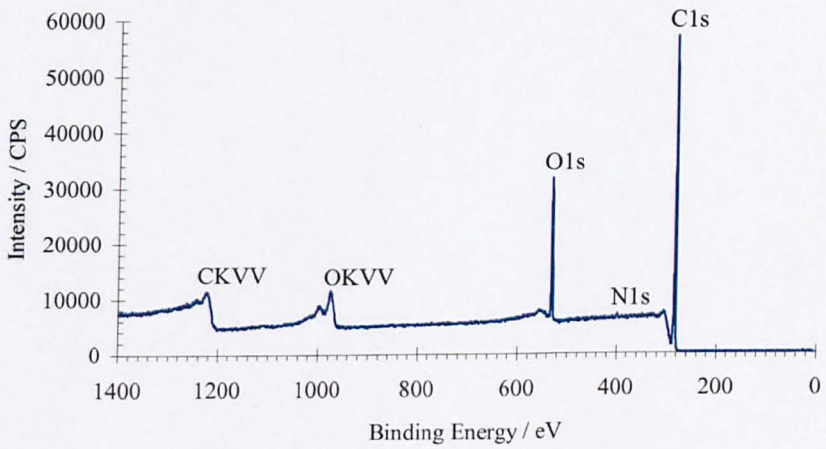

Figure 5.5 XPS wide scan of oxygen etched Ibidi channel for 3 minutes at different positions (a) the end of the channel, (b) the middle of the channel.

(a)

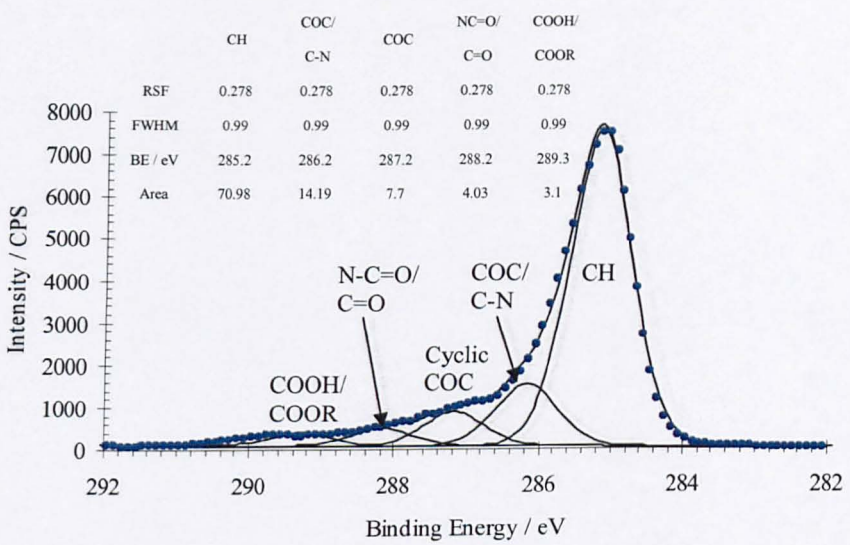

(b)

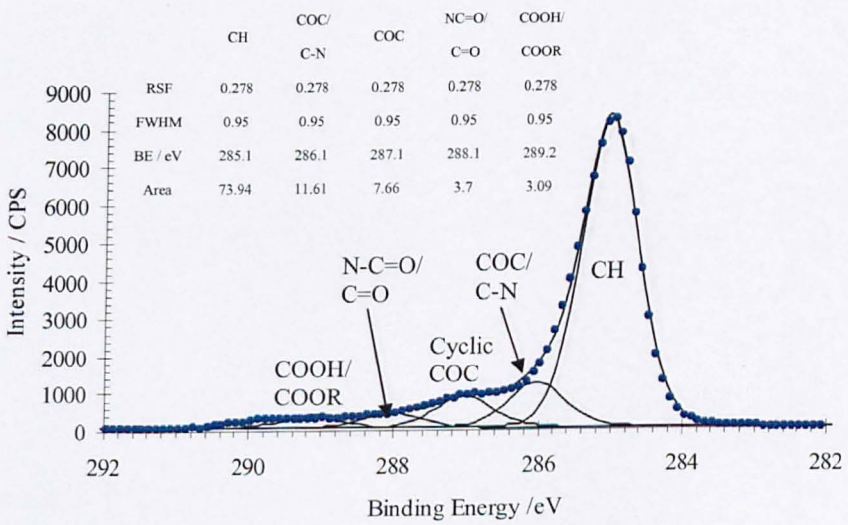

Figure 5.6 C1s narrow scan of oxygen etched Ibidi channel for 3 minutes at different positions (a) the end of the channel, (b) the middle of the channel.

(a)

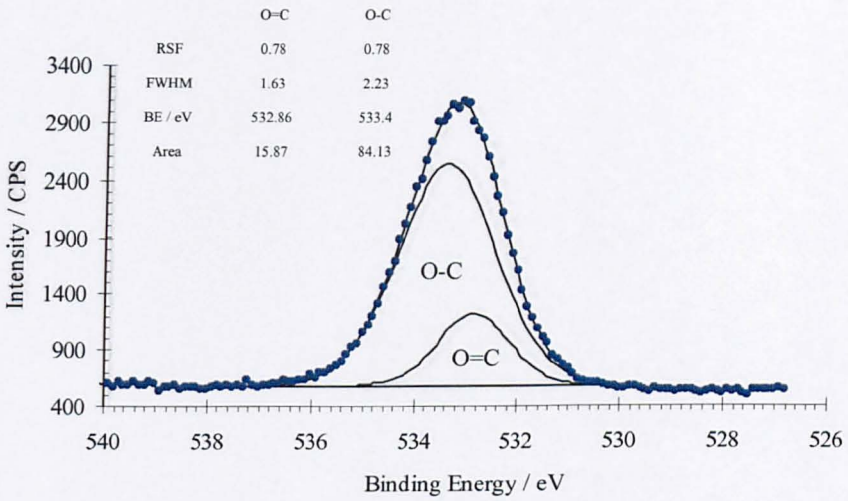

(b)

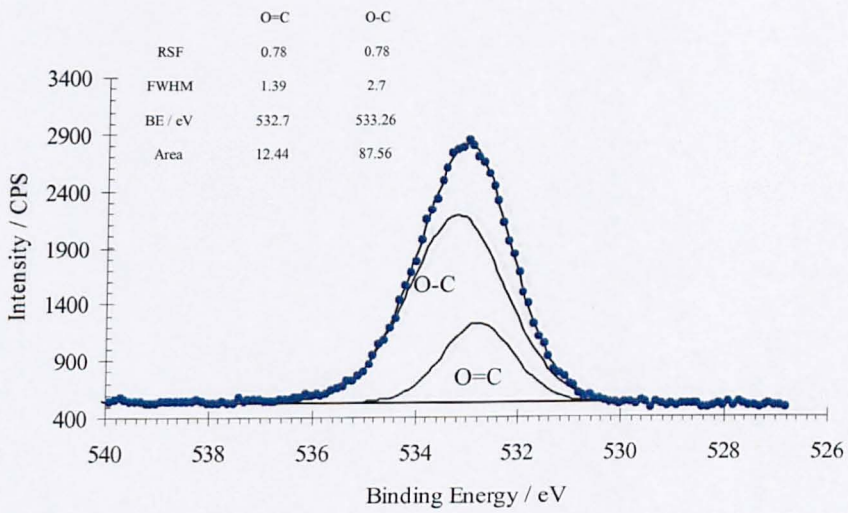

Figure 5.7 O1s narrow scan of oxygen etched Ibidi channel for 3 minutes at different positions (a) the end of the channel, (b) the middle of the channel.

(a)

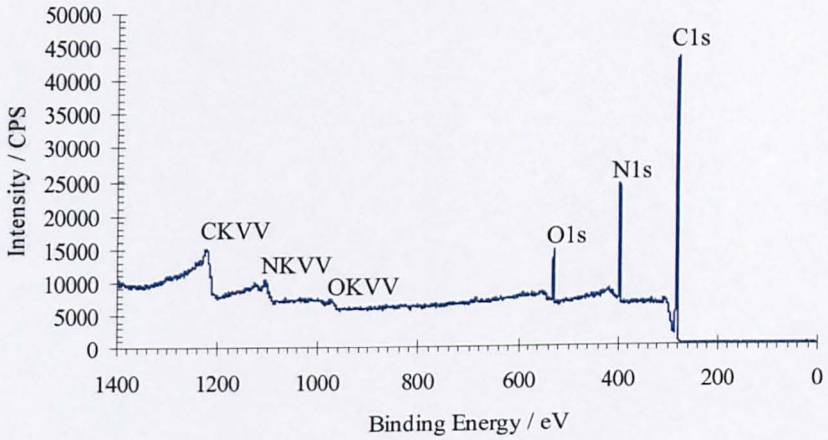

(b)

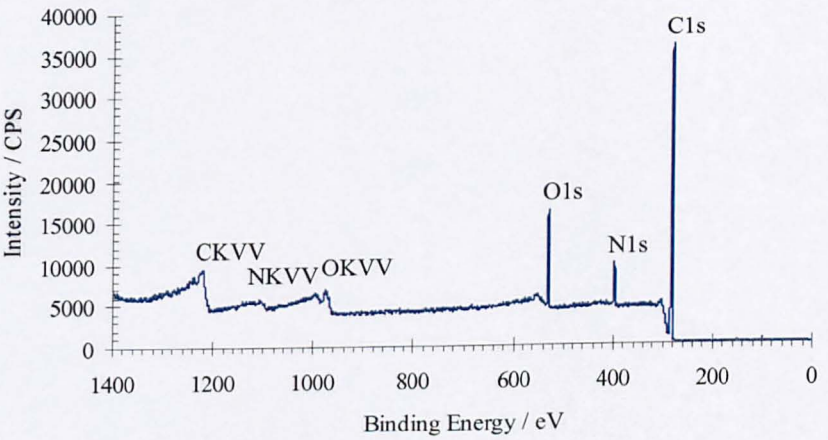

Figure 5.8 XPS wide scan of ppAAm deposited into Ibidi channel for 7 minutes at different positions (a) the end of the channel, (b) the middle of the channel.

(a)

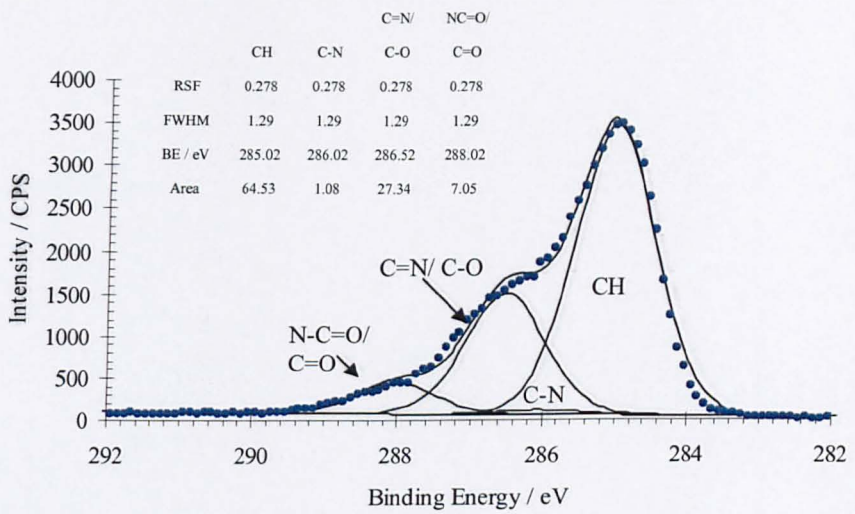

(b)

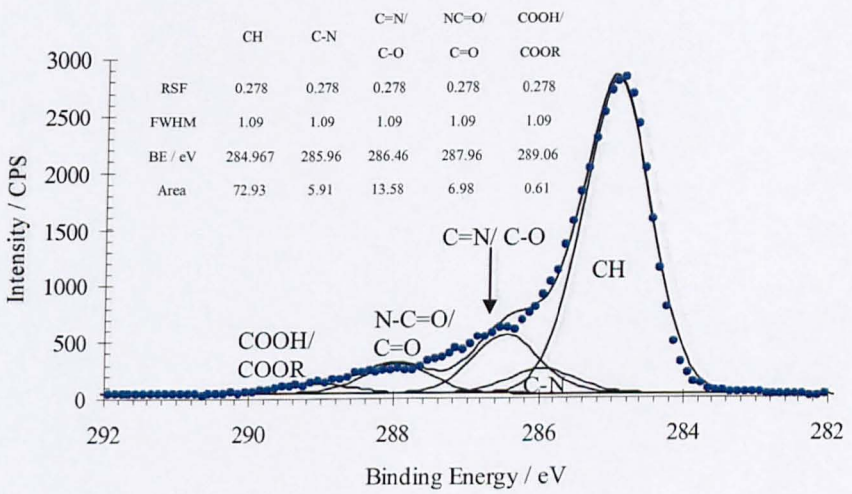

Figure 5.9 C1s narrow scan of ppAAm film deposited into Ibidi channel for 7 minutes at different positions, (a) the end of the channel and (b) the middle of the channel.

(a)

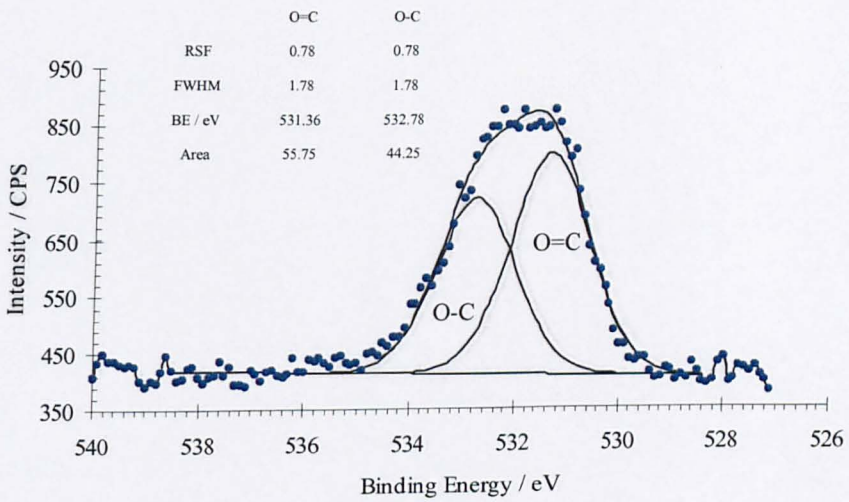

(b)

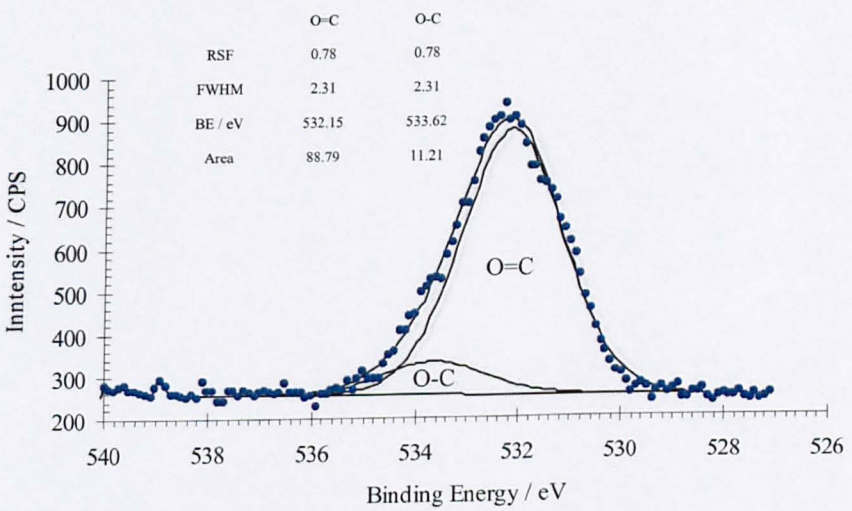

Figure 5.10 O1s narrow scan of ppAAm film deposited into Ibidi channel for 7 minutes at different positions, (a) the end of the channel and (b) the middle of the channel.

(a)

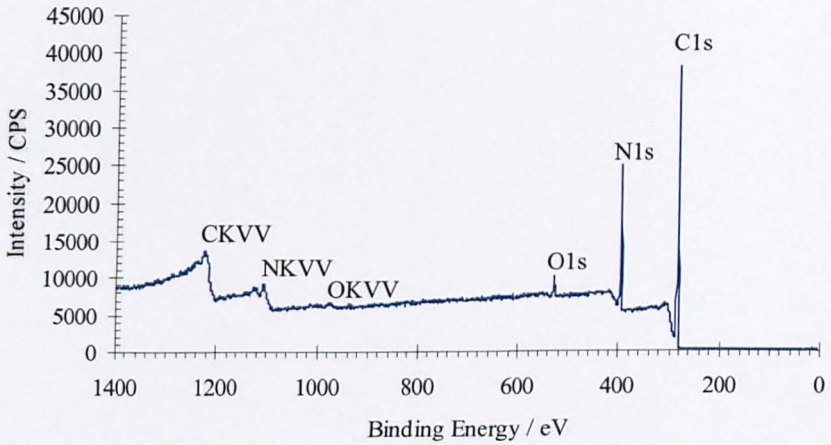

(b)

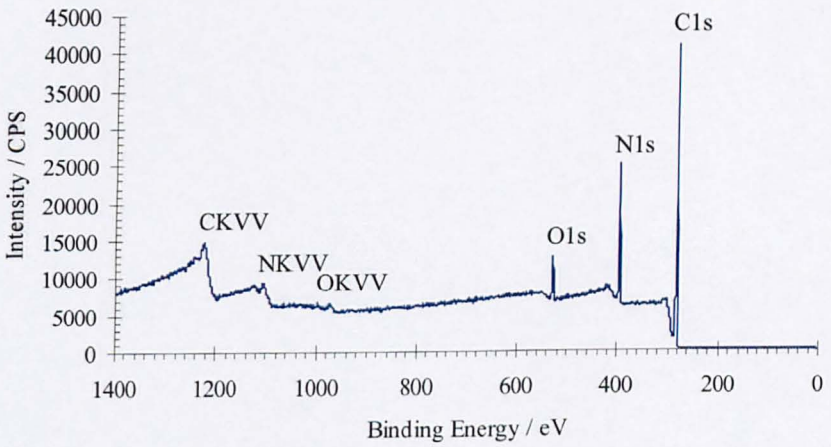

Figure 5.11 XPS wide scan of ppAAm film deposited into Ibidi channel for 20 minutes at different positions, (a) end of the channel and (b) the middle of the channel.

(a)

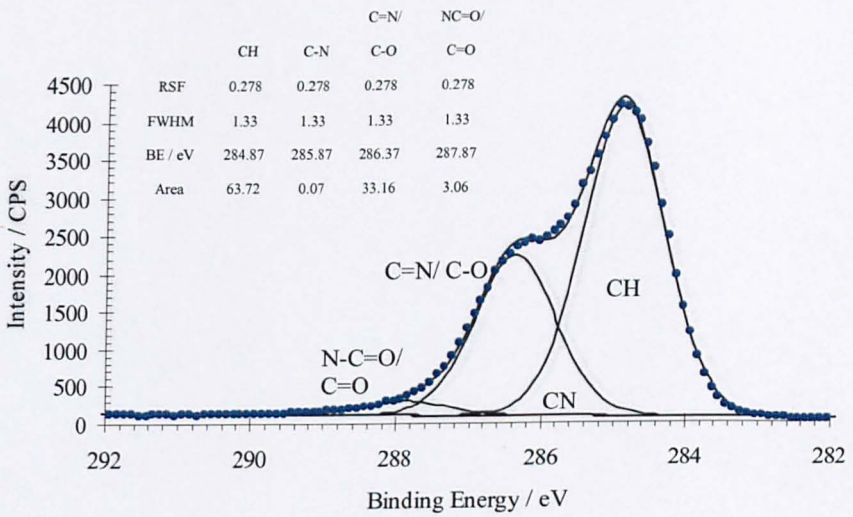

(b)

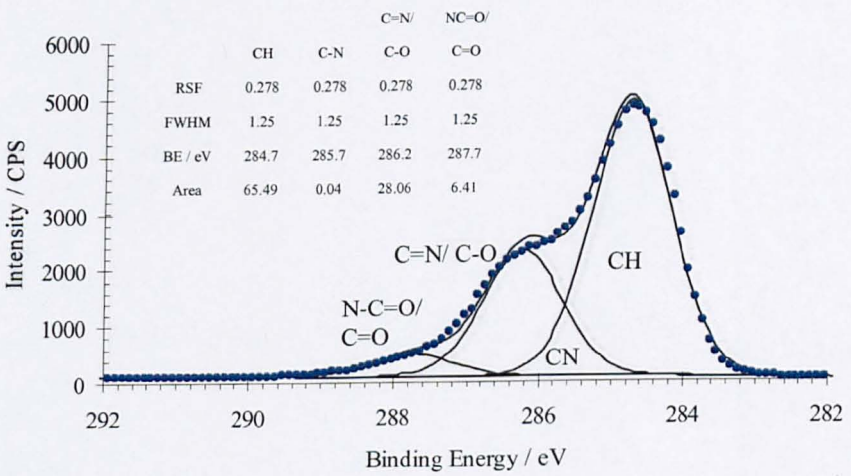

Figure 5.12 C1s narrow scan of ppAAm film deposited into Ibidi channel for 20 minutes at different positions, (a) end of the channel and (b) the middle of the channel.

(a)

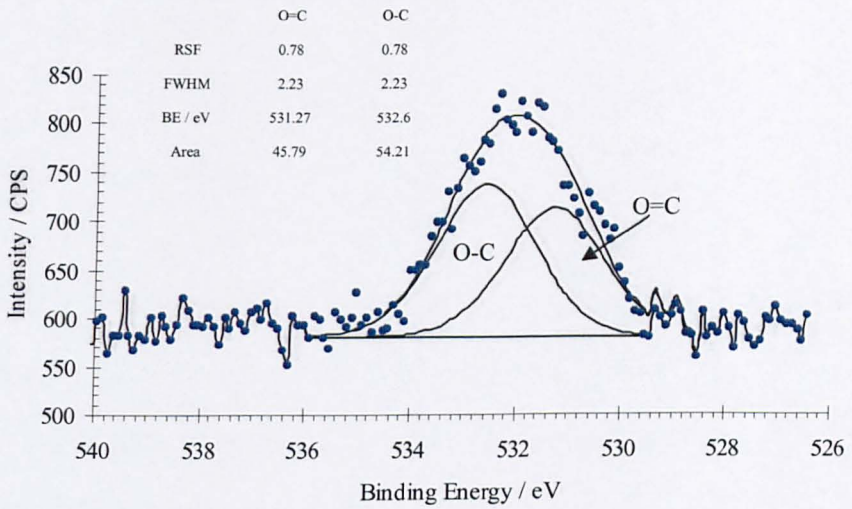

(b)

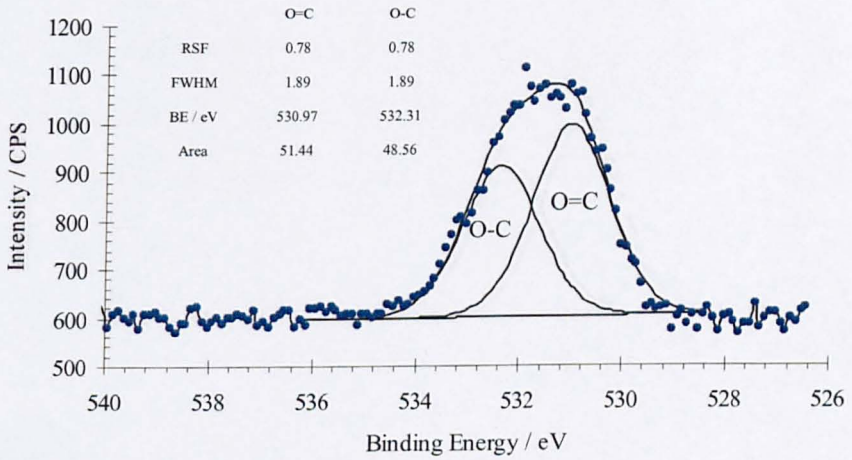

Figure 5.13 O1s narrow scan of ppAAm film deposited into Ibidi channel for 20 minutes at different positions, (a) end of the channel and (b) the middle of the channel.

At the edges of the channels, the C1s core level was fit with synthetic peaks representing amine (C-N), imine or alcohol/ester/ether environments (C=N/C-O), and carbonyl/amide (C=O/N-C=O) at shifts of 1, 1.5 and 3 eV respectively. The same component fitting was attributed to the C1s core level of the centre sample of channels coated with ppAAm for 20 mins. However, due to low penetration of the ppAAm to the centre of channels when coated for 7 mins, there were higher levels of oxygen present as shown by XPS analysis, leading to different fitting of the C1s core level. This is illustrated in figure 5.9b, where an additional synthetic component representing acid/ester functionalities at a shift of 4.1 eV was included. The binding energy of the symmetric single component N1s core level from ppAAm coatings was 399.5 eV (not shown). The O1s core level (Figure 5.4c, 5.7, 5.10 and 5.13) was fit into two synthetic components corresponding to O-C and O=C functionalities. The XPS results obtained for 10 mins ppAAm deposition were similar to 7 mins deposition times (results not shown).

b) Contact Angle

The contact angle of uncoated Ibidi sheet surface was (89 ± 4.1) °, indicating a very hydrophobic surface unsuitable for cellular adhesion. After oxygen etching of the sheet, the contact angle was found to be (21 ± 5) ° and after ppAAm coating for 3 mins, the contact angle was measured to be (72 ± 0.2) °. Contact angles along the channel were high at the ends of the channels and decreased through the channels to reach their lowest at the middle as summarised in figure 5.14.

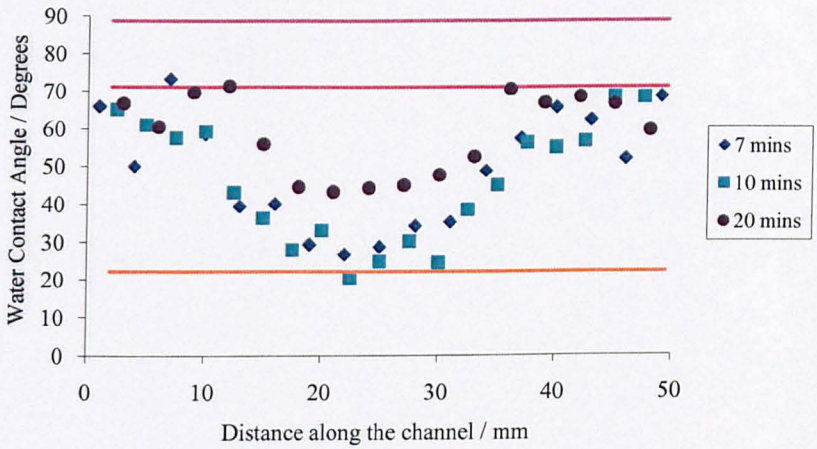

Figure 5.14 Water contact angle measurements of ppAAm films deposited into Ibidi channels for varying time periods, 7 (blue), 10 (green) and 20 (violet) minutes. The plum coloured line indicates the contact angle of an uncoated Ibidi sheet, the pink coloured line indicates contact angle of ppAAm coated Ibidi sheet for 3 mins and the orange coloured line indicates the contact angle of oxygen etched Ibidi sheet.

The contact angle of the longest ppAAm deposition (20 mins) was the highest, compared to a 7 and 10 mins deposition time, throughout the channels with the exception of the ends where all contact angles were similar. The difference between the contact angle at the ends and the middle of the channel of each deposition period narrowed with increasing deposition times of ppAAm. In addition, there was not an apparent variability in contact angle of 7 and 10 mins deposition periods (Figure 5.14).

The contact angle results promote the data obtained from XPS analysis of the ppAAm coated surfaces. This is illustrated in the pattern of contact angle which follows the increase in nitrogen composition of the ppAAm films leading to hydrophobic areas with high contact angle at the ends of the channel. On the other hand, there was less nitrogen and more oxygen in the middle of the channel, leading to less hydrophobic and more hydrophilic areas with low contact angle.

Figure 5.15 demonstrates the effects of nitrogen on water contact angle measured on the surfaces coated with ppAAm. Water contact angle was proportional to the nitrogen elemental composition of the surface. Nitrogen on the surface of Ibidi polymer decreased the original contact angle of the plastic from about 90 ° to lower than 70 °. Therefore, this creates a less hydrophobic surface promoting cellular adhesion for cell culture. Despite achieving the most hydrophilic surface with only oxygen plasma, previous experience with primary rat hepatocytes demonstrated low cellular attachment with oxygen rich surfaces.

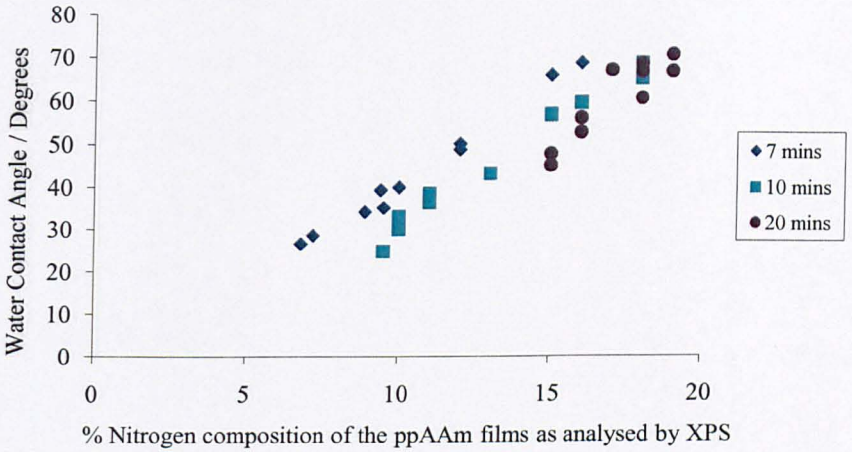

Figure 5.15 The relationship between water contact angle and nitrogen composition of the ppAAm coated channels. The channels were coated with ppAAm for 7, 10 or 20 mins.

5.4.2 Attachment of Huh-7 cells to Uncoated, Collagen Coated and ppAAm Coated Channels under Static and Media Flow

Phase-contrast images in Figure 5.16 showed that Huh-7 cells attached to both collagen and ppAAm coated channels to form confluent mono-layers of cells. However, the attachment on uncoated channels was patchy and reached confluency after 24 hrs of static culture in serum-free media (Figure 5.17). After 24 hrs of static culture in serum-free media, the cells plated into collagen and ppAAm coated channels were over confluent.

The channels incubated with media flow at a flow rate of 200 µl/min for 24 hrs, after attachment, are represented in Figure 5.18. The cells were less confluent compared o static cultures and the cells plated into uncoated channels showed a patchy cell distribution.

The live/ dead stain in Huh-7 cells revealed that all the cells were alive at the end of the experiment by taking up the fluorescent green stain (Figure 5.18). The shear stress applied during these flow experiments did not have damaging effects on the cells and their viability.

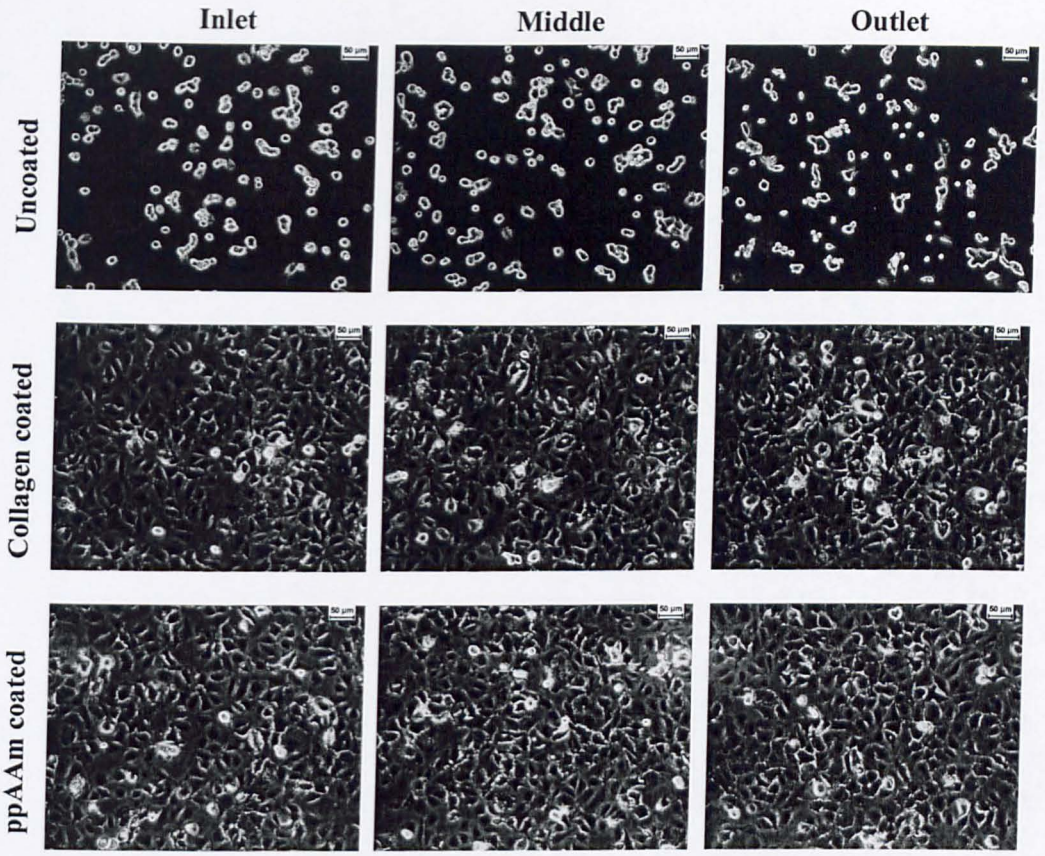

Figure 5.16 Phase-contrast images of Huh-7 cells after 3 hrs of seeding into uncoated, collagen coated and plasma coated channels, images were captured at the inlet, middle and outlet.

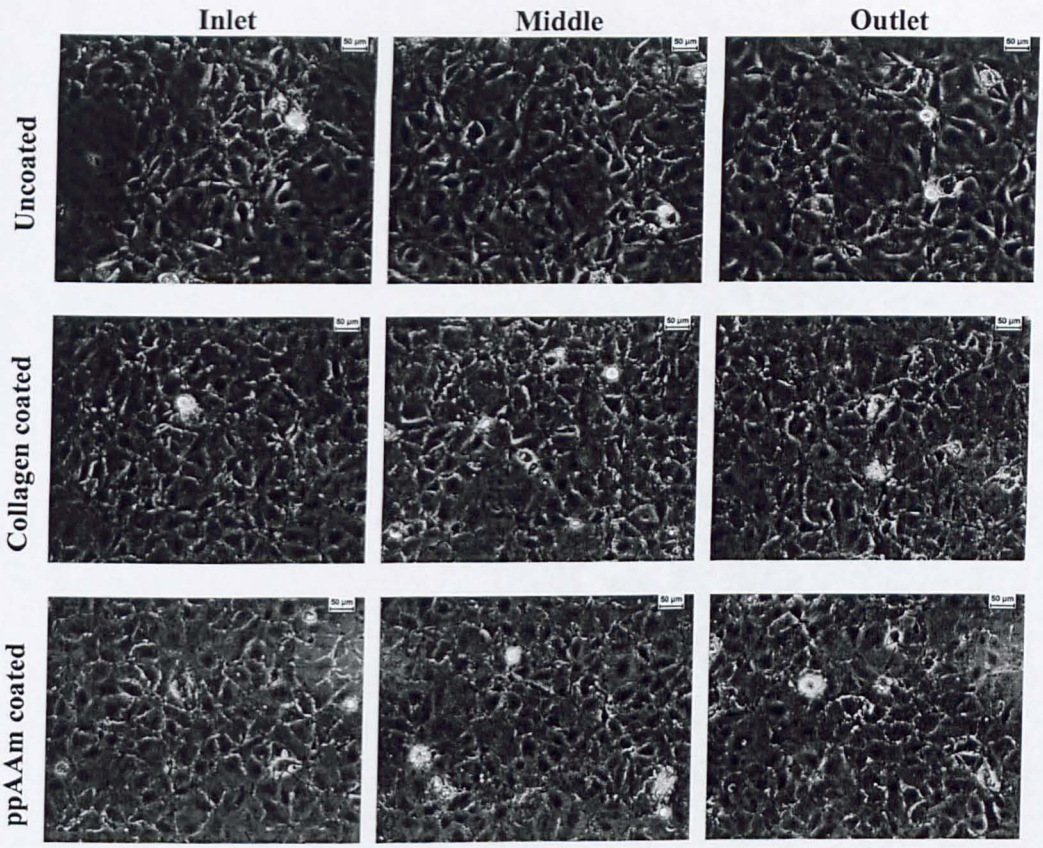

Figure 5.17 Phase-contrast images of Huh-7 cells after 24 hrs of seeding into uncoated, collagen coated and plasma coated channels, images were captured at the inlet, middle and outlet. After 3 hrs of attachment the media was changed to serum-free media under static conditions.

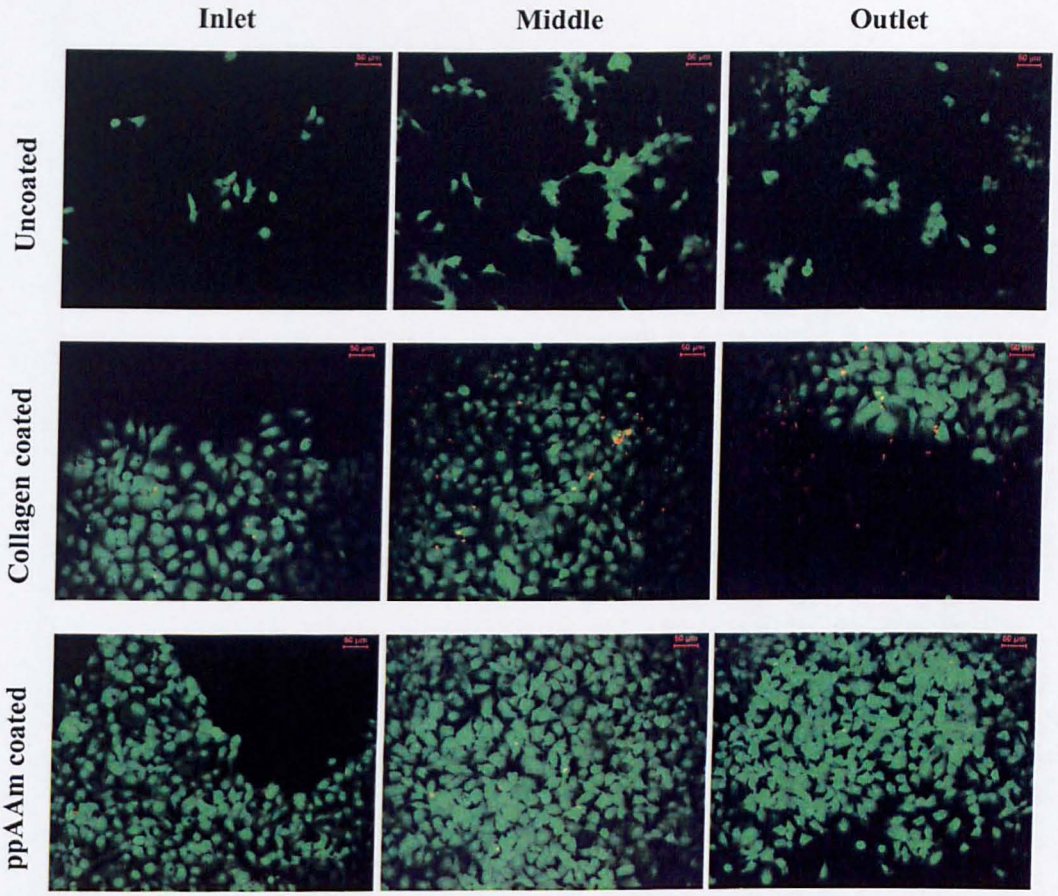

Figure 5.18 Live/ dead stain in Huh-7 cells after 24 hrs of seeding into uncoated, collagen coated and plasma coated channels, images were captured at the inlet, middle and outlet. After 3 hrs of attachment the media was changed to serum-free media and flow was initiated at a flow rate of 200 µl/min.

5.4.3 Attachment of PRH to Collagen Coated and ppAAm Coated Channels under Static and Media Flow

Figure 5.19 and Figure 5.20 show the attachment of PRH into collagen and ppAAm coated channels at 4 different seeding densities. After 1 hr from seeding and washing of unattached cells, 5×10^5 and 7.5×10^5 cells per channel showed the highest cells attachment on collagen coated channels. Fewer cells were attached using the following seeding densities, 2.5×10^5 and 1×10^6 cells per channel on the same surface. The cells plated into ppAAm coated channels showed very low attachment under the same conditions.

PRH, incubated under static conditions for 24 hrs after seeding, attached and spread on surfaces close to the ends of the channel, while the cells showed round morphology in the middle as illustrated with phase-contrast images in Figure 5.21. The live/dead stain in figure 5.22 showed that the cells were alive after 24 hrs both at the ends and the middle of the channel despite the round morphology of the later. On the other hand, PRH, incubated with media flow at a flow rate of 50 µl/min for 24 hrs, demonstrated live cells with attached and spread morphology throughout the channel (Figure 5.23).

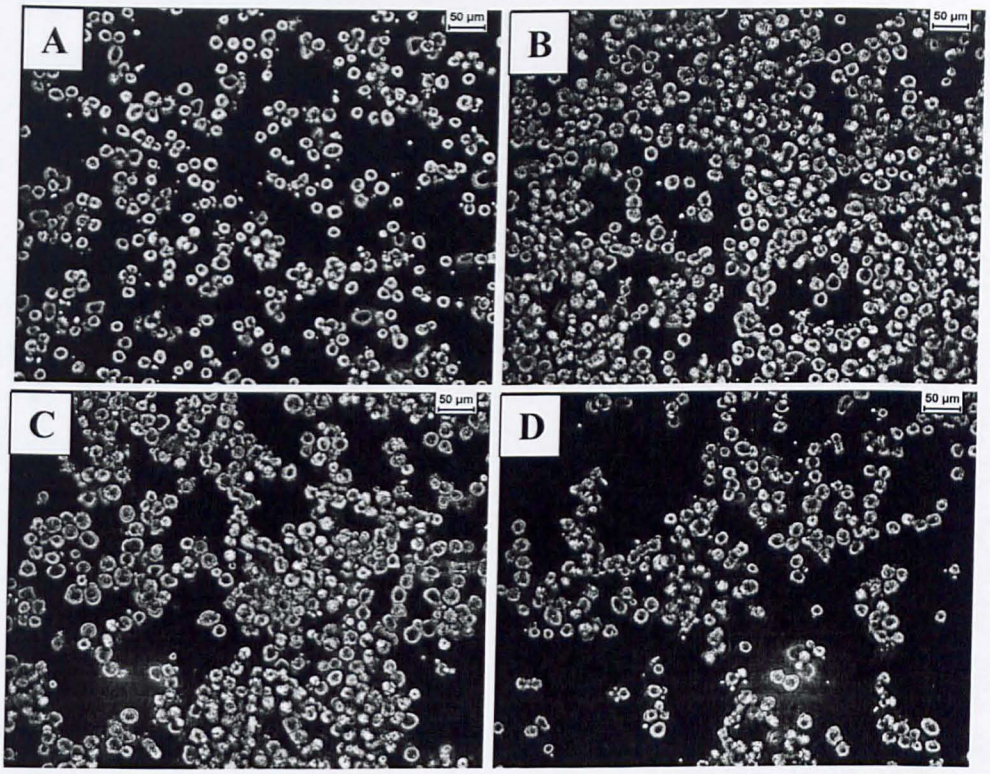

Figure 5.19 Phase-contrast microscopy images of PRH plated into collagen coated channels at (A) 250,000, (B) 500,000), (C) 750,000 and (D) 1,000,000 cells per channel after 1 hr from seeding. Cells were washed with serum-free media before microscopy.

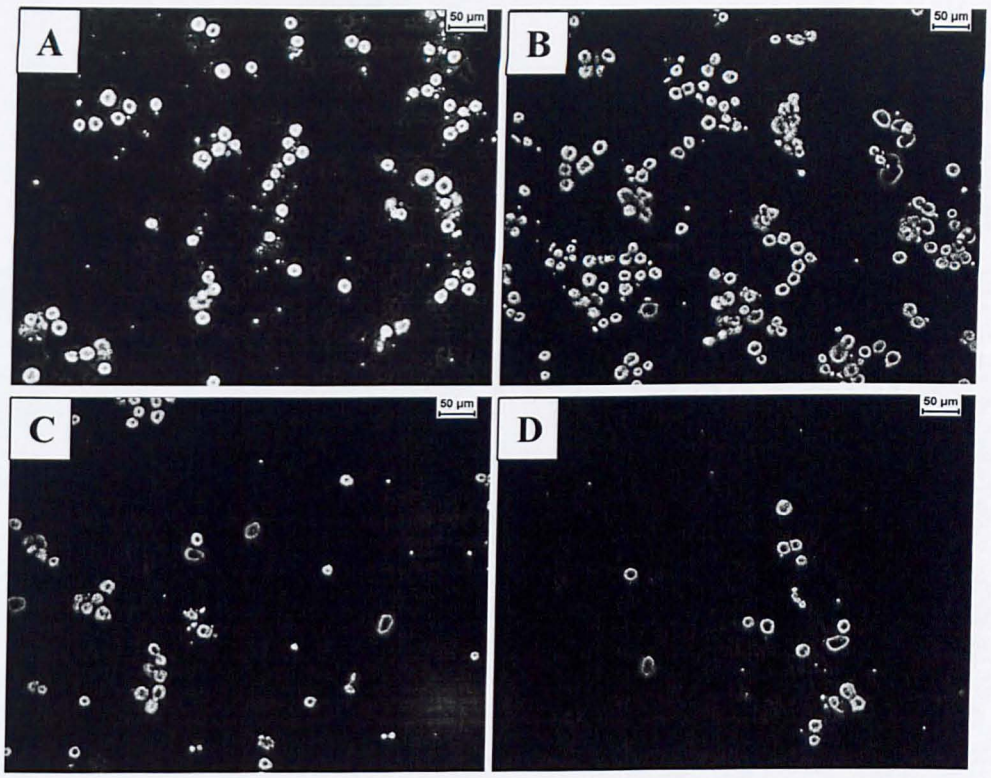

Figure 5.20 Phase-contrast microscopy images of PRH plated into ppAAm coated channels at (A) 250,000, (B) 500,000), (C) 750,000 and (D) 1,000,000 cells per channel after 1 hr from seeding. Cells were washed with serum-free media before microscopy.

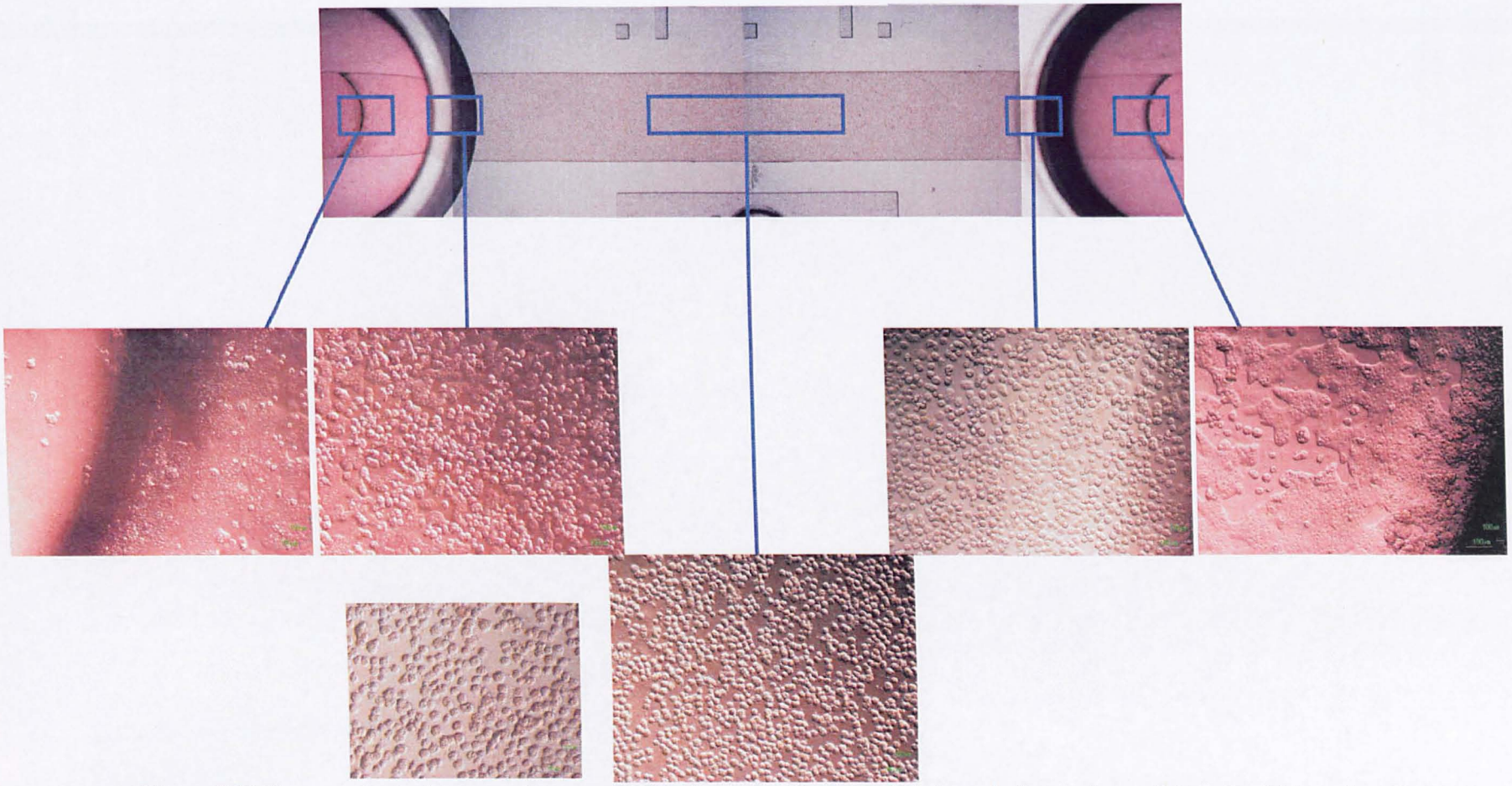

Figure 5.21 Phase-contrast microscopy images of PRH plated in collagen coated channels in a static condition after 24 hrs of seeding. Cells were plated in serum containing media for 1 hr which was then changed to serum-free. Images were taken from different areas.

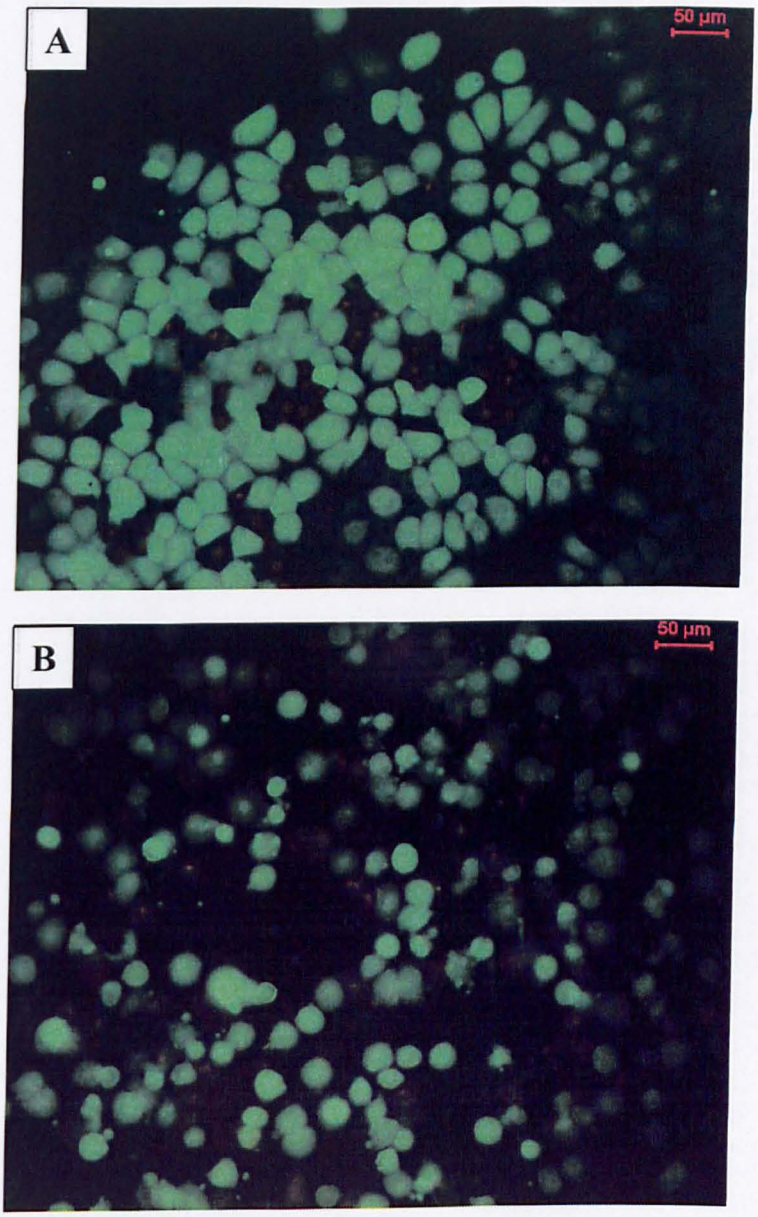

Figure 5.22 Live/ dead stain in PRH plated in collagen coated ibidi channels under static conditions, (A) image taken near the ends and (B) image taken in the middle of the channel after 24 hrs from seeding.

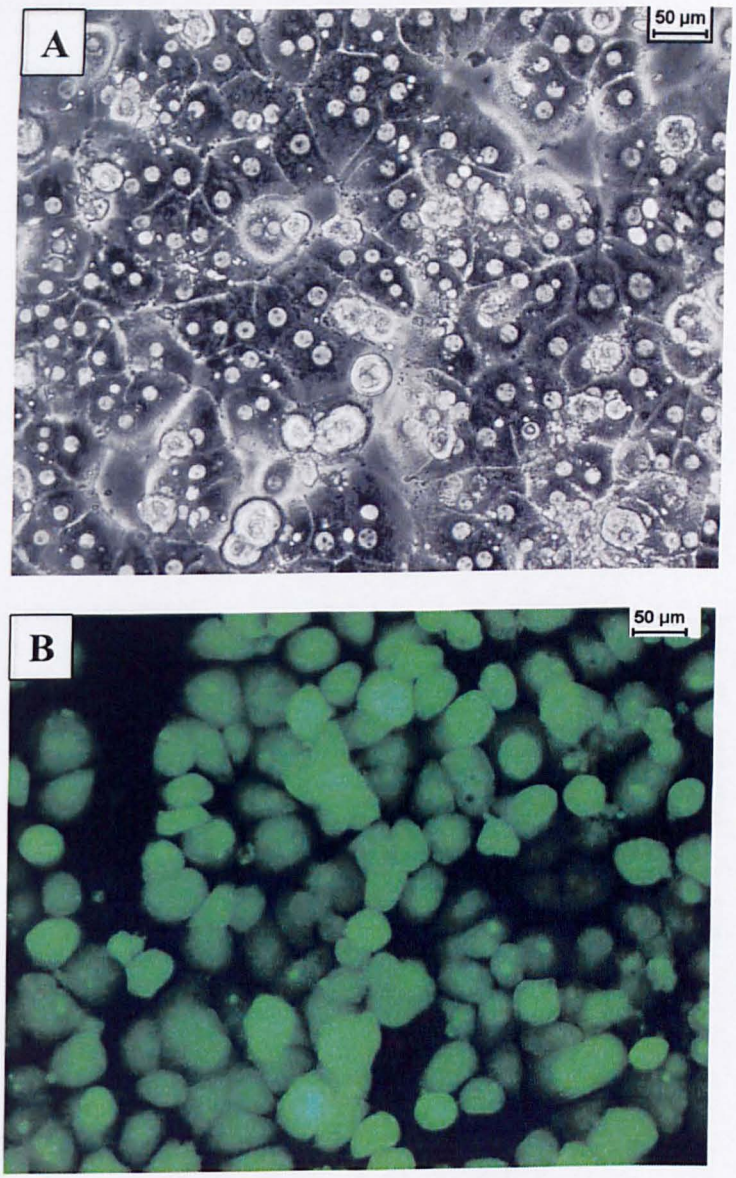

Figure 5.23 Images of PRH in collagen coated Ibidi channel after 1 hr attachment with static media and overnight incubation under media flow at a flow rate of 50 µl/min, (A) phase-contrast microscopy image and (B) live/ dead stain image (Images were taken from the middle of the channels).

5.5 Discussion

In this chapter, seeding Ibidi channels with both PRH and Huh-7 cells was achieved by coating the channels by adsorbed collagen and ppAAm. Collagen coating and media flow were demonstrated to be essential in seeding and maintaining the survival of PRH in the Ibidi chambers. However, Huh-7 cells attached to both adsorbed collagen and ppAAm coated channels and were found viable even under static conditions. The ppAAm film along the Ibidi channels was established, by XPS and contact angle measurements, to form a gradient of chemicals and hydrophilicity depending on the duration of ppAAm deposition.

5.5.1 ppAAm Surface Coating and Characterisation

ppAAm surface coating formed a layer of new functional groups on the surface of the Ibidi polymer leading to a decrease in surface hydrophobicity (contact angle) from about 90 ° to just under 70 °. The functional and elemental composition of the ppAAm film differs along the channel resulting in variation in water contact angles. The main reason for this is the duration of ppAAm deposition. At low deposition times (7 and 10 mins), the penetration of allylamine species into the centre of the channel was lower than with a longer deposition of 20 mins. This probably produced an uneven ppAAm film thickness along the channel with thicker deposits near the ends of the channels and thinner deposits at the centre. This effect was markedly significant at low deposition times as it is indicated by nitrogen elemental composition (Figure 5.3), C1s core level synthetic functionality fittings (Figure 5.9, 5.12) and water contact angle measurements (Figure 5.14). The results indicated that low deposition time for ppAAm coating generated thin films at the centre of the channel (and/or patchy) which did not cover the oxygen residues resulting from

oxygen etching. Therefore, this resulted in more oxygen functionalities (Figure 5.9b) and very low water contact angle at these sites (Figure 5.14).

This effect of low monomer residue penetration during plasma polymer deposition has been previously reported by our group when ppAAm was employed to coat porous PLA scaffolds (Barry *et al.*, 2005). The coated scaffolds had considerably higher nitrogen contents on their outer surface compared to the inner sites of the scaffolds.

5.5.2 Cell Culture

Huh-7 attached and spread on Ibidi polymer coated with ppAAm for 7_mins or collagen after few hrs of seeding. However, the attachment was poor on uncoated channels (Figure 5.16). Proliferation of Huh-7 was noticed after 24 hrs incubation under static conditions and not under flow through condition (Figure 5.17 and 5.18). This was probably stimulated by residual FCS in the serum-free media of the static culture which is not available in the flow through culture as it was diluted by the high volume of media and washed off by the flow. The flow rates used did not affect cell morphology and attachment even when started few hrs after seeding (3 hrs).

PRH attached and spread on collagen coated channels but did not attach onto ppAAm coated channels of various deposition times (Figure 5.19 and 5.20). The reasons for this were unclear and might be related to a more detailed composition of the ppAAm film. Previous work on PRH attachment to ppAAm deposited on glass cover-slips showed good cellular attachment with unaltered cell functionality. The penetration of allylamine residues into the channel to form the ppAAm deposit might

have formed a different deposit to the one obtained on the glass cover-slips or Ibidi sheets. The deposit of the channel was similar to the one on the glass and the sheets in terms of nitrogen composition and water contact angle. Other unknown physicochemical factors might have affected the differences observed in cellular attachment. Other factors that might influenced the PRH adhesion to ppAAm coated channels are the micro-environment of the channel with limited oxygen and nutrient supply during the attachment period, animal to animal and preparation to preparation variability. In depth investigation of the physicochemical properties of the ppAAm films using various techniques, such as secondary ion mass spectroscopy, might provide a better understanding of cell behaviour.

The poor adhesion of PRH to ppAAm was observed with the different seeding densities assessed, 2.5×10^5, 5×10^5, 7.5×10^5 and 1×10^6 cells per channel (Figure 5.20). However, on collagen coated channels, 2.5×10^5 and 1×10^6 showed low attachment and this might be because 2.5×10^5 is a low cell number for seeding the channels and lot of cells were washed off after 1 hr of attachment. This might be related to micro-environment of the channel that does not allow adequate nutrient and oxygen supply during seeding. Susceptible cells would probably die quicker in this culture compared to culturing the cells in a well plate and therefore low cell attachment is observed. The highest seeding density resulted in high cell number and limited nutrients and oxygen in the channel (100 µl of media) leading to poor attachment and cell death. The seeding density of 5×10^5 cells per channel was used for seeding PRH in all other experiments.

Incubating PRH under static condition for 24 hrs after plating resulted in spread cells with typical morphology near the ends of the channels and round and dead cells in the centre of the channel (Figure 5.21 and 5.22). The main reason for this was the starvation of the cells due to lack of the nutrients and oxygen in the centre comparing to areas near the ends where the reservoirs are located. There was no movement of the media but utilisation of nutrients and oxygen by the cells lead to a diffusion of more nutrients and oxygen from the media reservoir to some areas of the channels. However, the diffusion was limited by the length of the channel and therefore a gradient was created with high levels of the oxygen and nutrients at the reservoirs and this decreased gradually to reach low levels at the centre. When the PRH were incubated under media flow, all the cells showed good morphology after 24 hrs incubation (Figure 5.23). The flow was initiated after about 2 hrs from cell seeding, 1 hr for attachment and another hour to wash the cell and change media and set up the equipment. As there was a short period between cell seeding and media flow commencement, it was important to optimise the flow rate to minimise cellular detachment and encourage spreading, good morphology and viability. The flow rate utilised during the first 24 hrs post seeding was 50 μl/min and other experiments (results not shown) indicated that higher flow rates during this periods caused detachment and cell death due to high shear stress.

PRH are very demanding cells compared to hepatoma cell lines and this can be the principle reason for differences observed in this chapter with regards to cellular attachment and viability.

Various methods were used to seed PRH on 2-D surfaces in order to achieve a confluent monolayer of cells in conventional or fluidic cultures. These mainly employed two strategies, multiple seeding and long periods for attachment. For illustration, duplicate seeding was used by Bhatia and colleagues in the flat plate bioreactor where the PRH were seeded for 1 hour with shaking every 15 mins for each seeding (Allen and Bhatia, 2003). Kane *et al.*, also reported using the same method when plating a concentrated suspension of PRH twice with 40 mins adhesion time (Kane *et al.*, 2006). Both studies incubated the cells for an extra 24 hrs under static conditions to enhance adhesion of the cells. However, multiple seeding probably implicates keeping isolated PRH unattached as a cell suspension which can affect their viability. The other strategy was incubating the cells for 24 hours after seeding under static conditions to allow attachment (Bader *et al.*, 2000; Langsch and Bader, 2001; Leclerc *et al.*, 2004). However, this might favour the adhesion of unhealthy cells which will consequently affect long-term results and their interpretation. The method optimised in this chapter to seed Ibidi channels with PRH support the development of a confluent cell monolayer of PRH with minimal dead cells attached. A single seeding step is important especially if co-culture techniques are desirable because the cells are plated as quickly as possible after isolation and the only time they are in a suspension might be the time for purification, counting and attachment of the other cell type (Chapter 1). Changing the media after 1 hour of attachment enables the removal of unattached cells which might be unhealthy for the culture. This is reinforced by continuous flow of media. Moreover, starting the flow as soon as possible after cell adhesion supports the aim of the fluidic system by starting the *in-vivo* like *in-vitro* environment for the isolated cells by mimicking blood flow.

5.6 Conclusions

The ppAAm and collagen coating improved the attachment of Huh-7 cells into Ibidi channels. However, ppAAm coating failed to promote the adhesion of PRH observed in collagen coated channels. The ppAAm film contained a higher concentration of nitrogen on the surface of the channels which led to a decrease in hydrophibicity of the original channel surface. The ppAAm coating also introduced different functional groups into the surface of the channels, which might influence the first contact with the cells.

Although Huh-7 cells attached to all surfaces including uncoated channels which were very hydrophobic, the maximum adhesion was observed with ppAAm and collagen coated channels. The cell line also survived in the channel under both static and flow conditions applied for 24 hrs. PRH attached only to collagen coated channels. Using the developed seeding protocol, PRH did not show good morphology and started dying under static conditions and media flow was necessary to maintain their survival in the Ibidi channels.

The developed methods to seed and maintain both Huh-7 cells and PRH in culture in Ibidi channels will allow their investigation in future work. The next step is to use those methods to culture the cells for a longer duration than 24 hours and assess their functionality under both static and flow conditions.

Chapter Six

Functionality of Primary Rat Hepatocytes in Ibidi Micro-fluidic Channels

6.1 Introduction

The liver is a complex organ to simulate *in-vitro* for research and organ replacement. Currently, fluidic is one of the key areas being investigated by various groups to capitalise on the utilisation of liver cells *in-vitro*. The different fluidic models being studied include flat bioreactors, 3-D bioreactors, and fluidic bioreactors of rigid or suspended 3-D cell aggregates. These systems have a single cell component of liver cells (hepatocytes) or co-cultures of hepatocytes with other cell types (stellates or endothelial cells). Both primary and cell lines have been used in these systems.

Bhatia and colleagues have developed an *in-vitro* flat plate fluidic bioreactor that permited the maintenance of the cells under steady-state oxygen gradients. These oxygen gradients demonstrated an *in-vitro* zonation of liver function (CYP2B and CYP3A) and toxicity in co-cultures of rat hepatocytes and J2-3T3 cells in response to various inducers (dexamethasone, phenobarbital), growth factors (EGF) and acetaminophen (Allen and Bhatia, 2003; Allen *et al.*, 2005).

Griffith and colleagues have investigated a fluidic bioreactor based on pre-aggregated liver cells. This model was demonstrated to express various similarities to native liver or isolated hepatocytes when gene expression of cytochrome P450 enzymes and hepatic transcription enzymes were assessed in a 7 day old model. This model showed only a slight down regulation of some genes compared to other models and this was consistent with the decrease in albumin secretion and ureagenesis. The superior functionality of liver cells obtained from this liver model were mainly attributed to the morphological similarity to liver tissue with the presence of tight junctions, glycogen storage and bile canaliculi (Powers *et al.*, 2002; Sivaraman *et al.*, 2005).

These two examples of fluidic liver model differ in their use of liver cells because they targeted different physiological aspects of liver architecture. However, the promising results gathered from various studies support the progress of *in-vitro* liver studies and the capability of these models to be utilised in toxicology studies in the pharmaceutical industry and potentially in liver replacement therapies as an *ex-vivo* apparatus or *in-vivo* transplant.

3T3 mouse embryonic fibroblasts have been widely used in *in-vitro* co-culture models of the liver including fluidic bioreactors. 3T3 cells form a well-established cell line which does not exert functional similarities with hepatocytes. The cells are easy to maintain and have good adhesion properties to various substrates. Co-cultures of primary hepatocytes and 3T3 cells were demonstrated to perform better than mono-cultures of hepatocytes both in 2-D and 3-D geometries. (Bhandari *et al.*, 2001; Bhatia *et al.*, 1998; Bhatia *et al.*, 1999; Donato *et al.*, 1990)

Ibidi Channels have been used to culture various cells including 3T3 fibroblast, Rat1 cells and mouse podocytes (Ibidi website). To date, it was not reported in the literature that these channels have been used successfully to culture PRH. Culturing PRH in the Ibidi channel could mimic the effects obtained by Bhatia and colleagues and provide a more convenient and easy way to use the flat plate bioreactor for further investigations. This chapter summarises the culture of PRH in Ibidi channels using the fluidic characteristic of the channel to flow media through the cells and provide them with fresh nutrients and oxygen.

6.2 Aims and Objectives

The aim of this chapter was to determine the survival and functionality of PRH in the Ibidi channels under media flow for a period of 5 days. The following objectives were addressed:

- Examine the potential benefits of seeding PRH on the top of 3T3 cells in the collagen and ppAAm coated channels with regards to improving attachment and functionality of PRH.
- Assess the functionality in terms of EROD activity and albumin secretion of PRH and co-culture PRH on 3T3 cells in the channels at day 1, 2, 3, 4 and 5 of the culture under media flow.
- Support the functionality results by a qualitative viability live/dead stain of the cells at the end of the culture.

6.3 Materials and Methods

6.3.1 Materials

All materials used in these experiments have been described in the previous chapters with the exception of 3T3 cells which were a gift obtained from Cancer Research Laboratories, University of Nottingham.

6.3.2 Surface Coating

Ibidi channels were collagen coated as explained in chapter 5. During the assessment of the co-culture with 3T3 cells, ppAAm coated channels were also used and they were coated for 7 minutes as reported in chapter 5.

6.3.3 Cell Culture

a) Mono-culture of PRH in the Channels

After isolation, 5×10^5 cells were seeded per channel and incubated to attach for 1 hr in serum containing media under static conditions. Then, cells were washed with serum-free L-15 and media was changed to serum-free L-15. The reservoirs at both ends were filled with 1 ml of media.

b) Co-culture of PRH and 3T3 Cells in the Channels

3T3 cells were cultured in DMEM containing 4.5 g glucose, 25 mM HEPES and L-glutamine supplemented with 10 % FCS, antibiotic/antimycotic cocktail (100 U/ml penicillin, 100 µg/ml streptomycin and 250 ng/ml amphotericin B). At 70 to 80 % confluency, the cells were passaged by incubation in 5 ml of trypsin/EDTA solution for

5 mins. After that, 20 ml of media was added to deactivate trypsin/EDTA and cells suspension was centrifuged at 1000 rpm using MSE Mistral 1000 centrifuge (Scientific Laboratory Supplies, UK) for 5 mins. The supernatant was then aspirated and the cells were re-suspended in 20 ml of media. The cells were counted using a Neubauer haemocytometer and plated into the channels (100 µl, surface area of 2.5 cm^2). For the co-culture (Figure 6.1), 3T3 cells were incubated for 1 hr to attach in serum containing DMEM and then washed with serum containing PRH media to remove dead cells. After that, PRH were seeded at 5×10^5 cells per channel by filling the channel with 100 µl of cell suspension at one end and gently removing wash media at the other end using cotton buds.

Various seeding densities of 3T3 cells were assessed for co-culture experiments and these were 2.5×10^4, 5×10^4 and 15×10^5 cells per channel.

6.3.4 Staining 3T3 cells with Cell Tracker Orange™

Cell tracker (Invitrogen, UK) was dissolved in 10 µl of DMSO and then diluted in 10 ml of serum containing DMEM to a final concentration of 10 µM. The cells were centrifuged at 1000 rpm for 5 mins. The cell pellet was re-suspended in cell tracker solution and incubated under cell culture conditions for 25 mins. The cells were centrifuged again at the same conditions and re-suspended in serum containing DMEM and incubated under cell culture conditions for 30 mins. After that, the cells were centrifuged, washed with PBS and were then re-suspended in media and seeded into the channels. At the visualisation stage, the fluorescent stain in the cells was detected using absorbance of 548 nm and emission of 576 nm.

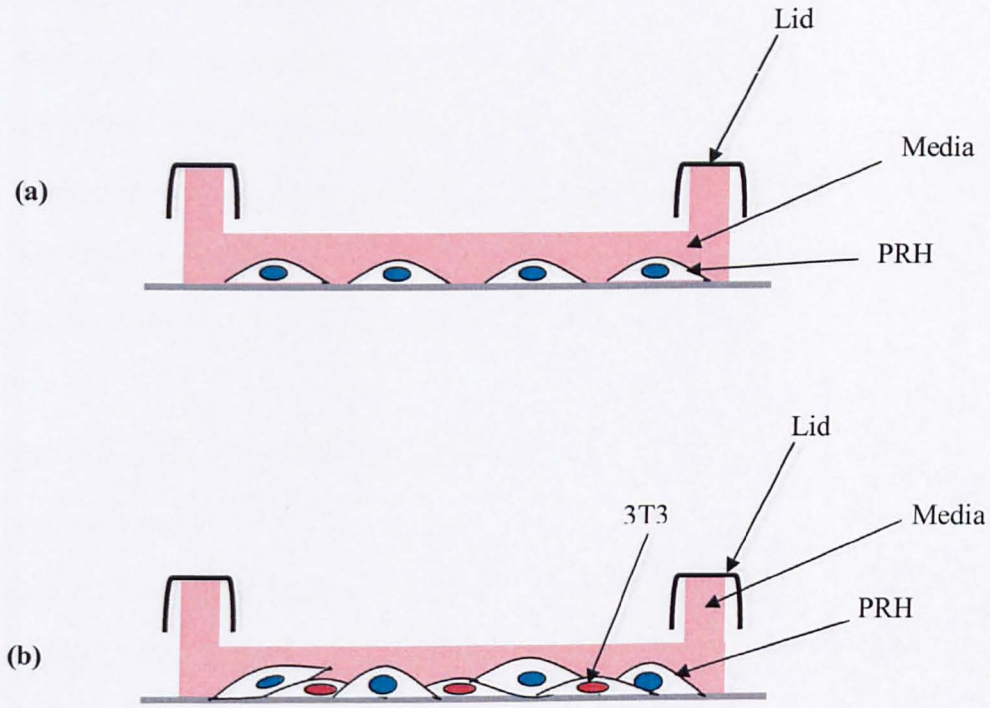

Figure 6.1: Schematic diagram of the flat plate (Ibidi) channel seeded with (a) mono-culture of PRH, (b) co-culture of 3T3 and PRH.

6.3.5 Long-term Flow Incubation of the Cells

The cells in the channels were assembled in the flow through set-up as described in chapter 5. PRH and co-cultures of PRH and 3T3 cells were incubated in the flow through set-up at a flow rate of 100 µl/min for 4 days post overnight attachment at a flow rate of 50 µl/min. The media reservoirs contained 50 mls of serum-free PRH media which was replaced with fresh media every day (day 2, 3, and 4). At the same time, phase-contrast images of the cells were captured to check changes in cell morphology, EROD assay was performed and samples were collected to measure albumin secretion. On day 5, the cells were stained with live/dead stain to examine cell viability.

6.3.6 Functionality of PRH in the Channels

a) EROD Assay

Before changing the media, the channels were removed from the set-up and incubated with resorufin for 30 mins. The solution was removed and aliquoted in a 96 well plate to finish the assay (Chapter 2). The cells were then washed with serum-free PRH media 3 times and re-mounted into the flow through set-up.

b) Albumin Secretion

The collected media was centrifuged at 5500 rpm, using Sigma 3k15 (Sigma, UK), to remove any cells from the media and the supernatant was stored at -20° C before assaying.

6.4 Results

6.4.1 Attachment of PRH into Channels Pre-seeded with 3T3 Cells on Collagen or ppAAm

Various seeding densities of 3T3 cells were used to pre-seed the channels and optimise PRH attachment. The phase-contrast images presented in Figure 6.2 showed that increasing the number of 3T3 cells increased number of dead cells in the channels 1 hr after seeding PRH. At 5×10^4 3T3 cells per channel, an optimum condition was obtained compared to 2.5×10^4 3T3 cells per channel where there were very few 3T3 cells and 15×10^4 3T3 cells per channels where more dead cells were observed.

There was a remarkable difference between the surface coating employed for this experiment as illustrated in Figure 6.2 and Figure 6.3. 3T3 cells attached to ppAAm coated channels, whereas the PRH plated on top showed very little adhesion compared to channels coated with collagen.

6.4.2 Morphology and Survival of Mono- and Co-culture of PRH in the Channels under Media Flow

Phase-contrast images demonstrated that the PRH had typical spread morphology with mono- and bi-nucleated cells after the first 24 hrs of seeding and incubation at a flow rate of 50 µl/min (Figure 6.4). This was also observed at day 2 after increasing the flow rate to 100 µl/min. However, the co-culture of PRH on 3T3 cells started aggregating into islands after day 3 as shown in Figure 6.5 and Figure 6.6. The mono-culture remained the same over the 5 day period (Figure 6.4, 6.5 and 6.6).

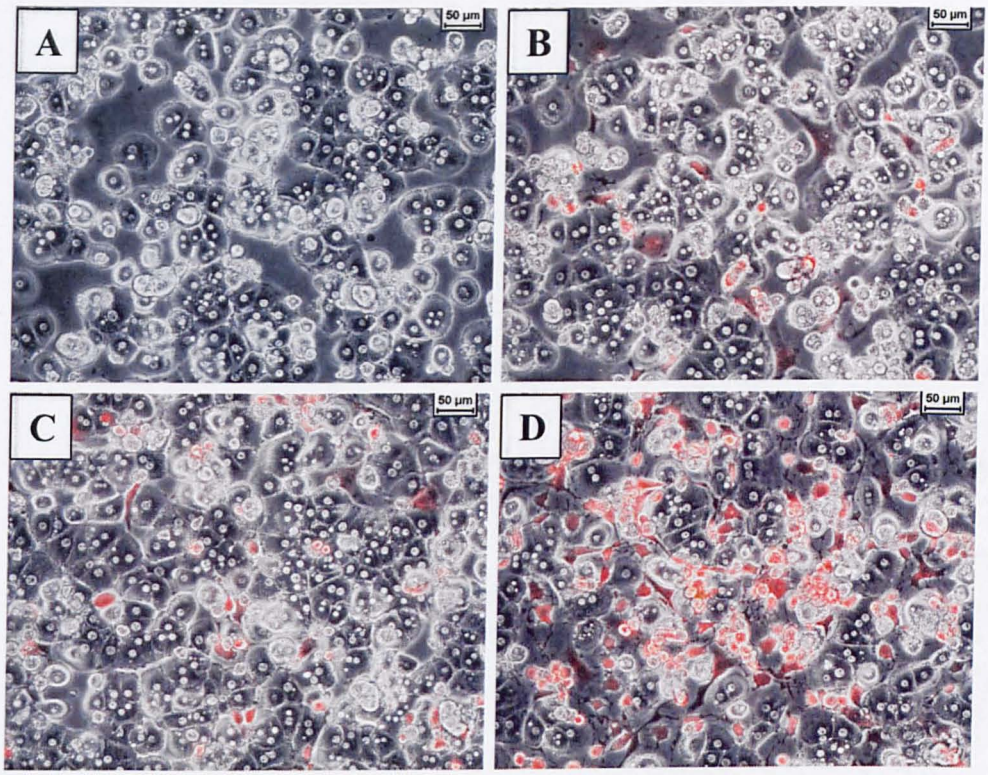

Figure 6.2 Phase-contrast microscopy images of PRH plated into collagen coated channels in mono- or co- culture with 3T3 cells, (A) mono-culture of PRH at 500,000, (B) co-culture with 25,000 3T3 cells), (C) co-culture with 50,000 3T3 cells and (D) co-culture with 150,000 cells 3T3 cells per channel after 24 hr after seeding. 3T3 cells were labelled with cell tracker orange™ (Images taken from the middle of the channels).

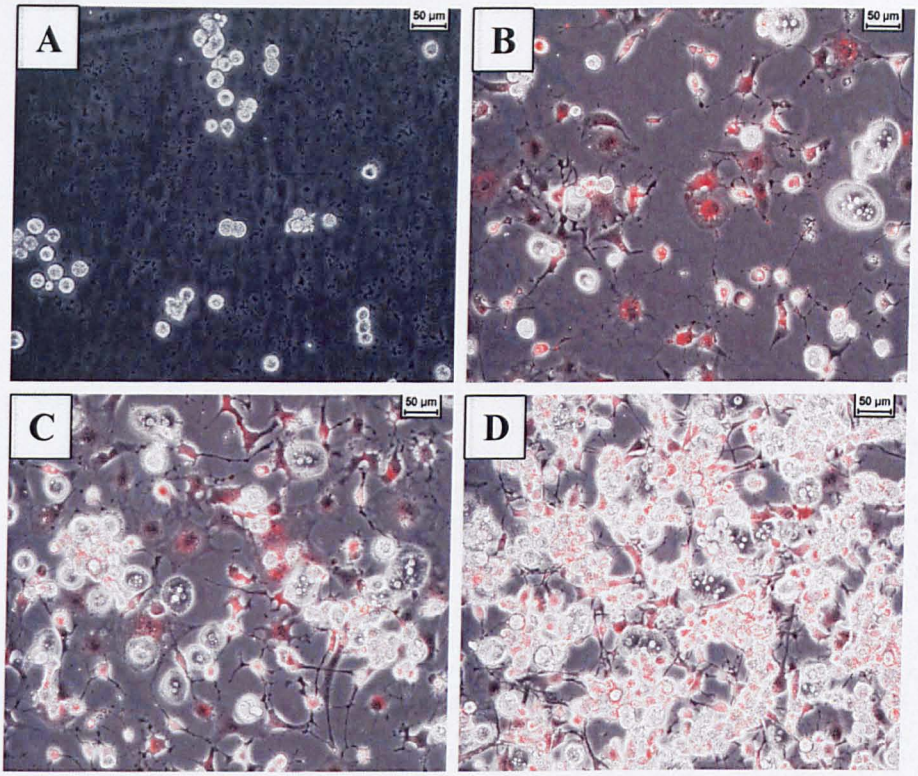

Figure 6.3 Phase-contrast microscopy images of PRH plated into ppAAm coated channels in mono- or co- culture with 3T3 cells, (A) mono-culture of PRH at 500,000, (B) co-culture with 25,000 3T3 cells), (C) co-culture with 50,000 3T3 cells and (D) co-culture with 150,000 cells 3T3 cells per channel after 24 hr after seeding. 3T3 cells were labelled with cell tracker orange™ (Images taken from the middle of the channels).

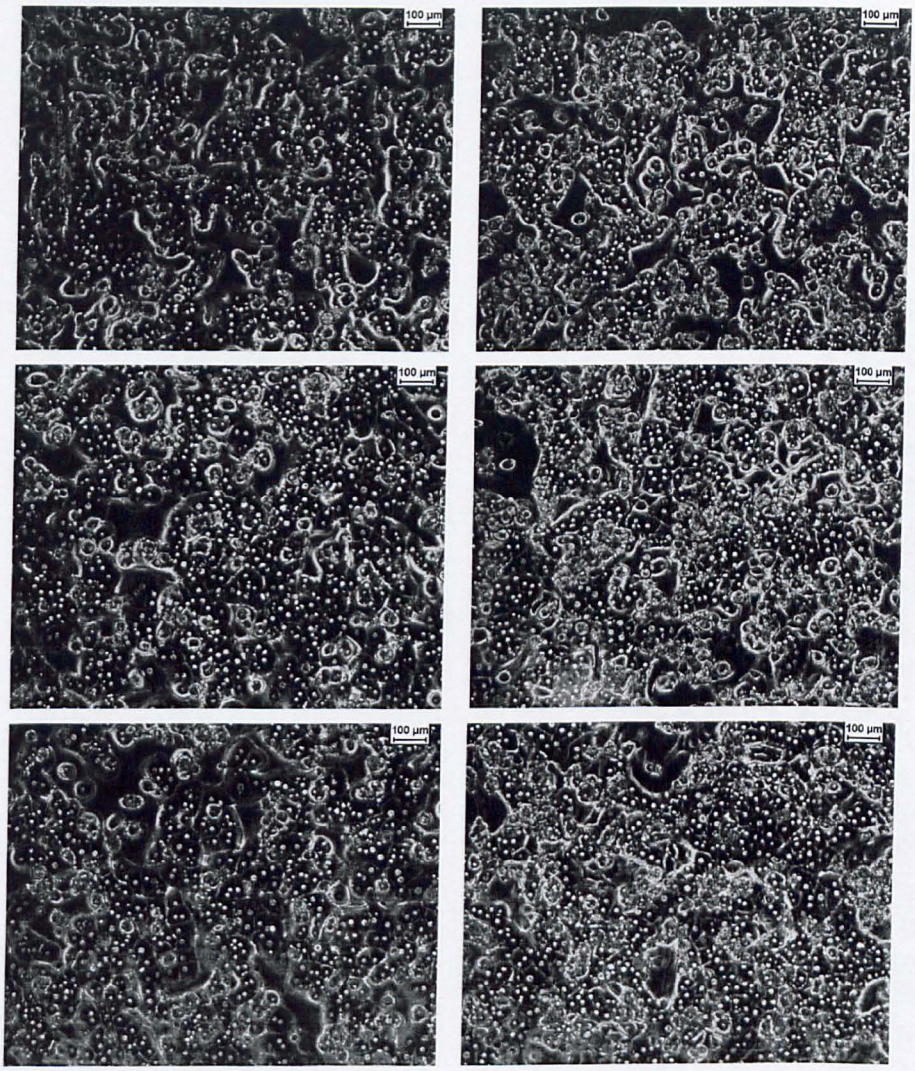

Figure 6.4 Phase-contrast microscopy images of PRH (left column) and PRH on 3T3 cells (right column) plated into collagen coated channels after 24 hrs from seeding. Images were captured at the inlet, middle and outlet of the channel (top to bottom). The cells were incubated in serum-free media at a flow rate of 50 µl/min after 1 hr attachment.

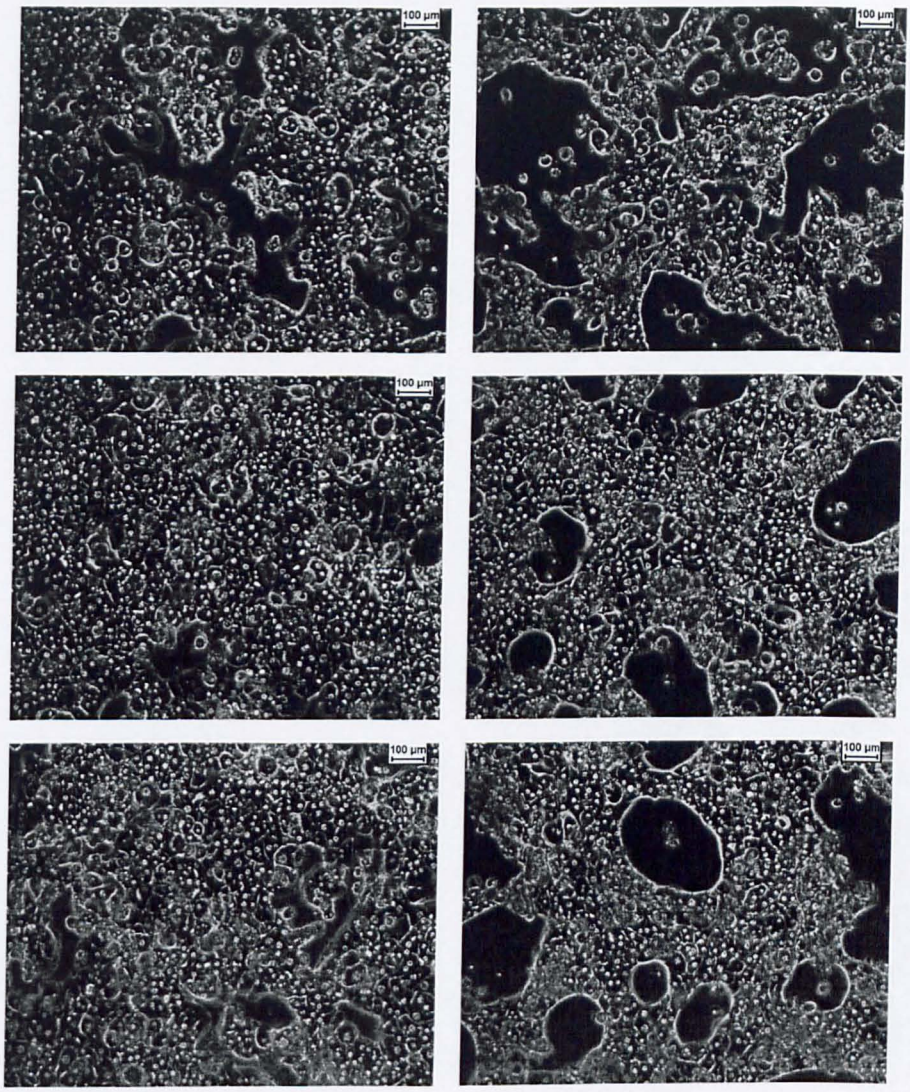

Figure 6.5 Phase-contrast microscopy images of PRH (left column) and PRH on 3T3 cells (right column) plated into collagen coated channels after 3 days under flow conditions at a flow rate of 100 µl/min. Images were captured at the inlet, middle and outlet of the channel (top to bottom).

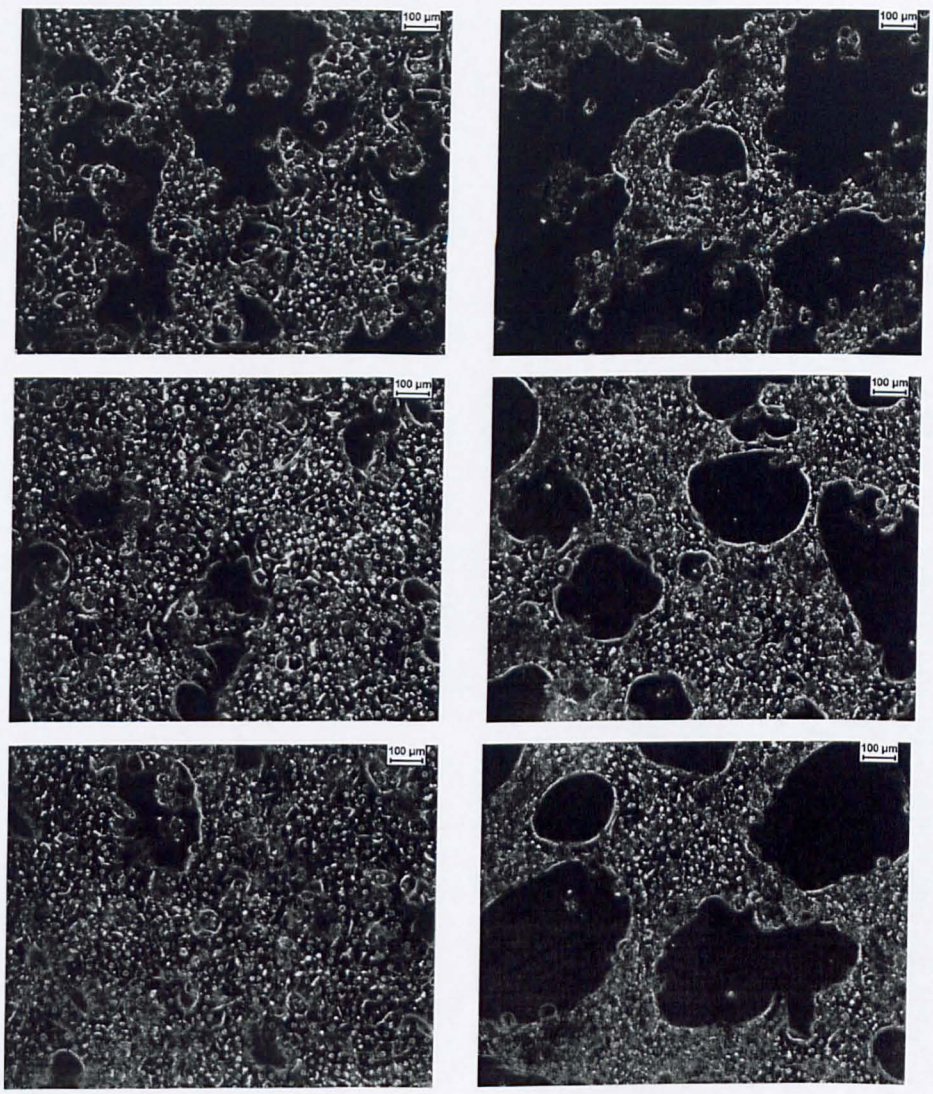

Figure 6.6 Phase-contrast microscopy images of PRH (left column) and PRH on 3T3 cells (right column) plated into collagen coated channels after 5 days under flow conditions at a flow rate of 100 µl/min. Images were captured at the inlet, middle and outlet of the channel (top to bottom).

Live/dead images in Figure 6.7 show that the majority of the cells were alive on day 5 in both cultures. However, there were more dead cells in the co-culture than the mono-culture.

All these observed features were evenly distributed throughout the channels as illustrated in the figures.

6.4.3 EROD Activity of PRH in Mono- and Co-culture with 3T3 Cells in the Channels under Media Flow

Figure 6.8 exemplifies a typical standard curve used for EROD activity measurements. The EROD activity of the PRH is reported in Figure 6.9. Resorufin production, which reflects EROD and cytochrome P450 activity, was more than 20 pmol per ml per min per channel for both mono- and co-culture on day 1 and decreased on day 2. After that, the activity increased for both culture conditions. Although the augmentation was slightly higher in the co-culture compared to mono-culture, this was not statistically significant.

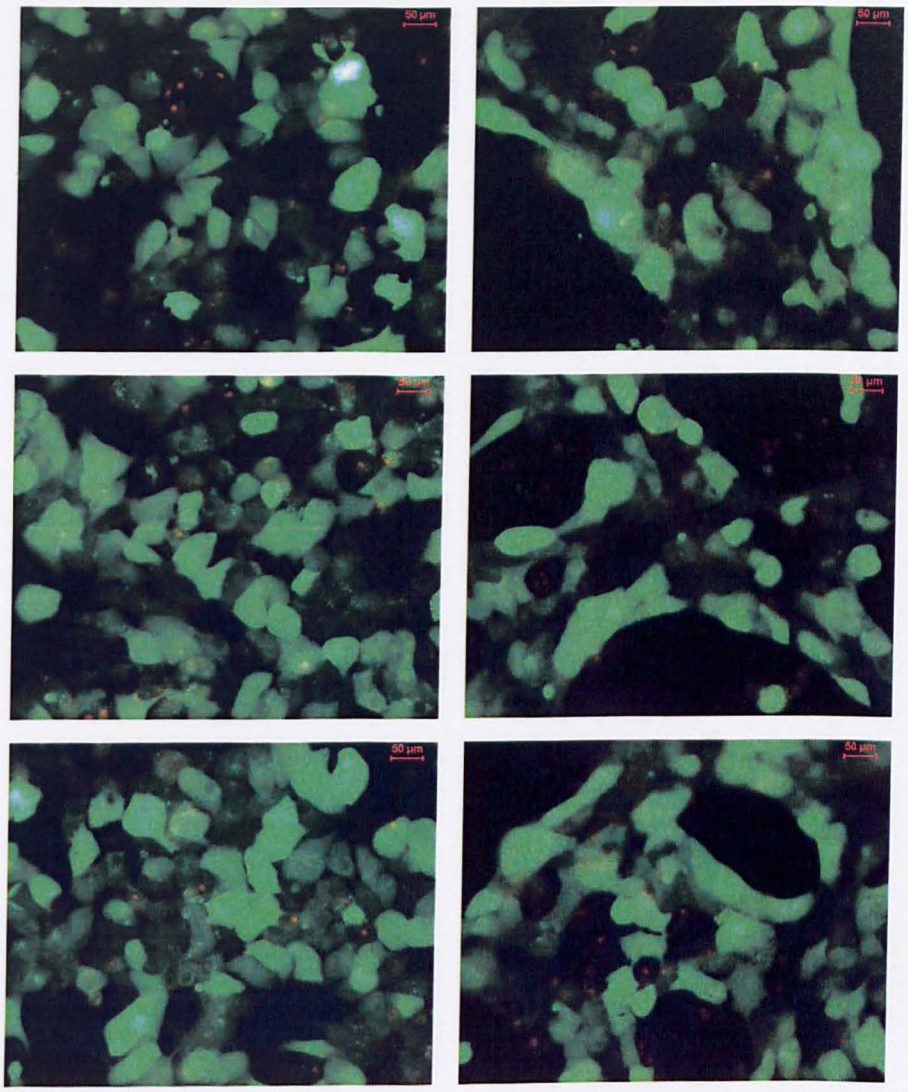

Figure 6.7 Live/dead stain images of PRH (left column) and PRH on 3T3 cells (right column) plated into collagen coated channels after 5 days under flow conditions at a flow rate of 100 µl/min. Images were captured at the inlet, middle and outlet of the channel (top to bottom).

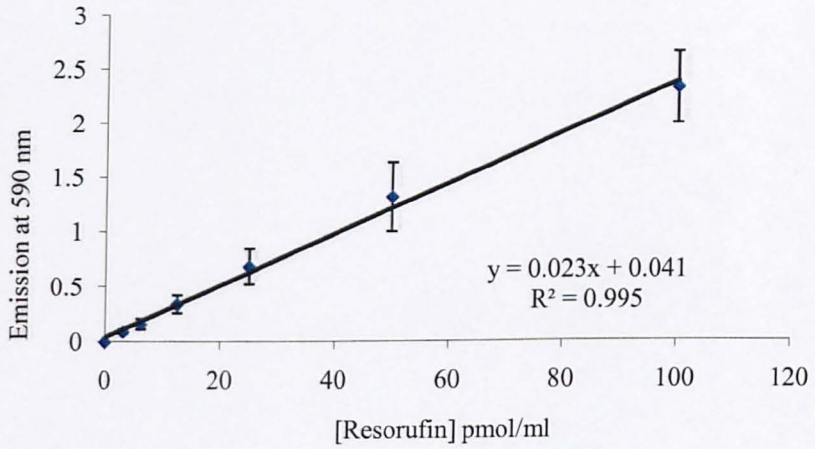

Figure 6.8 A representative resorufin standard curve. Emission of varying concentrations of resorufin solution at 590 nm. n = 12; error bars indicate ± SD.

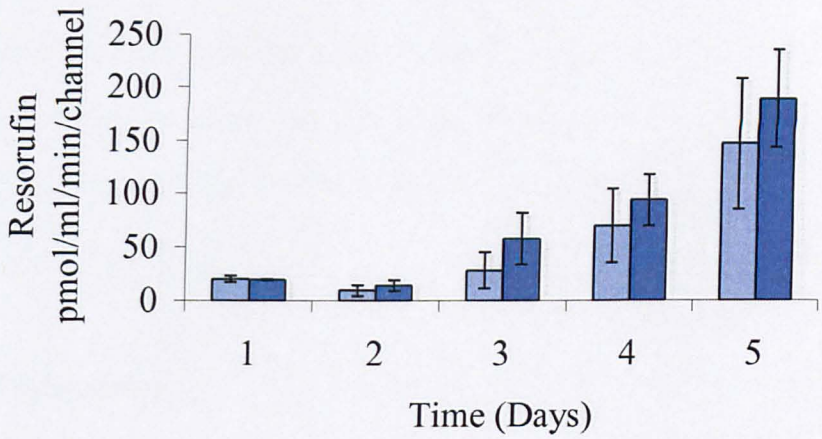

Figure 6.9 EROD activity of PRH ( ) and PRH on 3T3 cells ( ) plated into collagen coated channels and incubated with media flow at a flow rate of 50 µl/min for the first day and then at 100 µl/min for days 2, 3, 4 and 5.

6.4.4 Albumin Secretion of PRH in Mono- and Co-culture with 3T3 Cells in the Channels under Media Flow

Figure 6.10 illustrates a standard curve obtained for albumin ELISA. Albumin secretion of PRH in mono- and co-culture daily over 5 days under media flow is shown in Figure 6.11. The amount of albumin secreted by PRH was approximately 200 ng per ml per channel on day 1 post-isolation and seeding and then it decreased gradually over the time of the culture. On day 5, the amount of albumin measured in the media was just under 25 ng per ml per channel. There was not a statistically significant difference between the two culture conditions (mono- and co-culture).

6.5 Discussion

In this chapter, the Ibidi channel was demonstrated to be a prospective bioreactor for the culture of PRH under media flow. This work revealed that PRH were maintained viable in the Ibidi channel for five days and the cells expressed both EROD activity and albumin secretion. Co-culturing a second cell type with the PRH in the Ibidi channel was found to be feasible as displayed with 3T3 cell co-culture.

6.5.1 Cell Culture

The seeding density of 3T3 cells was optimised by seeding the channels with varying number of 3T3 cells for 1 hr before seeding PRH. At a seeding density of 15×10^4 3T3 cells per channel, there were many dead cells after plating PRH and this was probably due to lack of nutrients and oxygen in the channel compared to the high number of cells.

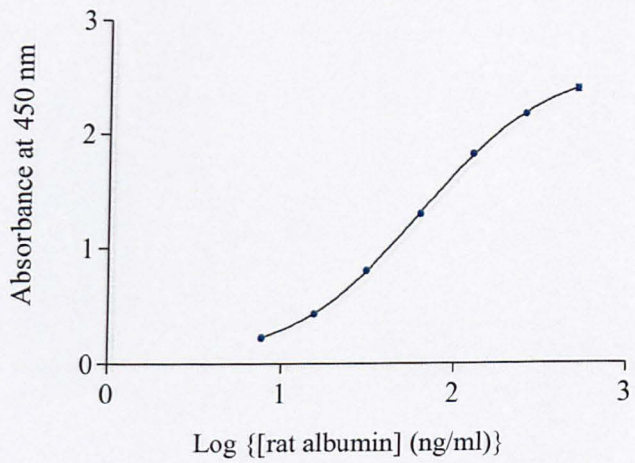

Figure 6.10 A representative albumin standard curve. Absorbance of varying concentrations of albumin at 450 nm. n = 3; error bars indicate ± SD.

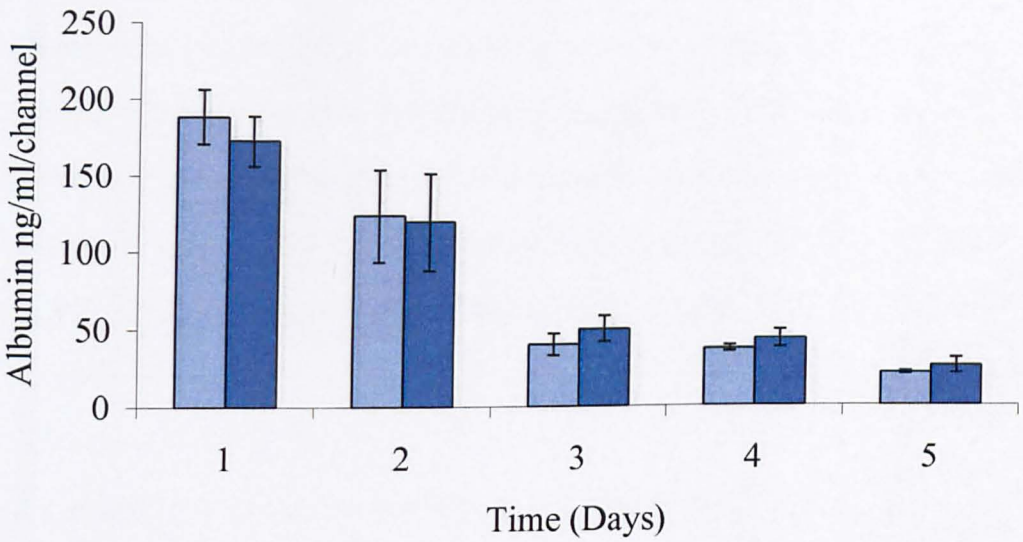

Figure 6.11 Albumin secretion of PRH ( ) and PRH on 3T3 cells ( ) plated into collagen coated channels and incubated with media flow at a flow rate of 50 µl/min for the first day and then at 100 µl/min for days 2, 3, 4 and 5.

On the other hand, at lower seeding densities of 3T3 cells, there were less dead cells when seeding the PRH.

Seeding 3T3 on ppAAm coated channels resulted in the attachment of 3T3 cells. However, this co-culture did not improve the adhesion of PRH into the ppAAm coated channels. This indicates that 3T3 cells did not improve the adhesion of PRH into the channels but they might have an effect on the functionality of PRH. This was probably because 3T3 cells were allowed to attach and spread into the channels for only 1 hr and this was not enough for the cells to start producing ECM proteins to improve attachment of PRH. In addition, those results indicated that PRH attached to the surface in between the adhered 3T3 cells.

The proportion of hepatocyte to non-parenchymal cells stated in the literature varies together with the order of cell seeding. As there is no rule dictating the benefits of one method over another, 3T3 cells were seeded first to form the co-culture. This facilitated optimising the number of 3T3 cells seeded to PRH:3T3 ratio of 10:1, and examining their effects on PRH attachment.

In the work reported by Bhatia's group (Allen *et al.*, 2005) and Park *et al.* (Park *et al.*, 2005), the 3T3 cells were seeded 24 hrs after plating PRH at a proportion of PRH:3T3 of 2:1 and 1:3 respectively. However, the two bioreactors were different from the Ibidi channel and permitted static incubation of cells before assembling the system and initiating the flow. This was not possible in the Ibidi channel because of limited oxygen and nutrients which leads to cell death under static cultures (Chapter 5).

The morphology of the PRH in both mono- and co-culture was typical hepatocyte morphology of 2-D monolayer after 24 hrs from seeding. Increasing the flow rate afterwards did not affect cell morphology. This revealed that the flow rate and the shear stress used was not harmful to the cells and did not cause any detachment. After 3 days, the cells in the co-culture started aggregating into islands and lost the 2-D monolayer morphology. This might be due to the contractile activity of 3T3 cells, the ECM produced and the flow of media

According to the data obtained from the manufacturer, the shear stress corresponding to the flow rates used ranges between 0.05 and 0.15 dyn/cm^2. This is within the range which was demonstrated by Tilles and co-workers to be safe for hepatocyte culture when they assessed albumin and urea production under increasing shear stress in a flat-plate bioreactor (Tilles *et al.*, 2001).

6.5.2 Functionality of the Cells

EROD activity of the PRH decreased after 2 days and then increased over the 5 day period in both cultures. On the other hand, albumin secretion decreased over time in both cultures. This pattern is usually observed in static hepatocyte cultures and co-cultures. This initial decrease in EROD and albumin is a consequence of cell isolation where the cells enter a phase of negative nitrogen balance and low mRNA encoding for some P450 enzymes. During this period the cells adapt to the *in-vitro* environment by altering some of their *in-vivo* functions. (Lecluyse *et al.*, 1996; Guillouzo, 1998)

The slight increase in EROD and albumin secretion in the co-culture was probably stimulated by the presence of 3T3 cells. Co-culture of PRH and non-parenchymal cells have been demonstrated in various studies to improve hepatocyte functionally as it mimics better the *in-vivo* environment of the cells (Bhandari *et al.*, 2001; Bhatia *et al.*, 1998; Bhatia *et al.*, 1999; Donato *et al.*, 1990; Guillouzo, 1998; LeCluyse *et al.*, 1996; Thomas *et al.*, 2005; Zinchenko *et al.*, 2006). Nevertheless, the increase seen in this work was not significantly different from the functionality observed in the mono-culture and this might be due to various reasons including the low number of 3T3 cells compared to studies previously reported in the literature, the order of plating the 3T3 cells first, cell-to-cell variation and the bioreactor used in the experiments. This has to be re-examined in the future to assess the effects of the above factors on the functionality of PRH and the benefits of the addition of another cell type in this bioreactor.

6.6 Conclusions

These results proved that Ibidi channels can be used for short-term culture of PRH *in-vitro*. The channel surface was hydrophobic and collagen surface coating was necessary prior to seeding. The use of ppAAm coating did not improve the cell adhesion of PRH even in the presence of pre-adhered 3T3 cells. The cells survived the micro-environment of the channels and the flow rates of the media applied for the culture period of five days. Their morphology and functionality was typical to a primary hepatocyte culture. The co-culture of PRH and 3T3 cells did not show any significant difference from the mono-culture in terms of functionality, but the method used could be harvested for the

formation of cell aggregates. The results obtained in this chapter form strong grounds for future studies of PRH behaviour in Ibidi channels in mono- and co-cultures.

This system can be used for long-term experiments to examine the morphology and basic liver functionality, zonation studies by varying flow rates and assessing enzyme expression along the channel, enzyme induction and zonation studies, co-culture with other primary non-parenchymal cells and to compare the new model with existing ones.

General Conclusions and Future Work

The liver is a structurally complex and metabolically important organ in mammals. The extensive use of the liver in multiple *in-vitro* applications renders the development of a reliable *in-vitro* liver model essential. Currently, there is an increased implementation of micro-fluidics in liver cell culture. In this work, two different micro-fluidic bioreactors were investigated. In this process, various factors known to affect the culture of liver cells were taken into account. The main factor examined here was the surface of the substrate. The conventional coating method, collagen, was compared to plasma polymerised allylamine (ppAAm). The ppAAm films were shown to change the chemical composition and the hydrophilicity of the upper surface of the substrate. The levels of nitrogen on the ppAAm films were higher than the uncoated glass or Ibidi chamber surface. Using x-ray photoelectron spectroscopy analysis, an estimate of the functional groups found on the ppAAm films was determined.

When the attachment and functionality of primary rat hepatocytes (PRH) seeded onto ppAAm and collagen gel coated coverslips was examined, no significance was found between the two coatings in the results collected. The functionality was measured in terms of albumin secretion and 7-Ethoxyresorufin-O-deethylase (EROD) activity over 48 hrs. The results also indicated that the ppAAm did not cause any unwanted toxic effects on the PRH. This study could be prolonged to investigate the long-term culture of PRH attached to ppAAm and compare it to collagen gel or adsorbed collagen coated coverslips.

The glass hexagonal bioreactor was developed to mimic the lobular structure of the liver. The nature of the channels etched into glass resulted in poor cellular adhesion and surface coating was necessary to seed both PRH and cells lines. Numerous coating techniques were assessed and ppAAm together with avidin-biotin seeding method were most appropriate for the micro-fluidic hexagonal bioreactor. The main reason for this was that the other methods, including collagen gel and poly(lactic acid), investigated produced thick coating that could block the channels and the flow of media during the experiments and/ or detached from the surface. The Huh-7 cells attached using biotin-avidin seeding technique were the only cells to maintain attachment during flow experiments after 24 hrs incubation. However, the viability of Huh-7 cells seeded onto ppAAm or using avidin-biotin decreased when incubated under media flow within 24 hours. The reasons for the cell death were unclear and many reasons could be possible including lack of oxygen and nutrients due to bioreactor design or absence of media flow. The results collected are promising and more work on investigating the reasons for cell death and optimising the bioreactor will be needed in order to use this system for PRH culture and functional studies. ppAAm could be also examined in more details to understand the ppAAm films and the mechanisms of cellular attachment

The Ibidi chamber was the second fluidic bioreactor assessed in this work. Two different coating methods were used to coat the internal surface of the chamber, adsorbed collagen and ppAAm. Huh-7 attached to both surfaces and survived under static and media flow for more than 24 hrs. However, PRH only adhered to the collagen and media flow was necessary for maintaining their viability. The viability and functionality of PRH in the Ibidi bioreactor was assessed over a period of 5 days

in mono-culture and co-culture with 3T3 cells. The results showed that the cells survived the 5 days incubation under media flow in the bioreactor and maintained EROD activity and albumin secretion. The presence of 3T3 cells in the culture did not improve the functionality of the PRH. These results could be the basis for initiating several studies investigating the Ibidi channels for short- and long-term PRH culture, including more understanding of the Ibid bioreactor and toxicology studies. Understanding the ppAAm coating in the Ibidi channels by investigating the ppAAm films in the channels and their composition could facilitate determining the mechanisms of cellular adhesion of certain cell types. This could also help understand the poor adhesion of PRH to ppAAm coated Ibidi channels observed in this work. Moreover, the Ibidi channels could be used for plasma treatment and gradient formation studies which could be then exploited in PRH mono- and co-culture studies.

Appendix

Appendix 1 Cell culture solutions

1.1 Preparation of HanksHEPES buffer (10x)

NaCl	1.37 M (80 g/L)
KCl	54 mM (4 g/L)
KH_2PO_4	4.4 mM (0.6 g/L)
$Na_2HPO_4.2H_2O$	3.6 mM (1.2 g/L)
HEPES	200 mM (47.6 g/L)
Phenol Red solution	20 mL
NaOH	100 mM (4 g/L)
Sterile distilled water	1000 ml

- Filter sterilise and treat as sterile.
- To make 1x buffer, dilute with sterile distilled water.
- Store at 4° C.

1.2 Preparation of bicarbonate/glucose solution

$NaHCO_3$	0.74 M (3.1 g/50 ml)
Glucose	0.28 M (2.5 g/50 ml)
Methionine	0.1 M (0.75 g/50 ml)
Sterile distilled water	50 ml

- Filter sterilise and store in aliquots at -20° C.

1.3 Preparation of working HanksHEPES buffer (1x, pH7.4)

- Add 2 ml bicarbonate/glucose solution per 100 ml HanksHEPES buffer (1x, pH 7.4). Solutions can be stored overnight at 4° C.

1.4 Preparation of 25 mM EGTA solution and 0.5 mM EGTA buffer

EGTA	0.48 g
Sterile 1x HanksHEPES (no bicarb/glucose)	25 ml
NaOH 1N	2.5 ml

- Make up to 50 ml with 1x HanksHEPES, filter sterilise and store at 4° C.
- Add 2ml 25 mM EGTA solution per 100mL working HanksHEPES buffer (1x, pH 7.4) to make 0.5 mM EGTA buffer. Solutions can be stored overnight at 4° C.

1.5 Preparation of 250 mM $CaCl_2$ solution and collagenase buffer

$CaCl_2$	1.84 g
Sterile distilled water	50 ml

- Filter sterilise and store at 4° C
- Add 2 ml 250 mM $CaCl_2$ solution per 100 ml working HanksHEPES buffer (1x, pH 7.4) to make 5 mM $CaCl_2$ buffer. Solutions can be stored overnight at 4° C.
- To the 5 mM $CaCl_2$ buffer, add collagense before perfusing the liver.

1.6 Preparation of 10x HBSS (for percoll) solution

NaCl	8 g
KCl	0.4 g
Na2HPO4.12H20	0.06 g
Glucose	1 g
KH2PO4	0.06 g
Distilled water	100 ml

- Filter sterilise and store at -20° C in 10 ml aliquots.

1.7 Preparation of working percoll solution

Percoll	90 ml
HBSS (10x)	10 ml

- Aliquot into 10 ml and store at 4° C

1.8 Preparation of culture medium

Serum containing media

Ingredient	*Volume*	*Final concentration*
Williams E, L-15, Dulbecco's Modified Eagle, Ham's 12 media	500 ml	N/a
L-glutamine (200 mM)	5 ml	2 mM
Antibiotic/antimycotic (100x solution)	5 ml	100 U penicillin 100 µg streptomycin 250 ng amphotericin B
Foetal calf serum (heat inactivated)	50 ml	10%

Serum-free media for primary rat hepatocytes

Ingredient	*Volume*	*Final concentration*
Williams E or L-15 media	500 ml	N/a
L-glutamine (200 mM)	5 ml	2 mM
Antibiotic/antimycotic (100x solution)	5 ml	100 U penicillin 100 µg streptomycin 250 ng amphotericin B
Insulin	500 µl (10 mg/ml solution)	10 µg/ml
Dexamethasone	500 µl (0.4 mg/ml solution)	0.4 µg/ml
Nicotinamide	5 ml (500 mM solution)	5 mM

Serum-free media for cell lines

Ingredient	*Volume*	*Final concentration*
Dulbecco's Modified Eagle, Ham's 12 Media	500 ml	N/a
L-glutamine (200 mM)	5 ml	2 mM
Antibiotic/antimycotic (100x solution)	5 ml	100 U penicillin 100 µg streptomycin 250 ng amphotericin B

- Medium should be dated and given a 2-week expiry (longer can be given for serum-free medium). Store at 4° C.
- All additives were aliquoted and stored at -20° C.

Appendix 2 Coating solutions

2.1 PLA solution

PLA	10 mg
Chloroform	10 ml

2.2 PBS-based 0.05 mg/ml collagen solution

Collagen stock solution (3.97 mg/ml)	PBS
0.03 ml	1.97 ml (2 ml / well in a 6-well plate)
0.013 ml	0.987 ml (1 ml / well in a 24-well plate)

- The concentration of collagen type I solution purchased from Upstate varied.

2.3 Collagen buffer for collagen gel coating

HBSS (x10) Ca^{2+}, Mg^{2+} free	1 ml
HEPES (1M)	250 µl
$NaHCO_3$ (7.5%)	500 µl
Distilled H_2O	5.3 ml

- Appropriate dilutions of Cellagen solution (0.3%) in the collagen buffer are needed to make various concentrations of collagen gel. The following was used :

Final collagen concentration	Volume of Cellagen solution to make 1 ml	Volume of collagen buffer to make 1 ml
0.02%	0.07 ml	0.93 ml

Appendix 3 Live / dead working solution

Ethidium homodimer-1	20 µl
Calcein AM	5 µl
Serum-free medium	10 ml

- Could be frozen at -20° C for use within 7 days.

Appendix 4 Solutions used for preparing SEM samples

4.1 Phosphate buffer (0.1 M, pH 7.2)

Sodium phosphate (monobasic)	2.76 g
sodium phosphate (dibasic)	2.84 g
Distilled water	200 ml

- Dilute 0.1 M phosphate buffer 1:2 with distilled H_2O to make 0.05 M phosphate buffer pH 7.2.

4.2 3% Glutaraldehyde

50% Glutaraldehyde solution	1.2 ml
0.1 M phosphate buffer	18.8 ml

4.3 1% Osmium tetroxide

2% Osmium tetroxide	2 ml
0.05 M phosphate buffer	2 ml

- Prepared 1% osmium tetroxide can be stored at -20° C for a month.

Appendix 5 7-Ethoxyresorufin-O-deethylase (EROD) assay

5.1 Krebs buffer

NaCl	7.013 g
KCL	0.358 g
KH_2PO_4	0.163 g
$NaHCO_3$	2.106 g
$MgCl_2$ anhydrous	0.244 g
$CaCl_2$	0.265 g
HEPES sodium salt	2.383 g
Glucose	1.802 g
Distilled water	1000 ml

- Store at 4° C.

5.2 7-Ethoxyresorufin 1 mM stock solution

7-Ethoxyresorufin	2.63 mg
Dimethyl sulphoxide (DMSO)	10 ml

- Store at 4° C in 200 µl aliquots.
- Dilute to 5 µM using Krebs buffer.

5.3 Dicoumarol 2 mM stock solution

Dicoumarol	1.0089 g
Dimethyl sulphoxide (DMSO)	15 ml

- Dilute to 10 µM using Krebs buffer.

5.4 β-glucuronidase enzyme (1600 units/ml)

β-glucuronidase enzyme 374000 units/g	1.35 g
Krebs buffer	15.75 ml

- Store at -20° C in 500 µl aliquonts.
- Dilute using sodium acetate buffer from 32000 units/ml to 1600 units/ml.

5.5 Sodium acetate buffer (0.1 M) pH 4.5

$CH_3COONa{\cdot}3H_2O$	4.101 g
Distilled water	500 ml

- Store at 4° C.

5.6 7-hydroxyresorufin

Step	Conc	Stock	Krebs (ml)
1	0.1 mM	2.35 mg	10
2	0.1 µM	10 µl from step 1	1
3	100 pmol/ml	100µl from step 2	10
4	50 pmol/ml	5 ml from step 3	5
5	25 pmol/ml	5 ml from step 4	5
6	12.5 pmol/ml	5 ml from step 5	5
7	6.25 pmol/ml	5 ml from step 6	5
8	3.125 pmol/ml	5 ml from step 7	5

Appendix 6 ELISA solutions

6.1 ELISA washing solution, pH 8

TBS, pH 8	1 sachet	
Tween 20	0.5 ml	0.05% v/v
Distilled water	1000 ml	

6.2 ELISA blocking solution, pH 8

TBS, pH 8	1 sachet	
BSA	10 g	1% w/v
Distilled water	1000 ml	

6.3 ELISA diluent solution, pH 8

TBS, pH 8	1 sachet	
BSA	10 g	1% w/v
Tween 20	0.5 ml	0.05% v/v
Distilled water	1000 ml	

6.4 Dilutions of calibrator albumin

Step	Conc (ng/ml)	Volume of stock	Sample diluent (ml)
1	500	5 µl	30
2	250	1 ml from step 1	1
3	125	1 ml from step 2	1
4	62.5	1 ml from step 3	1
5	31.25	1 ml from step 4	1
6	15.625	1 ml from step 5	1
7	7.8	1 ml from step 6	1
8	3.9	1 ml from step 7	1
9	1.95	1 ml from step 8	1
10	0.975	1 ml from step 9	1
11	0.49	1 ml from step 10	1

6.5 Dilutions of HRP conjugated anti-albumin

Step	Conc (ng/ml)	Volume of stock	Sample diluent (ml)
1	1:1000	5 µl	5
2	1:10000	1 ml from step 1	9
3	1:20000	1 ml from step 2	1
4	1:40000	1 ml from step 3	1
5	1:80000	1 ml from step 4	1

- Store all solution for ELISA at 4° C.
- Use within a month.

Appendix 7 Total protein assay

7.1 Bovine serum albumin dilutions

Step	Conc (mg/ml)	Stock	0.1 M NaOH
1	0.6	6 mg	10 ml
2	0.5	8.3 ml from step 1	1.7 ml
3	0.4	8 ml from step 2	2 ml
4	0.3	7.5 ml from step 3	2.5 ml
5	0.2	6.7ml from step 4	3.3 ml
6	0.1	5 ml from step 5	5 ml

Appendix 8 Avidin-Bition seeding method

8.1 Avidin buffer pH 7.4

FCS	5 ml
PBS	500 ml

- Keep sterile and store at 4° C.

8.2 Biotin buffer pH 6.5

FCS	5 ml
PBS	500 ml
HCl 1 mM	pH 6.5

- Keep sterile and store at 4° C.

8.3 Sodium periodate solution

Sodium periodate	10.7 mg
PBS	5 ml

- Use cold PBS and store at 4° C.
- Dilute this solution (10 mM) to 1 mM.

References

Akiyama, S. and Yamada, K. (1985). The interaction of plasma fibronectin with fibroblastic cells in suspension. *J Biol Chem*, **260**, 4492-4500

Alexander, M. and Duc, T. (1998). The chemistry of deposits formed from acrylic acid plasmas. *J Mater Chem*, **8**, 937-943.

Allen, J. And Bhatia, S. (2003). Formation of steady-state oxygen gradients in vitro. *Biotechnol Bioeng*, **82**, 253-262.

Allen, J., Khetani, S. and Bhatia, S. (2005). In vitro zonation and toxicity in hepatocyte bioreactor. *Toxicol Sci*, **84**, 110-119.

Amenta, F., Cavallotti, C., Ferrante, F. and Tonelli, F. (1981). Cholinergic Nerves in the Human Liver. *Histochem J*, **13**, 419-424.

Anderson, J. R., Chiu, D. T., Jackman, R. J., Cherniavskaya, O., Cooper McDonald, J., Wu, H., Whitesides, S. H. and Whitesides, G. M. (2000). Fabrication of topologically complexes three-dimensional microfluidic systems in PDMS by rapid prototyping. *Analytical Chemistry*, **72**, 3158-3164.

Bader, A., Knop, E., Kern, A. *et al.* (1996). 3-D coculture of hepatic sinusoidal cells with primary hepatocytes-design of an organotypical model. *Exp Cell Res*, **226**, 223-233.

Bader, A., De Bartolo, L and Haverich, A. (2000). High level benzodiazepine and ammonia clearance by flat membrane bioreactors with porcine liver cells. *J Biotechnol*, **81**, 95-105.

Baraldi, A., Comelli, G., Lizzit, S., Kiskinova, M. and Paolucci, G. (2003). Real-time X-ray photoelectron sepctroscopy of surface reactions. *Surf Sci Rep*, **49**, 169-224.

Barry, J., Silva, M., Shakeheff, K., Howdle, S. and Alexander, M. (2005). Using plasma deposits to promote cell population of the porous interior of 3D poly (D,L-lactic acid) tissue engineered scaffolds. *Adv Funct Mater*, **15**, 1134-1140.

Barry, J., Howard, D., Shakeheff, K., Howdle, S. and Alexander, M. (2006). Using a core-sheath distribution of surface chemistry through 3D tissue engineering scaffolds to control cell ingress. *Adv Mater*, **18**, 1406-1410.

Bars, R., Mitchell, A., Wolf, R. and Elcombe, C. (1989). Introduction of Cytochrome P-450 in cultured rat hepatocytes. The heterogenous localization of specific enzymes using immunocytochemistry. *Biochem. J.*, **262**, 151-158. Cited in: Lindros, K. (1997). Zonation of Cytochrome P450 Expression, Drug Metabolism and Toxicity in Liver. *Gen Pharmac*, **28**, 191-196.

Barton, D., Shard, A., Short, R. and Bradley, J. (2005). The effect of positive ion energy on plasma polmerisation: a comparison between acrylic and propionic acids. *J Phys Chem B*, **109**, 3207-3211.

Beamson, G., Briggs, D. (1992). *High Resolution XPS of Organic Polymers-The Scienta ESCA300 Database*, Wiley, Chichester, UK.

Beck, A., Candan, S., Short, R., Goodyear, A. and Braithwaite, N. (2001). The role of inos in the plasma polymerization of allylamine. *J Phys Chem B*, **105**, 5730-5736.

Beck, A., Phillips, J., Smith-Thomas, L., Short, R. and MacNeil, S. (2003). Development of a plasma-polymerized surface for the transplantation of keratinocyte-melanocyte coculture for patient with vitiligo. *Tissue Eng*, **9**, 1123-1131.

Berry, M. N., Edwards, A. M., and Barritt, G. J.(1991). Monolayer culture of hepatocytes. In *Laboratory techniques in biochemistry and molecular biology: isolated hepatocytes preparation, properties and applications* (Eds, Berry, M. N., Edwards, A. M. and J., B. G.) Elsevier, Amsterdam, pp. 263-354.

Bettinger, C., Weinberg, E., Kulig, K., Vacanti, J., Wang, y., Borenstein, J. and Langer, R. (2006). Three-dimensional microfluidic tissue-engineering scaffolds using a flexible biodegradable polymer. *Adv Mater*, **18**, 165-169.

Bhandari, R., Riccalton, L., Lewis, A., Fry, J., Hammond, A., Tendler, S and Shakesheff, K. (2001). A role for co-culture systems in modifying hepatocyte function and viability. *Tissue Eng*, **7**, 345-357

Bhatia, S., Balis, U., Yarmush, M. and Toner, M. (1998). Microfabrication of hepatocyte/fibroblast co-cultures: role of homotypic cell interactions. *Biotechnol prog*, **14**, 378-387.

Bhatia S., Balis, U., Yarmush, M. and Toner, M. (1999). Effect of cell-cell interactions in preservation of cellular phenotype: cocultivation of hepatocytes and nonparenchymal cells. *FASEB J*, **13**, 1883-1900.

Bioulac-Sage, P., Lafton, M., Saric, J. and Balabaud, C. (1990). Nerves and perisinusoidal cells in human liver. *J Hepatol*, **10**, 105-112.

Bouwens, L., De Blesser, P., Vanderkerken, K., Geerts, B. and Wisse, E. (1992). Liver cell heterogeneity: functions of non-parenchymal cells. *Enzyme*, **46**, 155-168.

Burt, A., Path, M., Le Bail, B., Balabaud, C. and Bioulac-Sage, P. (1993). Morphological investigation of sinusoidal cells. *Semin Liv Dis*, **13**, 21-38. Cited in: Jungermann, K. and Kietzmann, T. (1996). Zonation of Parenchymal and Nonparenchymal Metabolism in Liver. *Ann Rev*, **16**, 179-203.

Carlisle, E., Mariappan, M., Nelson, K., Thomes, B., Timmons, R., Constantinescu, A., Eberhart, R. and. Bankey, P. (2000). Enhancing hepatocyte adhesion by pulsed plasma deposition and polyethylene glycol coupling. *Tissue Eng*, **6**, 45-52.

Christoffels, V., Sassi, H., Ruijter, J., Moorman, A., Grange, T. and Lamers, W. (1999). A Mechanistic Model for the Development of Portcentral Gradients in Gene Expression in the Liver. *Hepatology,* **29,** 1180-1192.

Chu, P., Chen, J., Wang, L. and Huang N. (2002). Plasma-surface modification of biomaterials. *Mater Sci Eng R*, **36**, 143-206.

Codogno, P., Doyennette-Moyne, M. and Aubery, M. (1987). Evidence for a dual mechanism of chick embryo fibroblast adhesion on fibronectin and laminin substrata. *Exp Cell Res*, **169**, 478-489.

Daoust, R. (1958). The cell population of liver tissue and the cytological reference bases. *Am. Inst. Biol. Sci. Publ,* **4,** 3-10. Cited in: Sasse, D., Spornitz, U. and Maly, P. (1992). Liver Architecture. *Enzyme,* **46,** 8-32.

De Bank, P., Kellam, B., Kendall, D. and Shakesheff, K. (2003). Surface engineering of living myoblasts via selective periodate oxidation. *Biotechnol Bioeng*, **81**, 800-808.

De Bank, P., Hou, Q., Warner, R., Wood, I., Ali, B., MacNeil, S., Kendall, D Kellam, B., Shakesheff, K. and Buttery, L. (2003). Accelerated formation of multicellular 3-D structures by cell-to-cell cross linking. *Biotechnol Bioeng*, **97**, 1617-1625.

De Bartolo, L., Morelli, S., Lopez, L., et al., (2005). Biotransformation anf liver-specific functions of human hepatocytes in culture on RGD-immobilized plasma-processed membranes. *Biomaterials*, **2005**, 26, 4432-4441.

Dehili, C., Lee, P., Shakesheff, K. and Alexander, M. (2006). Comparison of primary rat hepatocyte attachment to collagen and plasma-polymerised allylamine on glass. *Plasmas Process Polym*, **3**, 474-484.

Desmet, V. (1987). Cholestasis: extrahepatic obstruction and secondary biliary cirrhosis. In *Pathology of the liver* (Eds, RNM, M., PP, A. and PJ, S.) Churchill Living stone, Edinburgh, pp. 364-423.

Desmet, V. (1994). Introduction: Organizational Principles. In *The Liver: Biology and Pathobiology*(Ed, Arias IM, B. J., Fausto N, Jakoby WB, Schachter DA and Shafritz DA) Raven Press, Ltd, New York, pp. 3-13.

Elia, H. and Sherrick, J. (1969). *Morphology of the liver,* Academic Press, New York. Cited in: Desmet, V. (1994). Introduction: Organizational Principles. In *The Liver: Biology and Pathobiology*(Ed, Arias IM, B. J., Fausto N, Jakoby WB, Schachter DA and Shafritz DA) Raven Press, Ltd, New York, pp. 3-13.

Erlinger, S. (1990). Role of intracellular organelles in the hepatic transport of bile acids. *Biomed Pharmacother,* **44,** 409-416. Cited in: Sasse, D., Spornitz, U. and Maly, P. (1992). Liver Architecture. *Enzyme,* **46,** 8-32.

Eves, P., Beck., A., Shard, A. and Mac Neil, S. (2005). A chemically defined surface for the co-culture of melanocytes and keratinocytes. *Biomaterials*, **26**, 7068-7081.

Feldmann, G. (1989). The cytoskeleton of the hepatocyte. Structure and functions. *J Hepatol,* **8,** 380-386. Cited in: Sasse, D., Spornitz, U. and Maly, P. (1992). Liver Architecture. *Enzyme,* **46,** 8-32.

Fitz, J. (1996). Cellular Mechanisms of Bile Secretion. In *Hepatology: A Textbook of Liver Disease*, Vol. 1 (Eds, Zakim, D. and Boyer, T.) Saunders Company, Philadelphia, pp. 362-375.

France, R., Short, R., Dawson, R. and MacNeil, S. (1998). Attachment of human keratinocytes to plasma co-polymers of acrylic acid/ octa-1,7-diene and allyl amine/ octa-1,7-diene. *J Mater Chem*, **8**, 37-42.

Gebhardt, R. (1992). Metabolic Zonation of the liver: Regulation and Implications for Liver Function. *Pharmac Ther,* **53,** 275-354.

Geerts, A., Bouwens, L. and Wisse, E. (1990). Ultrastructure and function of hepatic fat-storing and pit cells. *J Electron Microsc Tech,* **14,** 247-256.Cited in: Sasse, D., Spornitz, U. and Maly, P. (1992). Liver Architecture. *Enzyme,* **46,** 8-32.

Geller, S. (1965). Intralobular distribution of polyploid cells in rat liver. *Anat. Rec.,* **151,** 352-353.

Glicklis, R., Shapiro, L., Agbaria, R., Merchuk, J. and Cohen, S. (2000). Hepatocyte behaviour within three-dimensional alginate scaffolds. *Biotechnol Bioeng*, **67**, 344, 353.

Green, N. (1975). Avidin. *Adv Protein Chem*, **29**, 85-133.

Griffith, L., Swartz, M. (2006).Capturing complex 3D tissue physiology in vitro. *Nat Rev Mol Cell Biol*, **7**, 211.224.

Guillouzo, A., Morel, F., Ratanasavanh, D., Chesne, C. and Guguen-Guillouzo, C. (1990). Long-term culture of functional hepatocytes. *Toxicology in Vitro,* **4,** 415-427.

Guillouzo, A. (1998). Liver cell models in in vitro toxicology. *Environment Health Perspective,* **106,** 511-532.

Hamerli, P., Weigel, Th., Groth, Th. and Paul, D. (2003a). Surface properties of and cell adhesion onto allylamine-plasma-coated polyethylenterephtalat membranes. *Biomaterials*, **24**, 3989-3999.

Hamerli, P., Weigel, Th., Groth, Th. and Paul, D. (2003b). Enhanced tissue-compatibility of polyethylenterephtalat membranes by plasma aminofunctionalisation. *Surf Coat Technol*, **174-175**, 574-578.

Harsch, A., Calderon, J., Timmons, R. and Gross, G. (2000). Pulsed plasma deposition of allylamine on polysiloxane: a stable surface for neuronal cell adhesion. *J Neurosci Meth*, **98**, 135-144.

Hildebrand, R. and Karcher, B. (1984). Karyometry of nuclei in liver cells. Heterogeneity of nuclear volume and percentage of binucleate cells associated with veins. *Cell Tissue Res,* **235,** 669-673. Cited in: Sasse, D., Spornitz, U. and Maly, P. (1992). Liver Architecture. *Enzyme,* **46,** 8-32.

Ho, C., Lin, R., Chang, W., Chang, H. and Liu, C. (2006). Rapid heterogenous liver-cell on-chip patterning via enhanced field dielectrophoresis trap. *Lab Chip*, **6**, 724-734.

Hong, J. T. and Glauert, H. P. (2000). Effect of extracellular matrix on the expression of peroxisome proliferation associated genes in cultured rat hepatocytes. *Toxicology in Vitro,* **14,** 177-184.

Horn, T., Lyon, H. and Christoffersen, P. (1986). The Blood Hepatocytic Barrier: A Light Microscopical, Transmission- and Scanning Electron Microscopic Study. *Liver,* **6,** 233-245.

Jahn, W. (1980). The cytoskeleton of rat liver parenchymal cells. *Naturwissenschaften,* **67,** 568. Cited in: Sasse, D., Spornitz, U. and Maly, P. (1992). Liver Architecture. *Enzyme,* **46,** 8-32.

Jones, A., Schmucker, D., Mooney, A., Alder, A. and Ockner, R. (1976). Morphometric Analysis of Rat Hepatocytes after Total Biliary Obstruction.*Gastroenterology,* **71,** 1050-1060.

Jones, A. L., Schmucker, D. L., Mooney, J. S., *et al.* (1978). A quantitative analysis of hepatic ultrastructure in rats during hance bile secretion. *Anat Rec,* **192,** 272.

Jones, A. (1996). Anatomy of the Normal Liver. In *Hepatology: A Textbook of Liver Disease*, Vol. 1 (Eds, Zakim, D. and Boyer, T.) Saunders Company, Philadelphia, pp. 3-32.

Jones A. L., Schmucker D. L., Renston R. H., and Murakami T. (1980). The architecture of bile secretion: a morphological perspective of physiology. *Dig Dis Sci,* **25,** 609. Cited in: Jones, A. (1996). Anatomy of the Normal Liver. In *Hepatology: A Textbook of Liver Disease*, Vol. 1 (Eds, Zakim, D. and Boyer, T.) Saunders Company, Philadelphia, pp. 3-32.

Jungermann, K. and Katz, N. (1989). Functional Specialization of Different Hepatocyte Populations. *Physiol Rev,* **69,** 708-764.

Jungermann, K. and Kietzmann, T. (1996). Zonation of Parenchymal and Nonparenchymal Metabolism in Liver. *Ann Rev,* **16,** 179-203.

Jungermann, K. and Kietzmann, T. (1997). Role of Oxygen in the Zonation of Carbohydrate Metabolism and Gene Expression in Liver. *Kidney Int,* **51,** 402-412.

Jungermann, K. and Kietzmann, T. (2000). Oxygen: Modulator of Metabolic Zonation and Disease of the Liver. *Hepatology,* **31,** 255-260.

Kanamura, S., Kanai, K., Watanabe, J., Asada-Kubuta, M. and Oka, M. (1984). Development of Structural Heterogeneity of Mitochondria in Mouse Hepatocytes. *J Anat,* **139,** 295-305.

Kane, B., Zinner, M., Yarmush, M. and Toner, M. (2006). Liver-specific functional studies in a microfluidic array of primary mammalian hepatocytes. *Anal Chem*, **78,** 4291-4298.

Kanno, N., LeSage, G., Glaser, S., Alvaro, D. and Alpini, G. (2000). Functional heterogeneity of the Intrahepatic Biliary Epithelium. *Hepatology,* **31,** 555-561.

Kaufmann, P. M., Heimrath, S., Kim, B. S. and Mooney, D. J. (1997). Highly porous polymer matrices as a three-dimensional culture system for hepatocytes. *Cell Transplantation,* **6,** 463-468.

Kleinman, H., Klebe, R. and Martin, G. (1981). Role of collagenous matrices in the adhesion and growth of cells. *J Cell Biol*, **88,** 473-485.

Kojima, N., Matsuo, T. and Sakai, Y. (2006). Rapid hepatic cell attachment onto biodegradable polymer surfaces without toxicity using avidin-biotin binding system. *Biomaterials*, **27**, 4904-4910.

Krasteva, N., Groth, T. and Fey-Lamprecht, F. (2001). The role of surface wettability on hepatocyte adhesive interactions and function. *J Biomater Sci Polymer Edn*, **12,** 613-627.

Kumar, G. and Prabhu, N. (2007). Review of non-reactive and reactive wetting of liquids on surfaces. *Adv Colloid Interface Sci*, **133,** 61-89.

Langsch, A. and Bader, A. (2001). Longterm stability of phase I and phase II enzymes of porcine liver cells in flat membrane bioreactors. *Biotechnol Bioeng*, **76,** 115-125.

Leclerc, E., Sakai, Y. and Fujii, T. (2003). Cell culture in 3-dimensional microfluidic structure of PDMS (polydimethylsiloxane). *Biomed Microdevices,* **5,** 109-114.

Leclerc, E., Furukawa, K., Miyata, F., Sakai, Y., Ushida, T and Fujii, T. (2004a). Fabrication of microstructures in photosensitive biodegradable polymers for tissue engineering applications. *Biomaterials*, **25,** 4683-4690.

Leclerc, E., Sakai, Y. and Fujii, T. (2004b). Microfluidic PDMS (polymethylsiloxane) bioreactor for large-scale culture of hepatocytes. *Biotechnol Prog*, **20,** 750-755.

LeCluyse, E., Bullock, P. and Parkinson, A. (1996). Strategies for restoration and maintenance of normal hepatic structure and function in long-term cultures of rat hepatocytes. *Adv Drug Delivery Rev*, **22,** 133-186.

Lindros, K. (1997). Zonation of Cytochrome P450 Expression, Drug Metabolism and Toxicity in Liver. *Gen Pharmac,* **28,** 191-196.

Lodish, H., Berk, A., Zipursky, L., Matsudaira, P., Baltimore, D. and Darnell, J. (2000). Molecular cell biology. Freeman and Company, New York , chapter 22.

Loud, A. (1968). A quantitative stereological description of the ultrastructure of normal rat liver parenchymal cells. *J. Cell Biol.,* **37,** 27-46. Cited in: Sasse, D., Spornitz, U. and Maly, P. (1992). Liver Architecture. *Enzyme,* **46,** 8-32.

MacPhee, P., Schmidt, E. and Groom, A. (1992). Evidence for kupffer cell migration along liver sinusoids, from high-resolution in vivo microscopy. *Am J Physiol,* **236,** G17-G23.

Manso, M., Rossini, P., Malerba, A., Valsesia, A., Gribaldo, L., Ceccone, G. and Rossi, G. (2004). Combination of ion beam stabilisation, plasma etching and plasma deposition for the development of tissue engineering micropatterned supports. J *Biomater Sci Polymer Edn,* **15,** 161-172.

Matsumoto, T., Komori, R., Magara, T., Ui, T., Kawakami, M., Tokuda, T., Takasaki, S., *et al.* (1979). A study on the normal structure of the human liver, with special reference to its angioarchitecture. *Jikeikai Med J,* **26,** 1-40. Cited in: Saxena, R., Theise, N. and Crawford, J. (1999). Microanatomy of the Human Liver-Exploring the Hidden Interfaces. *Hepatology,* **30,** 1339-1346.

McIndoe, A. (1928). The structure and arrangement of the bile canaliculi. *Arch Pathol Lab Med,* **6,** 598.Cited in: Jones, A. (1996). Anatomy of the Normal Liver. In *Hepatology: A Textbook of Liver Disease*, Vol. 1 (Eds, Zakim, D. and Boyer, T.) Saunders Company, Philadelphia, pp. 3-32.

Michalopoulos, G. K. and Pitot, H. C. (1975). Primary culture of parenchymal liver cells on collagen membranes. *Experimental Cell Research,* **94,** 70-78.

Mitchell, S., Davidson, M., Emmison, N. and Bradley, R. (2004) Isopropyl alcohol plasma modification of polystyrene surfaces to influence cell attachment behaviour. *Surf Sci*, **561**, 110-120.

Mitra, S. (1966). The Terminal Distribution of the Hepatic Artery with Special Reference to Arterio-Portal Anastomosis. *J Anat,* **100,** 651-663.

Munzer, F. (1923). Uber die zweikernigkeit der leberzellen. *Arch. Mikrosk. Anat.* **98,** 249-282. Cited in: Sasse, D., Spornitz, U. and Maly, P. (1992). Liver Architecture. *Enzyme,* **46,** 8-32.

Nathanson, M. and Boyer, J. (1991). Mechanisms and regulation of bile secretion. *Hepatology,* **14,** 551-566. Cited in: Desmet, V. (1994). Introduction: Organizational Principles. In *The Liver: Biology and Pathobiology*(Ed, Arias IM, B. J., Fausto N, Jakoby WB, Schachter DA and Shafritz DA) Raven Press, Ltd, New York, pp. 3-13.

Neveu M. J., Hully J. R., Babcock K. L., Hertzberg E. L., Nicholson B. J., Paul D. L., and Pitot H. C. (1994). Multiple mechanisms are responsible for altered expression of gap junction genes during oncogenesis in rat liver. *J Cell Sci,* **107,** 83-95.

Newsholme, P., Procopio, J., Lima, M., Pithon-Curi, T. and Curi, R. (2003). Glutamine and Glutamate: Their Central Role in Cell Metabolism and Function. *Cell Biochem Funct,* **21,** 1-9.

Niiro, G. and O'morchoe, C. (1986). Pattern and Distribution of Intrahepatic Lymph Vessels in the Rat. *Anat Rec,* **215,** 351-360.

Oda, M., Tsukada, H., Kamatsu, H., Yoner, Y., Honda, K. and Tsuchiya, M. (1986). Mechanism of contraction and dilatation of sinusoidal endothelial fenetrae in the liver. *Hepatology,* **16,** 2469. Cited in: Sasse, D., Spornitz, U. and Maly, P. (1992). Liver Architecture. *Enzyme,* **46,** 8-32.

Oinonen, T., Mode, A., Lobie, P. and Lindros, K. (1996). Zonation of Cytochrome P450 Enzyme Expression in Rat Liver. *Biochem Pharmac,* **51,** 1379-1387.

Ostrovidov, S., Jiang, J., Sakai, Y. and Fujii, T. (2004). Membrane-based PDMS microbioreactor for perfused 3D primary rat hepatcoyte cultures. *Biomed Microdevices*, **6**, 279-284.

O'Toole, L., Beck, A., Ameen, A., Jones, F., Short, R. (1995). Radiofrequency-induced plasma polymerisation of propenoic acid and propanoic acid. *J Chem Soc-Faraday Trans*, **91**, 3907-3912.

Parikh, A. (2004). Mammalian Histology: Liver and gall bladder images, University of Delaware, www.udel.edu/Biology/Wags/histopage/ colorpage/clg/clg.htm, date: January 2004.

Park, J., Berthiaume, F., Toner, M., Yarmush, M. and Tilles, A. (2005). Microfabricated grooved substrates as platforms for bioartificial liver reactors. *Biotechnol Bioeng*, **90**, 632-644.

Pearson, R., Molino, Y., Williams, P., Tendler, S., Davies, M., Roberts, C. and Shakesheff, K. (2003). Spatial confinement of neurite regrowth from dorsal root ganglia within nonpourous microconduits. *Tissue Eng*, **9**, 201-208.

Pierschbacher, M. and Ruoslahti, E. (1984). Cell attachment activity of fibronectin can be duplicated by small synthetic fragments of the molecule. *Nature*, **309**, 30-33.

Pinkse, G., Voorhoeve, M., Noteborn, M., Terpstra, O., Bruijn, J. and de Heer, E. (2004). Hepatocyte survival depends on β1-integrin-mediated attachment of hepatocytes to hepatic extracellular matrix. *Liver International*, **24**, 218-226.

Pinzani M., Failli P., Ruocco C., Casini A., Milani S., Baldi E., Giotti A., and Gentilini P. (1992). Fat-storing cells as liver-specific pericytes. Spacial dynamics of agonist-stimulated intra-cellular calcium transients.*J Clin Invest,* **90,** 642-646.

Powers, M., Janigian, D., Wack, K., Baker, C., Beer Stolz, D. And Griffith, L. (2002a). Functional behaviours of primary rat liver cells in three-dimensional perfused microarray bioreactor. *Tissue Eng*, **8**, 499-513.

Powers, M., Domansky, K., Kaazempur-Mofrad, M. *et al.* (2002b). A microfabricated array bioreactor for perfused 3D liver culture. *Biotechnol Bioeng*, **78**, 257-269.

Qiao, L. and Farrell, G. (1999). The effects of cell density, attachment substratum and dexamethasone on spontaneous apoptosis of rat hepatocytes in primary culture. *In Vitro Cell Dev Biol Anim*, **35**, 417-424.

Radziuk, J. and Pye, S. (2001). Hepatic Glucose Uptake, Gluconeogenesis and the Regulation of Glycogen Synthesis. *Diabetes Metab Res Rev*, **17**, 250-272.

Rappaport, A., Borowy, Z., Loughheed, W. and Lotto, W. (1954). Subdivision of Hexagonal Liver Lobules into a Structural and Functional Unit. *Anat Rec*, **119**, 11-33.

Rappaport, A. (1958). The structural and functional unit in the human liver (liver acinus). *Ana. Rec*, **130**, 673-689.

Reid, L. M., Narita, M., Fujita, M., Murray, Z., Liverpool, C. and Roseberg, L. (1986). Matrix and hormonal regulation of differentiation in liver cultures. In *Isolated and cultured hepatocytes* (Eds, Guillouzo, A. and Guguen-Guillouzo, C.) Libbey, London, pp. 225-258.

Reid, L., Fiorino, A., Sigal, S., Brill, S. and Holst, P. (1992). Extracellular matrix gradients in the space of Disse: relevance to liver biology. *Hepatology*, **15**, 1198-1203.

Rieder, H., Meyer zum Buschenfelde, K.-H. and Ramadori, G. (1992). Functional spectrum of sinusoidal endothelial liver cells. Filtration, endocytosis, synthetic capacities and intercellular communication. *J Hepatol*, **15**, 237-250. Cited in: Desmet, V. (1994). Introduction: Organizational Principles. In *The Liver: Biology and Pathobiology*(Ed, Arias IM, B. J., Fausto N, Jakoby WB, Schachter DA and Shafritz DA) Raven Press, Ltd, New York, pp. 3-13.

Sasse, D., Spornitz, U. and Maly, P. (1992). Liver Architecture. *Enzyme*, **46**, 8-32.

Saxena, R., Theise, N. and Crawford, J. (1999). Microanatomy of the Human Liver-Exploring the Hidden Interfaces. *Hepatology*, **30**, 1339-1346.

Seglen, P. O. (1976). Preparation of isolated liver cells. *Methods cell biol*, **13**, 29-83.

Schwartz, M. (2001). Integrin signalling revisited. *Trends Cell Biol*, **11**, 466-470.
Shard, A., Whittle, J., Beck, A., *et al.* (2004). A NEXAFS examination of unsaturation in plasma polymers of allyamine and propylamine. *J Phys Chem B*, **108**, 12472-12480.

Sivaraman, A., Leach, J., Townsend, S. *et al.* (2005). A microscale in vitro physiological model of the liver: predictive screens for drug metabolism and enzyme induction. *Curr Drug Metab*, **6**, 569-591.

Talamini, M. A., Kappus, B. and Hubbard, A. (1997). Repolarisation of hepatocytes in culture. *Hepatology,* **25,** 167-172.

Terranova, V., Rao, C., Kalebic, T., Margulies, I. And Liotta, L. (1983). Laminin receptor on human breast carcinoma cells. *Proc Natl Acad Sci USA*, **80**, 444-448.

Thomas, R. ; Bhandari, R.; Barrett, D.; Bennett, A. ; Fry, J. ; Powe, D.; Thomson, B.; and Shakesheff, K. (2005). The effect of three-dimensional co-culture of hepatocytes and hepatic stellate cells on key hepatocyte functions in vitro. *Cells Tissues Organs*, **181**, 67-79.

Tilinin, I. S., Jablonski, A. and Werner, W. S. M. (1996). Quantitative surface analysis by Auger and X-ray photoelectron spectroscopy. *Prog Surf Sci*, **52**, 193-335.

Tilles, A., Baskaran, H., Roy, P., Yarmush, M. and Toner, M. (2001). Effects of oxygenation and flow on the viability and function of rat hepatocytes cocultured in a microchannels flat-plate bioreactor. *Biotechnol Bioeng*, **73**, 379-389.

Toh, Y., Ng, S., Khong, Y., Samper, V. and Yu, H. (2005). A configurable three-dimensional microenvironment in a microfluidic channels for primary hepatocyte culture. *ASSAY Drug Dev technol*, **3**, 169-176.

Traub, P., Look, J., Dermietzel, R., Brummer, F., Hulser, D. and Willecke, K. (1989). Comparative characterization of the 21 kD and 26 kD gap junction proteins in murine liver and cultured hepatocytes. *J Cell Biol,* **108,** 1039-1051.

Tseng, D. and Edelman, E. (1998). Effects of amide and amine plasma-treated ePTFE vascular grafts on endothelial cell lining in an artificial circulatory system. *J Biomed Mater Res*, **42**, 188-198.

Tsiaoussis, J., Newsome, P., Nelson, L., Hayes, P. and Pelvris, J. (2001). Which Hepatocyte Will It Be? Hepatocyte Choice for Bioartificial Liver Support Systems. *Liver Transpl,* **7,** 2-10.

Volpes, R., Van den Oord, J. and Desmet, V. (1991). Distribution of VLA family of integrins in normal and pathological human liver tissue. *Gastroenterology,* **101,** 200-206.

Wang, Y., Liu, H., Guo, H., Wen, H. and Liu, J. (2004). Primary hepatocyte culture in collagen gel mixture and collagen sandwich. *World Journal of Gastroenterology,* **10,** 699-702.

Wardle, E. (1987). Kupffer Cells and their Function. *Liver,* **7,** 63-75.

Webb, K., Hlady, V. and Tresco, P. (1998). Relative importance of surface wettability and charged functional groups on NIH 3T3 fibroblast attachment, spreading, and cytoskeletal organization. *J Biomed Mater Res*, **41**, 422-430.

Weibel, E., Staubli, W., Gnagi, H. and Hess, F. (1969). Correlated morphometric and biochemical studies on the liver cell. I. Morphometric model, stereologic methods. *J. Cell Biol.*, **42**, 68-91. Cited in: Desmet, V. (1994). Introduction: Organizational Principles. In *The Liver: Biology and Pathobiology*(Ed, Arias IM, B. J., Fausto N, Jakoby WB, Schachter DA and Shafritz DA) Raven Press, Ltd, New York, pp. 3-13.

Whittle, J., Bullet, N., Short, R., Douglas, C., Hollander, A. and Davies, J. (2002). Adsorption of vitronectin, collagen and immunoglobulin-G to plasma polymer surfaces by enzyme linked immunosorbent assay (ELISA). *J Mater Chem*, **12**, 2726-2732.

Wisse, E., Geerts, A., Bouwens, L., Van Bossuyt, H., Vanderkerken, K. and Van Goethem, F. (1991). Cell biological functions of sinusoidal cells. In *Oxford textbook of clinical hepatology*, Vol. 1 (Eds, McIntyre, N., Benhamou, J.-P., Bircher, J., Rizzetto, M. and Rodes, J.) Oxford University Press, Oxford, pp. 235-244.

Yamamoto, K. and Philips, M. (1986). Three Dimensional Observations of the Intrahepatic Lymphatics by Scanning Electron Microscopy of Corrosion Casts. *Anat Rec*, **214**, 67-70.

Yamamoto, A., Mishimam, S., Maruyama, N. and Sumita M (1999). Quantitative evalulation of cell attachment to glass, polystyrene, and fibronectin- or collagen-coated polystyrene by measurement of cell adhesive shear force and cell detachment energy. *Biomed Mater Res*, **50**, 114-124.

Yang, J., Chung, T., Nagaoka, M., Goto, M., Cho, c. and Akaike, T. (2001). Hepatocyte-specific porous polymer-scaffolds of alginate/galactosylated chitosan sponge for liver-tissue engineering. *Biotechnol Lett*, **23**, 1385-1389.

Yang, J., Bei, J. and Wang, S. (2002). Enhanced cell affinity of poly (D,L-lactide) by combining plasma treatment with collagen anchorage. *Biomaterials*, **23**, 2607-2614.

Yasuda, H. (1985). Plasma polymerization. Academic Press, Orlando.

Yokota, S. (1985). Functional differences between sinusoidal endothelial cells and intralobular or central vein endothelium in rat liver. *Anat Rec*, **212**, 74-80.

Zinchenko, S., Schrum, L., Clemens, M. and Coger, R. (2006). Hepatocyte and kupffer cells co-cultured on micropatterned surfaces to optimize hepatocyte function. *Tissue Eng*, **12**, 751-761.

http://www.udel.edu/biology/Wags/histopage/colorpage/clg/clgllp.GIF. September 2007. Mammalian Histology-B408, Department of Biological Sciences, University of Delaware. June 2004.

http://www.ibidi.de/products/slideI.html. 2007. Ibidi GmbH. March 2005.